Dissertation

Characterization of Phospholipid Scramblase 1 (PLSCR1) in the villous trophoblast of the human placenta

submitted by
Dr.med.univ.
Veronika Marlies BERGHOLD

for the Academic Degree
Doctor of Philosophy
(PhD)

at the
Medical University of Graz

carried out at
Institute of Cell Biology, Histology & Embryology
Medical University of Graz, Austria
&
Department of Obstetrics & Gynecology, Faculty of Medicine and Dentistry
University of Alberta, Edmonton, Canada

under the Supervision of
Univ.-Prof. Dr.rer.nat. Berthold Huppertz

2014

Statutory Declaration

I hereby declare that this dissertation is my own original work and that I have fully acknowledged by name all of those individuals and organisations that have contributed to the research for this dissertation. Due acknowledgement has been made in the text to all other material used. Throughout this dissertation and in all related publications I followed the guidelines of “Good Scientific Practice”.

Please note that parts of this thesis are already published:

- Berghold, V.M., Gauster, M., Hemmings, D.G., Moser, G., Kremshofer, J., Siwetz, M., Sundl, M. & Huppertz, B. 2014, "Phospholipid scramblase 1 (PLSCR1) in villous trophoblast of the human placenta", *Histochemistry and Cell Biology*, DOI 10.1007/s00418-014-1294-y.

November 2014, Graz, Austria

Further Publications:

- Gauster, M., Berghold, V.M., Moser, G., Orendi, K., Siwetz, M. & Huppertz, B. 2011, "Fibulin-5 expression in the human placenta", *Histochemistry and Cell Biology*, vol. 135, no. 2, pp. 203-213.
- Huppertz, B., Berghold, V.M., Kawaguchi, R. & Gauster, M. 2012, "A variety of opportunities for immune interactions during trophoblast development and invasion", *American Journal of Reproductive Immunology* (New York, N.Y.: 1989), vol. 67, no. 5, pp. 349-357.

Preface & Acknowledgements

The thesis was carried out through the PhD Program *Molecular Medicine*, Medical University of Graz, Austria at the Institute of Cell Biology, Histology & Embryology under the supervision of Berthold Huppertz with the support of Martin Gauster. The majority of experiments including most of cell line and first trimester explants work were performed there.

During my studies I spent six months (February – August 2013) at the lab of Denise G. Hemmings, Department of Obstetrics and Gynecology, University of Alberta, Edmonton, Canada, where the isolated primary trophoblast experiments completed the project.

The PhD program *Molecular Medicine*, Medical University of Graz mainly funded this study. Additionally, part of this study was supported by the START funding program and the Franz-Lanyar-Foundation of the Medical University of Graz granted to Gerit Moser (Project #358) and Martin Gauster (Project #359). The Canadian Institutes of Health Research (CIHR) granted further funding to Denise G. Hemmings (MOP 123488).

First of all, I would like to sincerely thank Berthold Huppertz for being my supervisor and for giving me the opportunity to work on this project. Although his time was limited, he was always informed about the progress and came up with new ideas. He picked me up when the project did not succeed as I hoped for. Furthermore, Berthold Huppertz encouraged me to present my work at various international conferences and workshops.

Particularly, I would like to thank Martin Gauster, who was my co-supervisor during the project. He always took time to discuss, teach me and think about new ways to advance the project.

I am very grateful to Monika Siwetz, for her introduction into various methods and her continuous support. Furthermore, I would like to thank Monika Sundl for all her help and I appreciate very much her staying late to help me finish important experiments.

I would like to thank Gerit Moser, Julia Kremshofer, Amin El-Heliebi, Julia König, Julia Fröhlich, Gregor Weiss and Stefan Wernitznig for our great time together, for the support and for being friends.

Thanks go to Astrid Hammer for her expertise with the laser-scanning microscope and to Tom Kroneis for the introduction into single cell analysis.

I would like to express my gratitude to Gottfried Dohr for giving me the opportunity to carry out my thesis at the Institute, to Beate Scheiber, Irmgard Ropitsch and Sandra Weber for administrative support and to Daniel Kummer and Rudolf Schmidt for technical support. And of course I want to thank all other members of the Institute of Cell Biology, Histology & Embryology for the great and valuable time during my thesis.

I also want to express my appreciation to Akos Heinemann (Institute of Experimental & Clinical Pharmacology) as a member of my thesis committee for his input and the idea with the washed platelet assay. Analysis of platelet aggregation was performed with the kind help of Martina Ofner.

I am very grateful to Sasa Frank, (Institute of Molecular Biology & Biochemistry), also a member of my thesis committee, for the siRNA protocol, which finally showed good results. Additionally, he provided HEK-293 and Hep G2 cells. I would like to thank Lada Brkić, who took the time to show me the specific method for siRNA transfection.

First trimester placenta samples were kindly provided by Andreas Glasner, Graz, Austria.

Deep appreciation goes to Denise G. Hemmings, whom I met in Japan and immediately invited me to join her lab in Edmonton, Canada. This gave me the opportunity to get new insights from a different lab. She was a great supervisor and friend. Her support and encouragement throughout my time in Canada was outstanding. I will always be grateful to her for picking me up from the airport, letting me stay at her house, the get-togethers (including TGIFs) and the awesome good-bye party. She also critically reviewed my manuscript and gave valuable input.

Denise G. Hemmings kindly provided primary trophoblasts from isolated term placentas. The cells were obtained from the laboratory of Larry Guilbert, University of Alberta isolated by Bonny Lowen and Meghan R. Riddell.

My thanks go to Martina Mackova for her methodical support, the rapid effort to find solutions for my questions and also the help with measurements of beta-hCG.

Further, I want to mention Sarah Post, Katie Kinatschuk, Daniel Kerage, Meagan Brown, Robert Patry and Shreya Amin. They gave me a warm and friendly welcome, were friends inside and outside the lab and showed me around Edmonton. Thanks to

Sheena (Xin) Fang, Heather Bronson and Kelycia Leimert for the theoretical support with qRT-PCR analysis.

I sincerely want to thank Andrea Berghold for statistical advice and Christian Berghold for his critical feedback and input for my project presentations as well as allowing me to perform hCG analysis at his lab with the help of Edda Streck, Marlies Weineiss, Markus Kampel, Ulrike Steindl-Podolsky, Marusa Hauke and Melanie Perhofer.

Particularly, I am very thankful to Andreas Kainer for his technical advice, his ImageJ software tutorial, his assistance in counting cell nuclei and his support throughout the project.

Last but not least I would like to thank my family and my friends who supported me throughout my thesis.

Table of Contents

Abbreviations and Definitions

ADP	adenosine diphosphate
ANOVA	repeated measures of variance
ATP	adenosine triphosphate
BeWo	human choriocarcinoma cell line
Br-cAMP	8-bromoadenosine 3′,5′-cyclic monophosphate
Ct	cycle threshold
DAPI	4',6-diamidino-2-phenylindole
DMEM/F-12	Dulbecco's Modified Eagle Medium / Nutrient Mixture F-12
DMSO	dimethylsulfoxide
dNTP	desoxyribonucleoside triphosphate
DTT	dithiothreitol
EDTA	ethylene diamine tetraacetic acid
FCS	fetal calf serum
FFPE	formalin-fixed paraffin-embedded
GCM-1	glial cells missing-1
H_2O	water
HBSS	Hank’s Balanced Salt Solution
hCG	human chorionic gonadotropin
HCMV	human cytomegalovirus
HEK-293	human embryonic kidney cells
Hep G2	human hepatocellular carcinoma cell line
HUVEC	human umbilical vein endothelial cells
IMDM	Iscove's Modified Dulbecco's Medium
JAR	human choriocarcinoma cell line
JEG-3	human choriocarcinoma cell line
MOI	multiplicity of infection
NGS	normal goat serum
PBS	phosphate buffered saline
PBS/T	mixture of PBS and 0.05% Tween 20
PC	phosphatidylcholine
PE	phosphatidylethanolamine
PEN	polyethylene naphthalate
PLSCR	phospholipid scramblase

RIN	RNA integrity number
RPLP0	ribosomal protein P0
PS	phosphatidylserine
RT	room temperature
RT-PCR	reverse transcription polymerase chain reaction
qRT-PCR	quantitative real-time polymerase chain reaction
SD	standard deviation
SEM	standard error of the mean
SM	sphingomyelin
TAE	Tris-acetate-EDTA
TBS	Tris-buffered saline
TBS/T	mixture of TBS and 0.05% Tween 20
TMEM16F	transmembrane protein 16F
TOP 1	DNA topoisomerase 1
YWHAZ	tyrosine 3-monooxygenase/tryptophan 5-monooxygenase activation protein

Abstract (German)

In der humanen Plazenta wird die äußerste Epithelschicht, die Abgrenzung zum mütterlichen Blut, aus dem vielkernigen Synzytiotrophoblasten gebildet. Der Synzytiotrophoblast entwickelt sich und wächst durch ständige Fusion mit den darunter liegenden einkernigen Zytotrophoblasten. Während des komplizierten Fusionsprozesses wird die reguläre Asymmetrie der Lipiddoppelschicht der Zellmembran vorübergehend aufgehoben. Phosphatidylserin, generell auf der zytoplasmatischen Seite gelegen, gelangt dabei auf die extrazelluläre Seite. Die Regulation dieser Membranarchitektur wird über verschiedene Phospholipidtransporter bewerkstelligt (sogenannte Flippasen, Floppasen und Scramblasen).

Microarray Experimente haben Phospholipid Scramblase 1 (PLSCR1) als den am stärksten exprimierten Transporter unter allen potentiellen Kandidaten identifiziert. Das Ziel dieser Studie war es, die räumliche und zeitliche Expression von PLSCR1 in der humanen Plazenta zu evaluieren, sowie eine mögliche Beteiligung an der Trophoblastfusion zu untersuchen.

In Plazenten des ersten und dritten Trimenons war PLSCR1 im Synzytiotrophoblasten, in Makrophagen und Endothelzellen sehr stark exprimiert. Im Gegensatz dazu zeigte der villöse Zytotrophoblast nur eine schwache immunhistochemische Färbung.

Für funktionelle Experimente wurde die Zelllinie BeWo als gängiges Trophoblast-Fusionsmodell, isolierte primäre Trophoblastzellen aus Plazenten des dritten Trimenons und villöse Explantatkulturen aus dem ersten Trimenon verwendet. Auf Protein- und mRNA-Ebene konnte in BeWo-Zellkulturen kein Unterschied in der Expression von PLSCR1 nach Forskolin induzierter Zellfusion beobachtet werden. In primären Trophoblastzellen, die mit Br-cAMP zur Fusion angeregt wurden, wurde eine verminderte PLSCR1-Expression auf Protein- und mRNA-Ebene festgestellt.

Um die Funktionalität des Transporters zu untersuchen, wurden RNA-Interferenz Experimente sowie ein Inhibitor für Scramblasen, R5421 (Aminoesterderivat) eingesetzt. Die Experimente mit small interfering RNA (siRNA, englisch für kleine eingreifende RNA) zeigten keinen Effekt auf die Fusionseffizenz nach erfolgreichem Knockdown von *PLSCR1*. Im Gegensatz dazu wurde nach Inhibition der PLSCR1-Aktivität mit R5421 ein Anstieg der *GCM-1* mRNA-Expression, der Sekretion der beta-Untereinheit des humanen Choriongonadotropin (beta-hCG) und der Zellfusionsrate

beobachtet. Wurde R5421 in primären Trophoblasten oder villösen Explantatkulturen angewendet, kam es jedoch zu keinem Einfluss auf die Fusionsrate.

PLSCR1 wurde in dieser Studie im villösen Kompartiment der Plazenta lokalisiert und dessen Expressionsrate analysiert. Diese Resultate deuten auf eine mögliche Beteiligung von PLSCR1 an einer negativen Regulation in der Trophoblastfusion hin.

Abstract (English)

The outermost layer of the human placenta facing maternal blood is called syncytiotrophoblast, a multinucleated epithelial layer. This syncytiotrophoblast develops and grows by fusion with underlying mononucleated cytotrophoblasts. During the complex process of villous trophoblast fusion the cell membrane's phospholipid asymmetry is abolished leading to phosphatidylserine exposure on the cell surface. Maintenance and transient abrogation of this membrane architecture is accomplished by different types of phospholipid transporters (flippases, floppases and scramblases).

Initial microarray studies revealed phospholipid scramblase 1 (PLSCR1) to have the highest expression among possible candidates. Therefore, the aims of this study were to analyze the spatio-temporal expression of PLSCR1 in the human placenta and to further elucidate its putative role in trophoblast syncytialization.

In first trimester and term placenta PLSCR1 was abundantly expressed in syncytiotrophoblast, macrophages and endothelial cells, while it was only slightly detected in cytotrophoblasts.

For functional studies, BeWo cells, the generally accepted trophoblast-fusion model, primary trophoblasts isolated from term placentas and first trimester placental explant cultures were used. In BeWo cells PLSCR1 mRNA and protein expression remained constant even after stimulation with forskolin to form multinucleated syncytia. However, when primary trophoblasts were stimulated with Br-cAMP, a decrease in PLSCR1 mRNA and protein expression was detected. Two approaches with RNA interference and a scramblase inhibitor, R5421 (ethaninidothioic acid) were used to define the functional role of PLSCR1 in trophoblast fusion. No changes in fusion efficiency were observed in *PLSCR1* siRNA down-regulated cells. On the contrary when PLSCR1 activity was inhibited with R5421 in BeWo cells increased *GCM-1* mRNA expression, beta-subunit of human chorionic gonadotropin (beta-hCG) protein secretion and cell fusion rates were observed. R5421 treatment in primary trophoblasts and villous explant cultures had no effect on trophoblast fusion.

In this study we focused on PLSCR1 localization and expression in the human placenta. The obtained results suggest a possible involvement of PLSCR1 in negatively regulating trophoblast fusion.

1 Introduction

Please note that parts of this chapter have been published in Berghold V.M. et al., *Histochemistry and Cell Biology*, 2014.

1.1 Human placenta

During pregnancy the human placenta connects the developing child to the uterine wall of the mother. This unique transient organ contains fetal cells and tissues derived from the blastocyst as well as maternal uterine cells and tissue. The placenta is responsible for exchange of maternal nutrients, gases, protective antibodies and in return waste products from fetal to maternal blood. Additionally, it produces a set of pregnancy regulating hormones, is a barrier for infections and protects the fetus from rejection through the maternal immune system (Benirschke, Burton & Baergen 2012a).

The development of the human placenta begins very early during pregnancy. After fertilization of the egg, symmetric cell division takes place and the blastocyst emerges which eventually implants into the maternal endometrium. Following asymmetric division two populations of cells originate within the blastocyst – an outer layer of trophoblast cells and an inner cell mass. The inner cell mass, referred to as embryoblast, evolves into embryo, umbilical cord, yolk sac and amnion. The outer trophoblast layer together with mesenchyme and blood vessels derived from the embryoblast form the chorion, the precursor of the fetal membranes including the placenta (Benirschke, Burton & Baergen 2012b).

When the blastocyst adheres and attaches to the uterine epithelium, trophoblast and uterine epithelial cells establish cell-cell contacts and trophoblast cells begin to proliferate and migrate into the endometrial epithelium. The trophoblast cells fuse with each other into a multinucleated mass, called the syncytiotrophoblast. This syncytiotrophoblast is one continuous, uninterrupted epithelial-like layer with no existing cell borders and no intercellular spaces. The inner layer of trophoblast cells of the blastocyst with no contact to maternal tissue remains mononucleated cells, referred as cytotrophoblasts (Benirschke, Burton & Baergen 2012b).

These first fusion events, which lead to the formation of the syncytiotrophoblast, are cell-cell fusion events. During embryonic development this only occurs during the peri-implantation period. Later on, only cyto-syncytial fusion takes place, where single

cytotrophoblast cells are incorporated into the existing syncytiotrophoblast (Potgens et al. 2002).

Trophoblasts differentiate either along the villous (fusion phenotype) or extravillous (proliferative/invasive phenotype) trophoblast pathway. Most of the trophoblasts are part of the villous developmental pathway and cover placental villi as a two-layered epithelium. The villous cytotrophoblasts continuously fuse with the overlying syncytiotrophoblast covering the floating chorionic villi to ensure maintenance and growth of the syncytiotrophoblast throughout pregnancy. The syncytiotrophoblast itself is a terminally differentiated tissue and is no longer able to proliferate (Benirschke, Burton & Baergen 2012b).

The remaining trophoblast cells, referred to as extravillous trophoblasts, are involved in the development of nonvillous parts of the placenta. These cells accomplish the attachment of the placenta to the uterus through anchoring chorionic villi. Extravillous trophoblasts migrate, form cell columns and are eventually found in the chorionic and basal plates, the chorion laeve, the decidua basalis and the maternal spiral arteries, where these cells induce the remodeling of the spiral uterine arteries to provide sufficient utero-placental perfusion (Benirschke, Burton & Baergen 2012c).

For a successful pregnancy it is essential to maintain the epithelial syncytiotrophoblastic cover on placental villi through sufficient fusion of cytotrophoblasts to balance normal sloughing via formation of syncytial knots of the syncytiotrophoblast layer. Dysfunction in the trophoblast fusion process may lead to different pregnancy disorders, e.g., preeclampsia; hemolysis, elevated liver enzymes and low platelets (HELLP)-syndrome; and intrauterine growth restriction (IUGR) (Lee et al. 2001, Langbein et al. 2008, Gauster et al. 2009).

1.2 Trophoblast Fusion

During the complex villous trophoblast differentiation and consequent fusion process several factors are involved including growth factors, hormones, cytokines, protein kinases, proteases, transcription factors, membrane proteins, and physiochemical factors (oxygen, calcium) (Gauster et al. 2009). Nuclei of the syncytiotrophoblast do not have the potential to replicate and there is hardly any transcriptional activity (Richart 1961, Huppertz et al. 1999). Consequently, the syncytiotrophoblast layer is completely dependent on fusing with mononucleated

cytotrophoblasts, which provides fresh cellular cytotrophoblast components such as nuclei, organelles, cytoplasm, membranes, proteins and RNA (Gauster et al. 2009). At the same time the syncytiotrophoblast sheds and deports aged and damaged components via so-called syncytial knots into the maternal blood (Askelund, Chamley 2011).

Whether the syncytiotrophoblast or cytotrophoblast cells initiate fusion is not clear. In favor of the syncytiotrophoblast degenerative changes as well as a syncytial signal preventing fusion until the diminution of this signal allows fusion have been proposed. If cytotrophoblasts alone would start the fusion process without feedback from the overlaying syncytiotrophoblast, it would either deplete or exceed the supply by cytotrophoblast components. Therefore, a cross talk between the two trophoblast layers is most likely before cytotrophoblasts differentiate and initiate the fusion process (Gauster, Huppertz 2010).

After the unknown stimulus in order to start villous trophoblast fusion, cytotrophoblasts divide in an asymmetric way. One cell remains in a progenitor state, while the other cell leaves the active cell cycle. This cell differentiates and accumulates high amounts of RNA, proteins and organelles and remodels its submembranous cytoskeleton. Additionally, cell adhesion proteins are degraded (Gauster, Huppertz 2010). During and prior to villous trophoblast fusion fusogenic proteins are up-regulated. One main representative is syncytin-1, an envelope protein of the endogenous defective retrovirus HERV-W (Mi et al. 2000). The placenta specific transcription factor, glial cells missing-1 (GCM-1) also initiates trophoblast differentiation and up-regulates *syncytin-1* gene expression in trophoblast cells (Yu et al. 2002).

Another essential aspect of syncytiotrophoblast fusion is the activation of the apoptosis-related machinery of caspases, specific proteases that degrade cytoskeletal and cell adhesion proteins (Fischer, Janicke & Schulze-Osthoff 2003). These caspases have been identified to play a role in terminal trophoblast differentiation by showing activated caspase 8 (Black et al. 2004, Gauster, Huppertz 2010, Gauster et al. 2010). Further, externalization of phosphatidylserine (PS) to the cell's surface occurs, another aspect of apoptosis (Huppertz et al. 1998).

Remodeling of the membrane architecture i.e. temporarily abolishing regular membrane asymmetry takes place to enable the two lipid bilayers of cells to fuse. The two membranes come into close contact, which results in local modifications of the lipid structures and results in merging of the two outer monolayers, forming a stalk and

consequently a fusion pore. This fusion pore expands until the complete membrane is able to merge (Monck, Fernandez 1996). In protein mediated membrane fusion it is suggested that proteins form gap-junction like structures, with hydrophilic channels that open at the beginning of fusion (Lindau, Almers 1995).

All these different factors and others not mentioned or yet unknown promote merging of the neighboring plasma membranes of the cytotrophoblast with the overlying syncytiotrophoblast during villous trophoblast fusion. Nevertheless, the mechanisms how adjacent membranes fuse are still poorly understood.

Syncytial fusion is only taking place in few tissues within the human body: syncytiotrophoblast, striated muscle fibres (Huppertz, Tews & Kaufmann 2001), foreign body giant cells, chondro- and osteoclasts (Vignery 2000) and sperm-egg fusion during fertilization. Similar to what has been described for trophoblast fusion, exposure of phosphatidylserine to the outer leaflet of the plasma membrane has also been indicated in the formation of myotubes in muscle cell differentiation (van den Eijnde et al. 2001) and sperm capacitation (Harrison, Gadella 2005).

1.3 Membrane Asymmetry

Physiologically, there is an asymmetric distribution of phospholipids across biological membranes (Bretscher 1972). The uncharged, choline-containing phospholipids, phosphatidylcholine (PC), sphingomyelin (SM) as well as glycosphingolipids are mainly located on the exofacial side of the plasma membrane (about 75% of PC and 80% of SM), additionally on luminal sides of internal organelles as the topological equivalent. On the other hand, the amine-containing, negatively charged phospholipids, phosphatidylethanolamine (PE), phosphatidylserine (PS), phosphatidic acid and phosphoinositides are predominantly positioned on the cytoplasmic side of the plasma membrane (almost 100% of PS and about 80% of PE) (Bretscher 1972, Bevers et al. 1994, Daleke 2003).

Responsible for this asymmetric transbilayer distribution of phospholipids and maintenance are flippases (also referred to as translocases) (Seigneuret, Devaux 1984) and floppases (Bitbol, Devaux 1988). Both classes of transporters require energy in terms of adenosine triphosphate (ATP) hydrolysis in order to translocate phospholipids against a concentration gradient. Flippases translocate PE and PS inwards from the outer to the inner leaflet of the plasma membrane (Seigneuret,

Devaux 1984). In return floppases export PE and PS outwards from the inner to the outer leaftlet (Bitbol, Devaux 1988).

In general flippases are integral membrane proteins, which belong to the type 4 subfamily (P4) of the P-type ATPase superfamily (Tanaka, Fujimura-Kamada & Yamamoto 2011). Members of the ATP-binding cassette transporter subfamily of ATP-dependent transporters were described to transport phospholipids outwards across the plasma membrane. However, there is evidence that these transporters not only function as floppases but also as flippases (Coleman, Quazi & Molday 2013).

In contrast to flippases and floppases, which accomplish maintenance of membrane asymmetry, the group of scramblases is responsible for its rapid and transient collapse. Scramblases catalyze unspecific transbilayer movement in both directions independent of energy along the concentration gradient, a phenomenon described as lipid scrambling (Sims, Wiedmer 2001, Daleke 2003).

Activation of scramblases occurs through an increase of intracellular calcium in conditions of cell activation, cell injury or apoptosis (Basse et al. 1996, Zhou et al. 1997). This results in PS exposure to the cell's surface that activates enzymes of the coagulation and complement cascade, as well as clearance of injured or apoptotic cells by the reticuloendothelial system (Sims, Wiedmer 2001). Four genes belonging to the phospholipid scramblase gene family (PLSCR1-4) have been described (Basse et al. 1996, Zhou et al. 1997, Wiedmer et al. 2000). Moreover, transmembrane protein 16F (TMEM16F) is involved in phospholipid scrambling across the plasma membrane during blood coagulation (Suzuki et al. 2010b, Yang et al. 2012a).

PLSCR1-4 mRNA expression was evaluated in different kinds of tissues. *PLSCR1* was detected in heart, lung, liver, kidney, pancreas, spleen, thymus, small intestine, colon, peripheral blood lymphocytes, prostate, testis, uterus and placenta, whereas it was not present in brain and skeletal muscle (Wiedmer et al. 2003). In the same study *PLSCR2* was solely detected in testis and consequently not analyzed in our samples. *PLSCR3* was found in all mentioned tissues except brain, liver and testis. *PLSCR4* was present in all tissues except peripheral blood lymphocytes and the only member detectable in brain tissues (Wiedmer et al. 2000).

1.4 Phospholipid Scramblase 1 (PLSCR1)

PLSCR1 is a multiply palmitoylated, calcium-binding, lipid-raft associated type II endofacial plasma membrane protein. The human PLSCR1 protein is composed of

318 amino acids and has a molecular mass of 35.1 kDa (Zhou et al. 1997). PLSCR1 has a long N-terminal cytoplasmic domain, an alpha-helix transmembrane region and a short extracellular tail (Zhou et al. 1997). The human PLSCR1 gene is located on chromosome 3q23 with a length of 29.7kb including 8 exons whereas the first exon is untranslated (Wiedmer et al. 2000).

PLSCR1 is normally detected in the plasma membrane and various internal membrane pools, often found in lipid rafts (Frasch et al. 2004, Sun et al. 2002, Wiedmer et al. 2003). As a posttranslational modification PLSCR1 is multiply palmitoylated, which is important for trafficking of PLSCR1 to the plasma membrane, where it functions as a membrane anchor and might also be involved in phospholipid translocation (Sahu et al. 2007). If PLSCR1 is not palmitoylated it localizes to the nucleus (Wiedmer et al. 2003).

PLSCR1 was originally described to catalyze rapid, bidirectional and unspecific distribution of phospholipids between the inner and outer leaflet of the plasma membrane in a calcium dependent manner resulting in collapse of the phospholipid asymmetry (Basse et al. 1996, Zhou et al. 1997). However, this scrambling activity remains controversial. In general, PLSCR1 is now considered a multifunctional molecule and may play a role in signaling pathways (Sahu et al. 2007).

When cells were exposed to a calcium ionophore and other inducers of injury or apoptosis an increase in phosphatidylserine exposure was observed (Zhao et al. 1998, Yu et al. 2003, Frasch et al. 2004). After UV-induced apoptosis cells overexpressing PLSCR1 demonstrated enhanced PS exposure and increased caspase-3 activation (Yu et al. 2003). Cells containing high amounts of PLSCR1 exposed to calcium ionophore A23187 responded with a rapid exposure of PS to the surface; however, in cells with lower amounts of PLSCR1 the effect was less prominent (Zhao, Zhou et al. 1998). In contrast, mice deficient in PLSCR1 presented normal PS exposure when blood cells obtained from the animals were stimulated (Zhou et al. 2002). Furthermore, Scott syndrome, a rare bleeding disorder where translocation of PS to the cell's surface is impaired, was initially assigned to PLSCR1 (Stout et al. 1997). Lately, TMEM16F has been identified to be involved in this disease (Suzuki et al. 2010b, Yang et al. 2012a).

Nevertheless, there has been new evidence for phospholipid reorganisation by PLSCR1. PS exposure induced by PLSCR1 is required for neuroendocrine compensatory endocytosis (Ory et al. 2013). Whether or not PLSCR1 is a true

scramblase needs to be further elucidated in the future. Nevertheless, there is evidence for its participation in rearranging phospholipids across membranes.

Among other functions PLSCR1 interacts as a signaling molecule with other cellular proteins such as immunoglobulin E type 1 receptor, c-Abl (acronym for abelson murine leukemia viral oncogene homolog 1) tyrosine kinase and epidermal growth factor receptor (Sahu et al. 2007).

The role of PLSCR1 in cancer is debated controversially. PLSCR1 has been described to be required for leukemic cell differentiation (Zhao et al. 2004). In colorectal cancer PLSCR1 may contribute to tumorigenesis and tumor progression. Due to elevated PLSCR1 plasma levels in patients it was proposed to serve as a prognostic biomarker (Kuo et al. 2011, Cui et al. 2012). On the other hand it has been shown that PLSCR1 has tumor suppressor functions against leukemia (Huang et al. 2006) and ovarian cancer (Silverman et al. 2002) by inducing growth arrest and apoptosis.

PLSCR1 is also an intracellular acute phase response protein, which is stimulated by tumor necrosis factor alpha and interleukin 1 beta in the liver (Lu et al. 2007). Moreover, the *PLSCR1* gene is activated by interferon alpha, beta and gamma (Der et al. 1998, Zhao et al. 2005), which trigger the principal viral defence mechanism of the innate immune system. PLSCR1 has been reported to play a role in this interferon-dependent antiviral response through antiviral activity, enhancement of antiviral gene expression and inhibition of virus replication (Zhao et al. 2005, Dong et al. 2004, Yang et al. 2012b).

PLSCR1 has been identified with an RNA interference mediated “gain of function” screen to contribute to inhibiting hepatitis C virus. Hepatitis C virus replication is highly dependent on intracellular membrane rearrangements. Scrambling of phospholipids is suggested as a possible mechanism by which PLSCR1 interferes with viral replication (Metz et al. 2012). In pregnant ewes PLSCR1 expression increased in endometrial stromal cells through interferon tau indicating a potential protection of the pregnant uterus against viral infection (Song et al. 2011).

Looking at pathologies related to pregnancy, Heikkilä et al. (2005) found an 11.0-fold up-regulation of PLSCR1 mRNA levels in two cases of early-onset preeclampsia (weeks 25+1 and 27+4) compared to age matched twin control placentas (Heikkila et al. 2005). *PLSCR1* mRNA expression was enhanced in isolated monocytes of patients with antiphospholipid syndrome (Amengual et al. 2013) and systemic lupus erythematosus (Suzuki et al. 2010a). In both conditions it is hypothesized that up-

regulation of PLSCR1 contributes to the prothrombotic tendency. In a small subgroup of patients with antiphospholipid syndrome and pregnancy morbidity, however, without thrombotic events, higher levels of *PLSCR1* mRNA expression were observed when compared to other patients (Amengual et al. 2013). This up-regulation may play an important role in this disease. Assessing the role of PLSCR1 in the human placenta and pregnancy complications, such as preeclampsia could be essential for a better understanding of pregnancy related pathologies.

2 Hypothesis

The present study tested the hypothesis that PLSCR1 plays an active role in human trophoblast differentiation and fusion by impairing regular membrane asymmetry. In addition to localization of PLSCR1 in the villous trophoblast compartment loss of function studies were performed to elucidate the effect of missing scramblase activity in trophoblast fusion. These investigations were carried out in three different model systems, trophoblast derived BeWo cells, isolated primary trophoblasts from term placentas and first trimester villous explant cultures.

3 Materials & Methods

This study was carried out at two institutions (Institute for Cell Biology, Histology & Embryology, Medical University of Graz, Austria and Department of Obstetrics and Gynecology, University of Alberta, Edmonton, Canada). Therefore, several methods have different approaches, which are referred to as *Method I* (performed in Graz) and *Method II* (performed in Edmonton) specified in materials and methods section and figure legends.

Please note that parts of this chapter have been published in Berghold V.M. et al., *Histochemistry and Cell Biology*, 2014.

3.1 Ethics statement

This study was approved by the ethical committees of the Medical University of Graz, Austria (Ethics approval reference number: 23-203 ex 10/11) and the University of Alberta, Canada (Ethics approval reference number: Pro00000925), where operational approval from Alberta Health Services in Edmonton, Alberta was granted. Written informed consent was obtained from each participant. Placental tissues were obtained from legal pregnancy terminations for psychosocial reasons (6 to 12 weeks of gestation), from pregnancies after normal term delivery or caesarean section (> 37 weeks of gestation), from pregnancies that developed preeclampsia at term or < 37 weeks of gestation as well as age-matched controls (< 37 weeks of gestation). Further, blood was drawn from healthy non-pregnant female and male volunteers for platelet aggregation assays.

3.2 RNA microarray analysis of primary trophoblasts and BeWo cells

Previously performed microarrays were screened for phospholipid membrane transporter data. The identified available transporters on the arrays were three phospholipid flippases (*ATP8B3, ATP8A1, ATP10A*, all belonging to the family of type 4 P-type ATPases) and four scramblases (*PLSCR1-4*). On the first array pooled primary trophoblast preparations were hybridized against Affymetrix HU133A chips. Ten preparations per cell type of first trimester and term placentas were used (Hiden et al. 2006). On the other array four independent passages of BeWo cells (n=4) were

analyzed with Applied Biosystems® Human Genome Survey Arrays (Gauster et al. 2010).

3.3 Analysis of the spatio-temporal PLSCR1 expression in placental tissues

3.3.1 Human first trimester and term placental tissue samples

First trimester and term human placenta samples were fixed in 4% formalin and subsequently embedded in paraffin (FFPE). Three categories in healthy human placenta sections were differentiated: mid first trimester samples from week 6 to 8 (group 1, n=21), late first trimester samples from week 9 to 12 (group 2, n=13) and samples from term placentas > 37 weeks (group 3, n=18). Further, placenta samples with a history of preeclampsia were examined in two categories: placentas with preeclampsia at term (group 4, n=4, compared to healthy controls from term placentas, group 3, n=18) and preeclampsia prior to 37 weeks (group 5, n=11, compared to age-matched controls, group 6, n=4).

3.3.2 Immunohistochemistry

FFPE tissues were cut in 5µm sections with a microtome (Microm HM440E). The sections were mounted on Superfrost® Plus slides (Menzel/Thermo Fisher Scientific, Braunschweig, Germany). Deparaffination was performed according to standard procedures, 5 min each xylol, xylol, xylol/ethanol, following 3 min each 100% ethanol, 96% ethanol, 96% ethanol, 70% ethanol, following repeated washing cycles in distilled water. Antigen retrieval was performed in the microwave oven by boiling slides in Dako Target Retrieval Solution pH 9.0 (Dako, Glostrup, Denmark) or 10 mM sodium citrate buffer pH 6.0. Each slide was cooked 3 times for 7 min in the microwave oven at 750 W. Tissues were immunostained either manually or with a Lab Vision Autostainer™ 360 (LabVison/Thermo Fisher Scientific, Fremont, CA, USA) using an UltraVision Large Volume Detection System HRP Polymer Kit (Lab Vision) according to the manufacturer's instructions. In brief, hydrogen peroxidase was used to block endogenous peroxidase for 10 min. Washing three times with Tris-buffered saline (TBS) containing 0.05% Tween 20 (TBS/T; Merck, Darmstadt, Germany) was followed by blocking for non-specific background staining with Ultra V Block for 5 min. Antibodies were diluted in Antibody Diluent (Dako) and incubated on slides for 30 min

to 1 h at room temperature (RT). Table 1 lists specifications of antibodies used and their respective dilutions. After washing, Primary Antibody Enhancer was added for 10 min, followed by washing with TBS/T. Slides were incubated with anti-rabbit HRP-labelled polymer for 15 min. The polymer complex was visualized by incubating the slides with AEC (3-amino-9-ethylcarbacole) Chromogen Single Solution (Lab Vision) for 10 min. Slides were rinsed with distilled water, then manually counterstained with hemalaun and mounted with Kaiser's glycerine gelatine (Merck).

3.3.3 Testing of antibodies against PLSCR1

Rabbit polyclonal anti-PLSCR1 antibody (cat. no: 11582-1-AP, Proteintech™, Eubio, Vienna, Austria) and rabbit polyclonal anti-scramblase 1 antibody (cat. no: ab96318, Abcam®, Cambridge, UK), two antibodies against PLSCR1, were tested on placental tissues (antibody dilutions ranging from 1:50 to 1:500). In order to obtain comparable staining patterns different concentrations of the two antibodies needed to be used. Further, an increase in the concentration above 10 µg/ml resulted in non-specific staining of every cell/tissue on the sections. The first anti-PLSCR1 antibody distributed by Proteintech™ showed specific staining at lower concentrations and was therefore chosen for the following PLSCR1 experiments, including staining pattern evaluation (Rabbit polyclonal anti-PLSCR1 antibody: 2.13 µg/ml working concentration; 1:250 dilution vs. rabbit polyclonal anti-scramblase 1 antibody: 5.2 µg/ml; 1:100).

3.3.4 Antibody pre-adsorption

Specificity of the anti-PLSCR1 antibody against PLSCR1 was assessed with the respective blocking peptide (antigen of human PLSCR1-gst fusion protein, cat. no: ag2172, Proteintech™, Eubio). In brief, anti-PLSCR1 antibody (2.135 µg/ml; 1:250; Proteintech™) was mixed in Antibody Diluent (Dako) with an excessive amount of blocking peptide (8 µg/ml; 1:100) corresponding to the PLSCR1 epitope. A mixture containing solely anti-PLSCR1 antibody served as control. The tubes were incubated while continually rotated for 1 h at RT. Immunohistochemistry was performed as described above.

3.3.5 Identification of macrophages

In order to verify if the PLSCR1-positive cells within the villous stroma are true macrophages, first trimester placenta tissue samples were co-stained using the rabbit polyclonal anti-PLSCR1 antibody (2.135 µg/ml; 1:250; Proteintech™) and a mouse anti-CD68 antibody (3.8 µg/ml; 1:100; clone KP1, Dako) diluted in Antibody Diluent (Dako). CD68 is a marker for cells of the monocyte/macrophage lineage. Staining was visualized by immunofluorescence using Alexa Fluor® 555 goat anti-mouse (H+L) and Alexa Fluor® 488 goat anti-rabbit IgG (H+L) (10 µg/ml; 1:200; Molecular Probes®, Life Technologies, Carlsbad, CA, USA) diluted in PBS.

3.3.6 Analysis of PLSCR1 staining intensity in placental tissues

PLSCR1 expression pattern in the human placenta was systematically evaluated by three independent observers. Each cell/tissue type of interest (syncytiotrophoblast, cytotrophoblasts, macrophages and endothelium) within one section was categorized. Therefore a staining scale from 0 to 3 (0 indicating no staining, 1 weak, 2 moderate and 3 strong staining) was used. The number of positive cells and the staining intensity of each cell/tissue type were taken into account. Each section was evaluated morphologically using an Axiophot microscope. Images were obtained with an AxioCam HRc digital camera (Zeiss, Oberkochen, Germany).

3.3.7 PLSCR1 in extravillous structures

FFPE first trimester decidua basalis sections were co-stained with anti-PLSCR1 (2.135 µg/ml; 1:250; Proteintech™) and mouse monoclonal antibody to HLA-G (0.5 µg/ml; 1:1,000; clone 4H84, BD Pharmingen™, BD Biosciences, Franklin Lakes, NJ, USA). HLA-G major histocompatibility antigen, class I, G or human leukocyte antigen G is expressed on the surface of trophoblast cells, almost exclusively on extravillous trophoblasts (McMaster et al. 1995).

3.4 BeWo cell cultures

BeWo cells, a human choriocarcinoma cell line that is fusion-competent, were purchased from the European Collection of Cell Cultures (ECACC, Salisbury, UK). As cultivating media DMEM/F-12 (Dulbecco's Modified Eagle Medium: Nutrient Mixture F-12; Gibco®, Life Technologies Cooperation) supplemented with 2% L-glutamine

(Gibco®), 1% penicillin/streptomycin (Gibco®), 1% amphotericin B (PAA Laboratories GmbH, GE Healthcare, Pasching, Austria), and 10% fetal calf serum (FCS; Gibco®) was used. The cells were grown at 37°C and 5% CO_2 in a conventional cell incubator. Media was changed every 48 h.

Cells were cultivated in 75 cm^2 flasks (Nunc, Thermo Fisher Scientific, Rochester, NY, USA) to approximately 80% confluence. For passaging, cells were washed with HBSS (Hank's Balanced Salt Solution; Gibco®) or PBS (Phosphate Buffered Saline; Gibco®), while Accutase™ (PAA) was used for cell detachment. Cell number was assessed with CASY® Technology Cell counter (Roche Applied Science, Mannheim, Germany).

For in vitro experiments 4 x 10^5 cells per well were grown in 4 ml medium on 6-well plates (Nunc), 1-2 x 10^5 cells per well in 2 ml medium on 12-well plates (Nunc) and 0.5-1 x 10^5 cells per well and chamber in 1 ml media on 24-well plates and 4-well plastic chamber slides (Permanox™ Plastic, Lab-Tek™, Nunc), respectively. Additionally, 5 x 10^4 BeWo cells were cultured on 12 mm fibronectin-coated coverslips (neuVitro, El Monte, CA, USA) in 1 ml media in 24-well plates. One day after seeding, BeWo cells were stimulated with forskolin (Sigma-Aldrich®, St. Louis, MO, USA) to differentiate and subsequently fuse into multinucleated syncytia. Forskolin was added at a final concentration of 20 µM for up to 48 h and was dissolved in DMSO (dimethylsulfoxide; Rotipuran®, Lactan, Graz, Austria).

3.5 Other cell line cultures

Other cell lines were used to evaluate PLSCR1 expression. The trophoblast-derived cell line JEG-3 as well as HUVEC, human umbilical vein endothelial cells, were purchased from ECACC. The second trophoblast-derived cell line JAR was obtained from the American Type Culture Collection (ATCC®, Washington, DC; USA). HEK-293, embryonic kidney cells and Hep G2 cells, derived from a hepatocellular carcinoma were a kind gift from Sasa Frank, Medical University of Graz. JEG-3, HUVEC, HEK-293 and Hep G2 cells were cultivated in DMEM (Gibco®) supplemented with 2% L-glutamine (Gibco®), 1% penicillin/streptomycin (Gibco®), 1% amphotericin B (PAA), and 10% FCS (Gibco®). JAR cells were cultivated in RPMI 1640 (Roswell Park Memorial Institute 1640 Medium, Gibco®) including the same supplements. Cells were grown on 12-well plates (Nunc) and 4-well plastic chamber slides (Nunc) and incubated at 37°C and 5% CO_2 in a conventional cell incubator with media renewal

every 48 h. As for BeWo cells Accutase™ (PAA) was used for cell detachment and cell number was assessed with CASY® Technology Cell counter (Roche Applied Science).

3.6 Isolation and culture of primary trophoblasts from term placentas

Villous trophoblasts were isolated from term placental tissues by trypsin/DNAse digestion and absorption onto immunoglobulin (Ig)-coated glass bead columns (Biotex, Edmonton, Alberta) as previously described (Yui et al. 1994, Kilani et al. 1997, Guilbert et al. 2002). Glass beats were coated with anti-CD9 (clone 50H.19, in-house preparation), anti-MHC class I (clone W6/32, Harlan Sera-Lab, Crawley Down, Sussex, UK) and anti-MHC class II (clone 7H3, in-house preparation) antibodies (Guilbert et al. 2002). Isolated trophoblasts were stored in liquid nitrogen (FCS with 10% DMSO). Cell purity was checked by vimentin staining revealing <0.01% mesenchymal cells in cell cultures. Primary trophoblasts were thawed and cell number was assessed with Bio-Rad TC10™ automated cell counter (Bio-Rad Laboratories, Hercules, CA, USA).

6.5 x 10^5 cells per well were seeded in 24-well plates (Nunc) and on fibronectin-coated coverslips (neuVitro, El Monte, CA, USA) in 24-well plates 4 h prior to treatment. Cells were grown in IMDM (Iscove's Modified Dulbecco's Medium; Gibco®) supplemented with 1% penicillin/streptomycin and 12% FCS in a conventional cell incubator at 37°C and 5% CO_2. To remove non-adherent cells before experiments cells were carefully washed twice with warm IMDM. Instead of forskolin, primary trophoblasts were stimulated to form multinucleated syncytia with the cell permeable cAMP analogue 8-bromoadenosine 3′,5′-cyclic monophosphate (Br-cAMP; Sigma-Aldrich®) at a final concentration of 100 µM. Br-cAMP was dissolved in H_2O and added to the cultures in IMDM. After 48 h media containing Br-cAMP was removed and regular media was added to the cells for another 24 h. Cells were harvested after a total of 72 h.

3.7 Human first trimester villous explant cultures

Villous explants were dissected from tissues of six first trimester placentas (week 7 to 9) with an approximate 5 mg moist mass each. The explants were

cultivated in DMEM/F-12 (Gibco®) supplemented with 2% L-glutamine (Gibco®), 1% penicillin/streptomycin (Gibco®), 1% amphotericin B (PAA) and 10% FCS (Gibco®) at 37°C, 5% CO_2 and 2.5% O_2 in an XVIVO incubation system Model G300C (BioSpherix, Lacona, NY, USA) for 48 h. The physiological oxygen tension of first trimester placenta around gestational week 8 is about 20 mm Hg (Jauniaux et al. 2000). To reflect similar culture conditions 2.5% O_2 was used for villous explant cultivation.

3.8 RNA interference

Small interfering RNA (siRNA) experiments were performed for functional studies in BeWo cells as well as HUVEC cells. HUVEC cells were initially used as a control for the siRNA transfection protocols, since these cells are easier to transfect than BeWo cells (data not shown). Similar functional studies with siRNA were attempted in primary trophoblast cultures but were unsuccessful given the difficulty transfecting these cells.

Four different transfection systems: HiPerFect® Transfection Reagent (Qiagen®, Hilden, Germany) siRNA Prime Kit (PAA), Nanofectin (PAA) and jetPEI® (Polyplus transfection™, Illkirch Cedex, France) were tested.

Four different siRNAs (GeneSolution siRNA, Qiagen®) directed against *PLSCR1* (Hs_*PLSCR1*_3 target sequence: ACGTAAGATTCAGGAAACGAA, Hs_*PLSCR1*_4 target sequence: CGGGTGTTGGCGCAAAGGTTA, Hs_*PLSCR1*_5 target sequence: CAGCGCCACAGCCTCCATTAA, Hs_*PLSCR1*_6 target sequence: CCAGTGTATAA-TCAGCCAGTA) were used. The effect of the different siRNAs on *PLSCR1* knockdown was evaluated with one single siRNA and mixtures of different siRNAs. Eventually, all four siRNAs were mixed in equal amounts for knockdown experiments, which resulted in best knockdown efficiency. A non-silencing (scrambled) siRNA (Ctrl_Control 1 target sequence: AATTCTCCGAACGTGTCACGT) served as a negative control. According to Qiagen the scrambled siRNA sequence has no homology to any known mammalian gene.

Two different protocols were available for siRNA transfection. Both were used and evaluated for experiments. The traditional protocol includes cell seeding on day 1 and is followed by formation of cell complexes and transfection on day 2. On the other hand, the fast-forward or reverse transfection protocol includes first complex formation

and subsequent transfection by adding the cell suspension on the preformed complexes.

Experiments were carried out trying to optimize cell seeding number, siRNA concentration, siRNA mixture vs. use of a single siRNA, transfection reagent concentration, traditional protocol vs. reverse transfection protocol, starving cells before transfection and duration of transfection with siRNA (3 h, 24 h vs. 48 h). Additionally, the effect of silencing with siRNA on cell viability was evaluated with an LDH release assay (as described in 3.10).

The three transfection reagents HiPerFect®, siRNA Prime Kit and jetPEI® turned out not to be useful in BeWo cells. Only the use of Nanofectin resulted in an adequate knockdown of *PLSCR1*.

After optimization the protocol with Nanofectin included the following: Cells were seeded in 12-well plates (1 x 10^5 cells / well) or chamber slides (5 x 10^4 cells / chamber) one day prior to transfection. One hour before transfection, cells were washed with HBSS or PBS and starved in DMEM/F12 lacking serum and supplements for 1 h. Transfection complexes were prepared by mixing 40 pmol (0.5 µg siRNA) for 12-well plates and 20 pmol (0.25 µg siRNA) for chamber slides of the respective siRNAs with Nanofectin reagent in the ratio 1:5 (µg of siRNA : µl of Nanofectin siRNA reagent) in 100 µl / 50 µl serum and supplement-free media. After incubation of Nanofectin and siRNA for 20 min, the transfection complexes were added drop-wise onto the cells, while gently swirling the plates and chamber slides. Cells with media containing siRNAs and Nanofectin complexes were incubated for 3 h after which the mixture was removed and replaced with regular media containing all supplements. 24 h after transfection, cells were stimulated with 20 µM forskolin / 0.2% DMSO for 48 h. Supernatants were collected and cells were harvested for downstream analysis after a total of 72 h treatment (48 h forskolin treatment).

3.9 Scramblase Inhibitor R5421 experiments

The scramblase inhibitor R5421, ethanimidothioic acid N-{[N-butylthio-N-methylamino]-carbonyloxy}-methyl ester (Endotherm GmBH, Saarbrücken, Germany; see Ref. (Dekkers et al. 1998) for formula) was used as a second approach to evaluate inhibition of PLSCR1 activity. R5421 was dissolved in DMSO at a stock concentration of 10 mM.

R5421 has been studied in human platelets and erythrocytes, where it inhibits the externalization of phosphatidylserine to the cell's outer membrane leaflet (Dekkers et al. 1998, Gonzalez et al. 2009, Smith et al. 2001). Appearance of phosphatidylserine on the outside of platelets forms a procoagulant surface initiating the blood coagulation cascade (Williamson et al. 1995). Therefore, before BeWo and primary trophoblast cells as well as villous explant experiments were performed, the effectiveness of R5421 to inhibit scramblase activity was assessed using a platelet aggregation assay. The assay was used to determine a valid concentration of R5421 which inhibits platelet aggregation and, thus, lipid scrambling.

3.9.1 Platelet Aggregation Assay

Venous blood from healthy donors was collected into plastic tubes containing 3.8% sodium citrate. Platelet rich plasma was obtained by centrifugation at 400 x g for 20 min at RT. Washed platelets were prepared by adding 100 µl 2% EDTA to 2 ml platelet rich plasma with centrifugation at 1000 x g for 15 min. This was followed by two washing steps with washing buffer (140 mM NaCl, 10 mM $NaHCO_3$, 2.5 mM KCl, 0.9 mM Na_2HPO_3, 2.1 mM MgCl2, 22 mM $C_6H_5Na_3O_7$, 0.055 mM Glucose, 0.053 mM BSA, pH 6.5). Thereafter, the pellet was resuspended in 2 ml Tyrode buffer (10 mM Hepes, 134 mM NaCl, 1 mM $CaCl_2$, 12 mM $NaHCO_3$, 2.9 mM KCl, 0.34 mM Na_2HPO_4, 1 mM $MgCl_2$, 0.055 mM glucose, Ph 7.4). Fibrinogen (250 µg/ml; Sigma-Aldrich®) was added just before stimulation of washed platelets with adenosine diphosphate (ADP). The best ADP concentration (1-2.5 µM) which induced near half-maximal aggregation was determined for each donor. This concentration was used for further experiments of the same donor. Washed platelets were pre-incubated with various concentrations of R5421 (0.1 µM, 1 µM, 2.5 µM, 5 µM, 10 µM, 25 µM) or vehicle control (0.4% DMSO) for 10 min. Washed platelets aggregation was induced with ADP and recorded at 37°C with constant stirring (1000 rpm) in an APACT 4004 aggregometer (Haemochrom Diagnostika, Essen, Germany). Data were obtained as percent of maximum light transmission, with non-stimulated washed platelets being 0% and Tyrode buffer being 100%.

3.9.2 BeWo cells and primary trophoblasts scramblase inhibitor R5421 experiments

The effect of R5421 on BeWo cell viability was tested with media containing increasing concentrations of R5421 (5 µM, 10 µM, 15 µM, 20 µM, 25 µM, 30 µM,

50 µM) or DMSO (0.5%) alone as a control for 48 h. Subsequently, LDH release was measured after 48 h (as described below) and normalized to total cell protein.

The concentration of R5421 that successfully inhibited platelet aggregation with minimal toxicity in BeWo cells was 25 µM and this was chosen for further experiments. Higher concentrations of R5421 were not tolerated by BeWo cells and resulted in increased cell death.

2×10^5 BeWo cells per well were seeded in 12-well plates and 5×10^4 cells on fibronectin-coated-coverslips in 24-well plates one day prior to experiments and incubated with media containing solvent control (DMSO, 0.45%), 20 µM forskolin alone, 25 µM R5421 alone or 25 µM R5421 and 20 µM forskolin for 48 h.

Primary trophoblasts were seeded at 6.5×10^5 cells per well in 24-well plates and on fibronectin-coated-coverslips in 24-well plates 4 h prior to treatment. Instead of forskolin, primary trophoblasts were treated with 100 µM Br-cAMP in order to fuse into multinucleated syncytia. Inhibitor experiments included incubation with IMDM media containing solvent control (DMSO, 0.25%), 100 µM Br-cAMP alone, 25 µM R5421 alone or 25 µM R5421 and 100 µM Br-cAMP. After 48 h media was changed and after a total of 72 h cells were harvested or fixed for downstream analysis.

Human first trimester villous explants were treated with R5421 at various concentrations (1 µM, 2 µM, 5 µM, 10 µM, 20 µM, 50 µM). 0.5% DMSO served as vehicle control. Explants were cultivated at 2.5% O_2 for 48 h.

3.10 Cell cytotoxicity

Conditioned media from BeWo cells and villous trophoblast explant cultures were assessed immediately after harvesting for cytotoxicity by LDH Cytotoxicity Detection Kit (Takara Bio Inc., Eubio) according to the manufacturer's instructions. In brief, after centrifugation at 6,000 x g for 10 min, supernatants were carefully obtained. Following 30 min incubation in the dark of 100 µl supernatant and 100 µl kit reaction mixture (2.5 µl catalyst (diaphorase/NAD+, lyophilisate) and 112.5 µl dye solution per reaction), LDH activity was determined at 492 nm absorbance with an Anthos 2010 Microplate Absorbance Reader (Anthos Labtech Instruments GmbH, Salzburg, Austria). Samples exceeding the detection limits of the assay were diluted and the dilution factor was taken into account for calculations. Measurements were normalized to total protein per well.

3.11 Human chorionic gonadotropin (hCG) release from cultured BeWo cells and primary trophoblasts

3.11.1 Method I

The remaining supernatants of BeWo cells and explants were used for hCG concentration analysis with a chemiluminescent immunoassay on ADIVA Centaur® XP Immunoassay System (Siemens Healthcare Diagnostics, Vienna, Austria) used in routine laboratory diagnostics. According to the manufacturer's manual stable amounts of two antibodies against hCG were used. The lite-reagent contained a polyclonal goat anti-hCG-antibody (approx. 0.1 µg/ml), which was labelled with an acridinium ester and the solid-phase contained a monoclonal mouse anti-hCG antibody (approx. 0.02 mg/ml) covalently bound to paramagnetic particles. These two antibodies bind specifically to different epitopes of the free beta-subunit as well as to the beta-subunit of the intact hCG. The system automatically dispensed 50 µl of sample together with 100 µl of lite-reagent and 450 µl solid phase. This was incubated for 7.5 min at 37°C. Afterwards the samples were separated and cleaned with deionised water and 300 µl of an acidic reagent and 300 µl of an alkaline reagent were dispensed in order to start the chemiluminescence reaction. Measurements, presented in mIU/ml, were normalized to total cell protein per well.

3.11.2 Method II

Conditioned media from BeWo cells and primary trophoblast cultures were collected and centrifuged at 6,000 x g for 10 min. The supernatants were collected and stored at -20°C for subsequent beta-hCG analysis by an enzyme linked immune sorbent assay (ELISA), using an ELISA 1911 kit (DRG diagnostics, Marburg, Germany). In brief, 25 µl of standard solutions and samples were added to microtiter wells. Each standard solution and sample was analyzed in duplicates. 100 µl of the enzyme conjugate (anti beta-hCG antibody conjugated to horseradish peroxidase) was added to each well and incubated at RT for 1 h. Wells were washed 5 times with 400 µl distilled water. 100 µl of substrate solution (tetramethylbenzidine) was added to each well and incubated for 15 min at RT. To stop the reaction 50 µl stop solution (0.5 M H_2SO_4) was added to each well. Absorbance was measured at 450 nm with an EL 808 absorbance microplate reader (Bio-Tek Instruments Inc., Winooski, VT, United States). When beta-hCG concentrations were above the linear dynamic range of the

standard curve, the samples were diluted and the dilution factor was taken into account for calculation. Measurements were normalized to total RNA per well.

3.12 Phospholipid Profile of BeWo cells

Membrane lipid profile of PS, PC and PE was analyzed by mass spectrometry in BeWo cells after 48 h incubation in presence or absence of 20 µM forskolin at the Core Facility Mass Spectrometry – Lipidomics (ZMF – Center for Medical Research) at the Medical University of Graz. All cellular membranes including plasma membrane and membranes of organelles were analyzed with this method.

3.13 Immunofluorescence and assessment of syncytialization in BeWo cells and primary trophoblasts

BeWo cells and primary trophoblasts cultured in 24-well plates on fibronectin-coated coverslips were fixed for 10 min in ice-cold methanol at -20°C prior to immunofluorescence staining. Cells were rehydrated in PBS and blocking was performed for 1 h in 10% normal goat serum (NGS). Anti-PLSCR1 antibody (5.33 µg/ml; 1:100, Proteintech™) and mouse monoclonal anti-desmosomal protein (1:200, Clone ZK-31, Sigma-Aldrich®) were diluted in 1% NGS and incubated overnight. On the following day after careful washing, coverslips were incubated for 30 min with Alexa Fluor® 594 goat anti-rabbit IgG (H+L) and Alexa Fluor® 488 goat anti-mouse IgG (H+L) (10 µg/ml; 1:200; Molecular Probes®) diluted in 1% NGS. Nuclei were visualized with 20 µM DAPI (4',6-diamidino-2-phenylindole; Molecular Probes®) diluted in PBS for 10 min. Coverslips were carefully removed from culture wells and mounted with Vectashield® Mounting Media (Vector Laboratories, Burlingame, CA, USA) on Superfrost® Plus slides.

Double immunofluorescence microscopy was performed on a confocal laser scanning microscope Leica SP2 (Leica Lasertechnik GmbH, Heidelberg, Germany). Excitation wavelengths for detection of UV, green, and red fluorescing compounds were 405, 488 and 543 nm, respectively. Fluorescence emission was recorded at 430–450 nm (UV), 500–535 nm (green) and 555–620 nm (red).

To assess stained cells three pictures were obtained for each coverslip of the different independent experiments with a Leica DM6000B (Leica Microsystems, Wetzlar, Germany) fluorescent microscope connected to an Olympus DP72 digital

camera (Olympus, Tokyo, Japan). The non-commercial free ImageJ software was used for counting of nuclei. Counting frames were applied to cover approximately 70% of every image. The total number of nuclei was marked and automatically counted by the software as well as the number of nuclei within multinucleated syncytia. Cell fusion rates were determined by comparing the number of nuclei in syncytia to the total number of nuclei. A true syncytium was defined if there was a minimum of three nuclei within an intact membrane. Syncytia of two nuclei were not taken into account, since it is not possible to distinguish between cells undergoing fusion or mitosis at this stage.

3.14 Staining of BeWo cells and first trimester villous explant cultures

BeWo cells for siRNA experiments and forskolin treatment were additionally cultured on chamber slides and consequently stained by immunocytochemistry. Treated BeWo cultures were washed in PBS, air dried and fixed in acetone for 10 min prior to manual immunocytochemical staining. The protocol described for automated immunohistochemical staining was used with the following exceptions: cells in chamber slides were rehydrated in TBS alone which was also used for the washing steps and primary antibodies were incubated for 1 h.

Primary antibodies used for immunocytochemical staining were anti-PLSCR1 (2.135 µg/ml; 1:250; Proteintech™), anti-beta-hCG (1:10; clone H-298-12, mouse monoclonal antibody, BioLogo, Kronshagen, Germany) and anti-E-cadherin (1:200; clone 24E10, rabbit monoclonal antibody, Cell Signaling Technology®, Boston, MA, USA). All antibodies were diluted in Antibody Diluent (Dako).

Double immunofluorescence staining was also performed with the antibodies against PLSCR1 and beta-hCG, with rehydration of cells in chamber slides and washing steps in PBS instead of TBS. As secondary antibodies a mixture of Alexa Fluor® 555 goat anti rabbit IgG (H+L) and Alexa Fluor® 488 goat anti mouse IgG (H+L) (10µg/ml; 1:200; Molecular Probes®) diluted in PBS was used. Nuclei were stained with DAPI (1:2,000; Molecular Probes®) diluted in PBS. Finally, slides were dried and mounted with ProLong® Gold Antifade Reagent (Molecular Probes®).

Immunohistochemical staining of FFPE samples of first trimester villous explant cultures treated with R5421 was performed as described earlier. Primary antibodies included Ki67 (1.1 µg/ml; 1:75; clone MIB-1, monoclonal mouse antibody, Dako), anti-cytokeratin-7 (1:2,000; clone OV-TL 12/30, monoclonal mouse antibody, NeoMarkers,

Eubio) and anti-cleaved caspase-8 (1:100; Asp391, clone 18C8, monoclonal rabbit antibody, Cell Signaling Technology®). IgG1 (1 µg/ml; 1:100; clone DAK-GO1, mouse monoclonal antibody, Dako) served as negative control. All antibodies were diluted in Antibody Diluent (Dako). Ki67 is expressed during all active phases of the cell cycle but absent in resting cells, thus served as a cell proliferation marker. Cytokeratin-7 was used as an epithelial marker, identifying trophoblast in placenta sections. Cleaved caspase-8 is involved in apoptosis and in trophoblast fusion (Black et al. 2004, Gauster et al. 2010, Gauster, Huppertz 2010).

Table 1: *Primary antibodies used in immunohistochemistry, immunocytochemistry and immunofluorescence*

Antigen (Clone/Cat. No)	Company	Working Dilution	Working Conc.	Host/ Isotype	Antigen Retrieval Buffer (FFPE samples)
PLSCR1 (cat.no: 11582-1-AP)	Proteintech™, Eubio (Vienna, Austria)	1:100 1:250	5.33 µg/ml 2.13 µg/ml	Rabbit IgG pc	Dako target retrieval solution pH 9.0
Scramblase 1 (cat.no: ab96318)	Abcam®, (Cambridge, UK)	1:100	5.2 µg/ml	Rabbit IgG pc	Dako target retrieval solution pH 9.0
CD 68(clone KP1)	Dako (Glostrup, Denmark)	1:100	3.8 µg/ml	Mouse IgG1 mc	Dako target retrieval solution pH 9.0
HLA-G (clone 4H84)	BD Pharmingen™ (BD Biosiences, Franklin Lakes, NJ, USA)	1:1,000	0.5 µg/ml	Mouse IgG1 mc	Dako target retrieval solution pH 9.0
Ki67 antigen (clone MIB-1)	Dako (Glostrup, Denmark)	1:75	1,1 µg/ml	Mouse IgG1 mc	10 mM sodium citrate buffer pH 6.0
Cytokeratin-7 (clone OV-TL 12/30)	NeoMarkers, Eubio (Vienna, Austria)	1:2,000	#	Mouse IgG1 mc	10 mM sodium citrate buffer pH 6.0
cleaved Caspase-8 (Asp391) (clone 18C8)	Cell Signaling Technology® (Boston, MA, USA)	1:100	#	Rabbit IgGmc	10 mM sodium citrate buffer pH 6.0
IgG1 (clone DAK-GO1,)	Dako (Glostrup, Denmark)	1:100	1 µg/ml	Mouse IgG1 mc	10 mM sodium citrate buffer pH 6.0
desmosomal protein (clone ZK-31)	Sigma-Aldrich® (St. Louis, MO, USA)	1:200	0.23 µg/ml	Mouse IgG1 mc	cell culture*
beta-hCG (clone H-298-12)	BioLogo, (Kronshagen, Germany)	1:10	#	Mouse IgG1 mc	cell culture*
E-Cadherin (clone 24E10)	Cell Signaling Technology®, (Boston, MA, USA)	1:200	#	Rabbit IgG mc	cell culture*
Cytomegalovirus (clone 8B1.2)	Millipore Corporation, (Billerica, MA, USA)	1:800	1.25 µg/ml	Mouse IgG2a mc	cell culture*

mc, monoclonal; pc, polyclonal; FFPE: formalin fixed paraffin embedded
* not applicable for acetone/methanol fixed cells
# not indicated by the distributor on the datasheet

3.15 Western Blot

3.15.1 Method I

BeWo cells, grown on 12-well plates (1-2 x 10^5 cells per well), were washed and lysed in 150 µl per well RIPA buffer (Sigma-Aldrich®) containing Protease Inhibitor Cocktail 25x (Roche Diagnostics, Indianapolis, IA, USA).

First trimester villous explants were transferred into the same protein lysis buffer and mixed with homogenizer (Ultra-Turrax® T10 basic; IKA®, Staufen, Germany) for approximately 30 s.

Protein concentration was assessed according to the Lowry protocol prior to gel electrophoresis. The same amount of total protein of each sample (ranging from 30 to 60 µg) was used for immunoblots. Samples were heated up to 90°C for 10 min containing 4x NuPage® LDS sample buffer (Novex®, Invitrogen™, Life Technologies Cooperation) and 10x NuPage® sample reducing agent (Novex®). Then samples were applied to precast 10% NuPage® Bis-Tris Mini Gels (Novex®). Proteins were separated at 120 V for 90 min in NuPage® MOPS SDS running buffer (Novex®).

Semidry blotting of proteins onto a 0.45 µm nitrocellulose membrane (Amersham Hybond ECL, GE Healthcare) was performed at 0.35 A for 30 min. Blotting efficiency was evaluated by Ponceau S solution (Sigma-Aldrich®) staining of the membranes for 1 min. Immunodetection was carried out with a chemiluminescent immunodetection kit (Western Breeze™, Novex®) according to the manufacturer's instructions. The membrane was blocked for 30 min with a specific blocking solution provided by the kit. A mixture of antibodies (primary antibody & normalization control antibody) was diluted in blocking solution and incubated overnight at 4°C on a shaker. As primary antibodies either anti-PLSCR1 (0.762 µg/ml; 1:700; Proteintech™) or anti-E-cadherin (1:1,000; clone 24E10, rabbit monoclonal antibody, Cell Signaling Technology®) were used. Anti-beta-actin antibody (0.155 µg/ml; 1:20,000; clone AC-15, mouse monoclonal antibody, Abcam®) served as protein normalization control. Anti-mouse and anti-rabbit secondary antibody solution was applied for 30 min. The membrane was incubated with chemiluminescence substrate for 5 min. Images were acquired with FluorChem Q System (Alpha Innotech, Cell Biosciences, Santa Clara, CA, USA) and band densities were analyzed with Alpha Innotech view software 2.0.1.1. Results are presented as a ratio of relative PLSCR1/E-cadherin and beta-actin band densities, with respective controls set to hundred percent. Experiments were performed in triplicates.

3.15.2 Method II

Primary trophoblasts and BeWo cells were grown on 24-well plates (6.5 x 10^5 primary trophoblasts and 0.5-1 x 10^5 BeWo cells per well). After experiments the cells were washed and lysed in 50 µl per well protein lysis buffer containing 10 mM Tris-HCl pH 7.4, 15 mM NaCl, 1% Triton X100, 5 mM EDTA, Protease Inhibitor 1:100 and 1 mM dithiothreitol (DTT). Protein concentration was assessed using the Protein Assay BCA™ (Pierce, Thermo Scientific) prior to gel electrophoresis. 60 µg of total protein from each sample were applied to each lane. Gels were prepared as follows: 10% SDS gel including 1.5 M Tris pH 8.8, 10% SDS, 30% acrylamide, 10% APS and 10 µl TEMED and stacking gel including 0.5 M Tris pH 6.8, 10% SDS, 30% acrylamide, 10% APS and 5 µl TEMED. First, proteins were separated at 130 V for 15 min until the protein front reached the running gel and then run at 180 V for another 45 min in 10x Tris/glycine/SDS buffer.

Wet transfer of proteins onto a 0.45 µm nitrocellulose membrane (Amersham Hybond ECL) was done at 0.15 A for 90 min. The membrane was blocked with 25% Odyssey blocking buffer (Li-COR, Lincoln, Nebraska, USA) in PBS containing 0.5% Triton-X100 (PBS/T) for 1 h followed by incubation with the anti-PLSCR1 antibody (0.762 µg/ml; 1:700; Proteintech™) diluted in blocking buffer overnight at 4°C and visualized with Alexa Fluor® 680 goat anti-rabbit IgG (H+L) (10 µg/ml; 1:200; Molecular Probes®). Membranes were washed with PBS/T for 1 h, subsequently reincubated with anti-alpha-tubulin (0.02 µg/ml; 1:10.000; cat. no: ab15246, rabbit polyclonal antibody, Abcam®) overnight at 4°C and again visualized with Alexa Fluor® 680 goat anti-rabbit IgG (H+L) (10 µg/ml; 1:200; Molecular Probes®).

Semi-quantitative analysis was performed on an LI-COR® Aerium automated infrared imaging system (LI-COR®, Lincoln, NB, USA). Results are presented as a ratio of relative PLSCR1 and alpha-tubulin band densities, with respective controls set to hundred percent. Experiments were performed from cells pooled from a minimum of two wells.

3.16 Quantitative real-time PCR (qRT-PCR)

3.16.1 RNA Isolation (TRIzol® method)

BeWo cells were washed in HBSS or PBS and directly lysed in cell culture dishes with TRIzol® Reagent (Ambion®, Life Technologies Cooperation). Total RNA was

isolated according to the user manual. In brief, for BeWo cells grown on 6-well plates 1 ml of TRIzol® was used per well. For phase separation 100 µl of 1-Bromo-3-Chloropane was added per tube. Tubes were inverted 22 times and incubated at RT for 15 min, following centrifugation at 12,000 x g and 4°C for 15 min. The colorless aqueous phase, containing RNA was carefully transferred into a new tube. 500 µl of isopropanol was added to each sample, inverted and incubated at RT for 10 min following again centrifugation at 12,000 x g and 4°C for 10 min. The supernatant was discarded and the remaining pellet washed with ice-cold ethanol (70%), centrifuged at 12,000 x g and 4°C for 10 min and dried for 45 min. Isolated RNA was dissolved in 50 µl H_2O on a shaker at 55°C. RNA was mixed with 6X loading dye (Peqlab, Biotechnologie GMBH, Erlangen, Germany) and RNA quality was assessed with 1.5% denaturing agarose gels (Biozym, Vienna, Austria) containing GelRed™ (Biotium, Hayward, CA, USA) in Tris-acetate-EDTA (TAE) buffer separated at 75 V for 1 h. RNA quantity and purity was determined using a NanoDrop™ 1000 Spectrophotometer (Thermo Scientific). RNA was stored at -80°C.

3.16.2 RNA isolation (RNeasy® Mini Kit)

BeWo and primary trophoblasts grown in 24-well plates were washed and directly lysed in cell culture dishes with RLT buffer (Qiagen® proprietary buffer containing 40 µl of 1 M DTT per 1 ml RLT). Total RNA was isolated using silica-membrane RNeasy® spin columns of the RNeasy® Mini Kit (Qiagen®) according to the user manual. In brief, 350 µl RLT buffer was added per well and cell lysates were transferred into a tube and mixed using a vortex mixer. The lysate was directly pipetted onto a QIAshredder spin column and centrifuged for 2 min at full speed. 350 µl of 70% ethanol were added and mixed by pipetting. Then samples were transferred to an RNeasy spin column and centrifuged for 15 s at ≥ 8.000 x g. The flow-through was discarded following additions of different buffers (provided by the RNeasy® Mini Kit) and centrifugation steps. Finally, 50 µl RNase free water was pipetted directly onto the spin column membrane and tubes were again centrifuged for 1 min at ≥ 8.000 x g to elute RNA.

RNA quality was assessed with ethidium bromide staining of 1.5% denaturing agarose gels (Biozym) and RNA quantity and purity was determined using a NanoDrop™ 1000 Spectrophotometer (Thermo Scientific). RNA was stored at -80°C.

3.16.3 cDNA transcription

After the quality check, RNA was reverse transcribed with the High-Capacity cDNA Reverse Transcription Kit (Applied Biosystems®, Life Technologies Cooperation). In brief, kit components (2 µl 10X RT buffer, 0.8 µl 25X dNTP (desoxyribonucleoside triphosphate) mix, 2 µl 10X RT random primers and 1 µl MultiScribe™ Reverse Transcriptase) and 500 ng of total RNA of each sample were mixed to a total reaction volume of 20 µl. Samples were incubated at 25°C for 10 min, 37°C for 120 min and 85°C for 10 s on GeneAmp® PCR System 9700 (Applied Biosystems®). cDNA was stored at -20°C.

3.16.4 Quantitative real-time PCR

PerfeCTa® SYBR® Green FastMix® for iQ™ (Quanta Biosciences, Gaithersburg, MD, USA) and QuantiTect Primer Assays (Qiagen®) were used for quantitative real-time polymerase chain reaction (qRT-PCR). Primer Assays for genes of interests were *PLSCR1* (Hs_PLSCR1_1_SG QuantiTect Primer Assay), *PLSCR3* (Hs_PLSCR3_2_SG QuantiTect primer assay), *PLSCR4* (Hs_PLSCR4_1_SG QuantiTect primer assay), *TMEMF16* (also referred as anoctamin 6; Hs_ANO6_1_SG QuantiTect primer assay), *GCM-1* (Hs_GCM1_1_SG QuantiTect primer assay), *beta-hCG* (Hs_CGB_1_SG QuantiTect Primer Assay), t*yrosine 3-monooxygenase/tryptophan 5-monooxygenase activation protein* (Hs_YWHAZ_2_SG QuantiTect primer assay), *DNA topoisomerase* 1 (Hs_TOP1_1_SG QuantiTect primer assay) and *ribosomal protein P0* (Hs_RPLP0_1_SG QuantiTect Primer Assay). *YWHAZ*, *TOP1* and *RPLP0* were used as endogenous reference genes. *YWHAZ* and *TOP1* were chosen as appropriate endogenous references where stable transcription has been described in the placenta (Drewlo, Levytska & Kingdom 2012).

8 µl cDNA (diluted 1:8, corresponding to 25 ng RNA), 2 µl 10x QuantiTect Primer Assay and 10 µl 2x SYBR® Green mastermix were used per well. Expression levels were analyzed in duplicates in a volume of 10 µl per well in a 96-well plate (Roche Diagnostics) with Bio-Rad MyiQ Thermal Cycler (Bio-Rad Laboratories). PCR started with an initial 10 min denaturation step at 95°C and was succeeded by 40 cycles of two-step cycling at 95°C for 10 s and 60°C for 30 s. Cycle threshold (Ct) values were calculated by the Bio-Rad MyiQ Thermal Cycler software. Samples of siRNA and R5421 experiments were normalized to the expression of *YWHAZ* and *TOP1*. *Beta-hCG* and *PLSCR1-4* expression in different cell lines was normalized to *RPLP0.*

3.17 Single cell analysis

In order to evaluate the involvement of PLSCR1 in membrane rearrangement of BeWo cell fusion more precisely, a single cell analysis approach was performed.

BeWo cells were grown on PEN (polyethylene naphthalate) membrane glas slides (Applied Biosystems®) and stimulated with forskolin for syncytialization. After 48 h of incubation BeWo cells were stained with an anti-beta-hCG antibody (1:10; clone H-298-12, mouse monoclonal antibody, BioPrime®) using an adapted fast immunocytochemistry staining protocol of less than 1 h duration to maintain RNA integrity. Using a laser capture microdissection device (P.A.L.M., Carl Zeiss Microscopy) beta-hCG positive syncytia and non-stained control cells were selected and marked with a line, then cut with a pulsed laser beam and catapulted into the cap of a 200 µl tube containing 30 µl RLT buffer. Consequently RNA was isolated with RNeasy® Micro Kit (Qiagen®). An on-column DNase digestion was performed while RNA isolation to ensure elimination of genomic DNA contamination. One-step reverse transcription PCR (RT-PCR) on a GeneAmp® PCR System 9700 (Applied Biosystems®) was performed. Reagents included 6 µl 5X buffer, 1.2 µl dNTP mix, 1.2 µl reverse transcriptase, 10 µl isolated RNA, 6.6 µl H2O and 4x 1.2 µl primers of beta-hCG (1:10; fwd: AGGTCACTTCACCGTGGTCT and rev: GCACAGATGG-TGGTGTTGAC, bp394) and RPLP0 (1:10; fwd: AACAACCCAGCTCTGGAGAA and rev: TGATGCAACAGTTGGGTA, bp236) per reaction. Samples were incubated at 50°C for 30 min, 95°C for 15 min, following 35 cycles of 94°C for 30 s, 60°C for 30 s and 72°C for 1 min, with a final step of 72°C for 5 min. One-step RT-PCR products were mixed with 6X loading dye (Peqlab) and separated on 1.5% denaturing agarose gels (Biozym) containing GelRed™ (Biotium) in TAE buffer at 75 V for 1 h.

Additionally, RNA quality was analyzed via RNA integrity number (RIN) with 2100 BioAnalyzer (Agilent Technologies, Santa Clara, CA, USA) at the ZMF (Center for Medical Research).

In order to maintain RNA integrity different strategies were attempted. First, DEPC-(diethylpyrocarbonate) water to inactivate RNase enzymes was used for all water-soluble solutions made from scratch. Additionally ProtectRNA™ RNase Inhibitor (Sigma-Aldrich®) was added to all solutions reagents for immunocytochemical staining. RNAlater® (Ambion®), an RNA stabilization solution that protects and preserves RNA in tissues and cells was applied to membranes for 1 h prior to immunocytochemical staining.

3.18 Cytomegalovirus infection of isolated human primary trophoblasts

Human cytomegalovirus (HCMV), a *Herpes viridae* family member, ubiquitously present is a common cause of congenital infection that may lead to permanent sequelae (Kenneson, Cannon 2007). HCMV infection of the placenta precedes the infection of the fetus, however, does not necessarily cause HCMV infection in the offspring (Fisher et al. 2000). Two mechanisms of transmission to the fetus have been proposed. Through direct contact with maternal blood HCMV passages the syncytiotrophoblast to the underlying cytotrophoblasts where viral replication is possible and supported. The second route suggests infection via the uterine wall, where extravillous trophoblasts are infected and the infection spreads retrograde through the cell columns to the anchoring villi (Fisher et al. 2000).

In order to study a possible involvement of PLSCR1 in infection with HCMV human primary trophoblasts isolated from term placentas were used. The cells were infected with HCMV at various multiplicities of infection (MOI). MOI represents the ratio of virus to the total number of cultured cells to be infected. Primary trophoblasts were seeded 4 h prior to treatment as described above and infected with 1 MOI and 10 MOI for a total of 6 h. Appropriate amounts of HCMV of a clinical isolate (generously provided by Denise G. Hemmings, University of Alberta) was added to IMDM media containing 1% FCS. After 6 h cells were either lysed for consequent Western Blot analysis or fixed in methanol for consequent immunofluorescence staining against a mouse anti-cytomegalovirus monoclonal antibody (1.25 µg/ml; 1:800; clone 8B1.2; Millipore Corporation, Billerica, MA, USA) and anti-PLSCR1 antibody (5.33 µg/ml; 1:100, Proteintech™) as described above.

3.19 Statistical analysis

Spatio-temporal PLSCR1 expression of immunohistochemistry staining in placental tissues was evaluated on a staining scale ranging from 0-3 (0 indicating no staining, 3 strong staining) by three independent observers. To determine statistical significances Kruskal-Wallis test and Mann-Whitney U test were used.

Differences among groups in cell culture experiments, protein expression as well as hCG measurements of supernatants and fusion rates through nuclei counts were assessed with repeated measures of variance (ANOVA). For post-hoc analysis the Duncan test was applied.

Gene expression profiles of qRT-PCR analysis and statistical evaluation of the obtained data was performed with the non-commercial free *Relative Expression Software Tool – REST-2009* (http://www.gene-quantification.de/rest.html) (Pfaffl, Horgan & Dempfle 2002).

Data are either presented as mean ± SD or mean ± SEM, as appropriate. A p-value of less than 0.05 was considered statistically significant.

4 Results

Please note that parts of this chapter have been published in Berghold V.M. et al., *Histochemistry and Cell Biology*, 2014.

4.1 Microarray analysis of phospholipid scramblases and flippases in the human placenta

Human primary trophoblast and BeWo cells were previously analysed by microarray (Gauster, Huppertz 2010, Hiden et al. 2006). Isolated primary trophoblast cells were pooled from first trimester placenta preparations (n=10) and term placenta preparations (n=10), while BeWo cell cultures of four independent experiments (n=4) were used. Available data was screened for known phospholipid transporters located within the plasma membrane. The arrays detected three flippases (*ATP8B3, ATP8A1, ATP10A*, all belonging to the family of type 4 P-type ATPases) and all four scramblases (*PLSCR1-4*), while floppases were not included on the arrays.

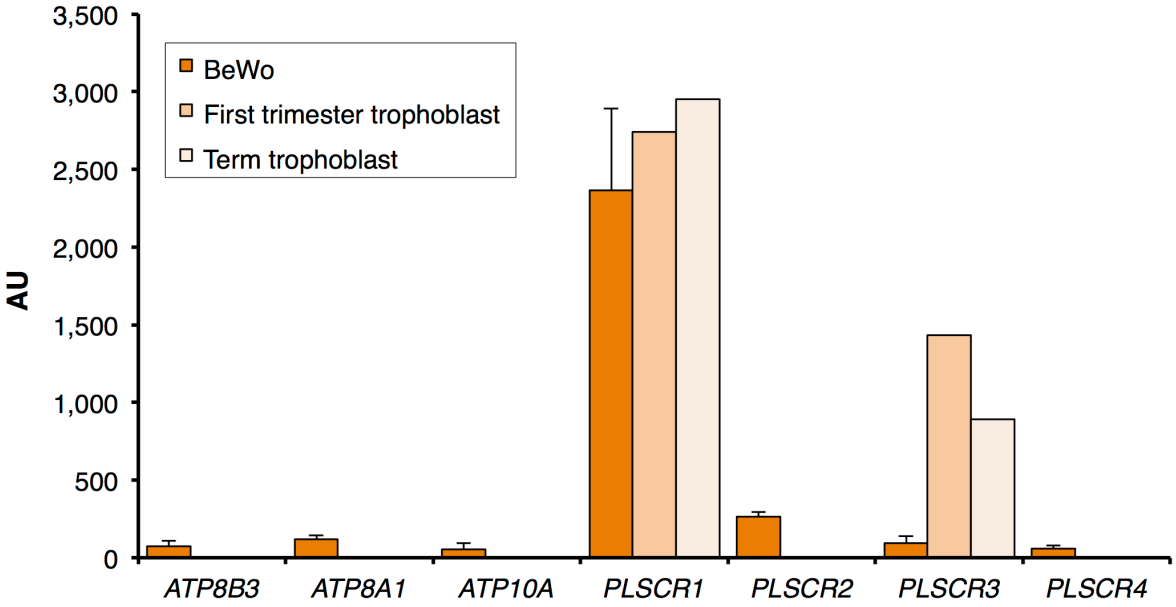

Figure 1: *Expression of phospholipid flippases and scramblases in human placenta.*

Microarray expression analyis of three phospholipid flippases (*ATP8B3, ATP8A1, ATP10A*) and four scramblases (*PLSCR1-4*) in isolated primary trophoblast cells pooled from first trimester placentas (n=10), term placentas (n=10) and BeWo cell cultures (n=4). AU = arbitrary units based on chemiluminescence intensity. This data has been published in Berghold V.M. et al., *Histochemistry and Cell Biology*, 2014.

PLSCR1 was identified to show the strongest expression among all candidates in primary trophoblast and BeWo cells (Fig. 1). *PLSCR1* was highly present in BeWo cells (2364 arbitrary units, a.u.), first trimester trophoblasts (2739 a.u.) and term trophoblasts (2954 a.u.). The second strongest expressed transporter was *PLSCR3* in first trimester trophoblasts (1434 a.u.), in term trophoblasts (889 a.u.), however, it only showed marginal expression in BeWo cells (91 a.u.). All other analysed transporters showed weak expression in BeWo cells, whereas were not expressed in primary trophoblasts (Fig.1).

4.2 Immunohistochemistry of PLSCR1 in the human placenta

Before starting systematic analysis of the spatio-temporal expression of PLSCR1 in human placental specimens, two anti-PLSCR1 antibodies were evaluated on placental tissues. The two PLSCR1 antibodies (one from Proteintech™, one from Abcam®) revealed similar staining patterns (Fig. 2A, B). However, the antibody distributed by Proteintech™ required lower concentrations to achieve a specific staining pattern and was chosen for further experiments (Fig. 2A).

Specificity of the PLSCR1 antibody from Proteintech™ was investigated by pre-absorption of the antibody with the respective blocking peptide. Placental sections stained for PLSCR1 without addition of the blocking peptide showed the specific staining pattern on placental sections. Pre-incubation with the blocking peptide completely abrogated staining of adjacent serial sections (Fig. 2C, D).

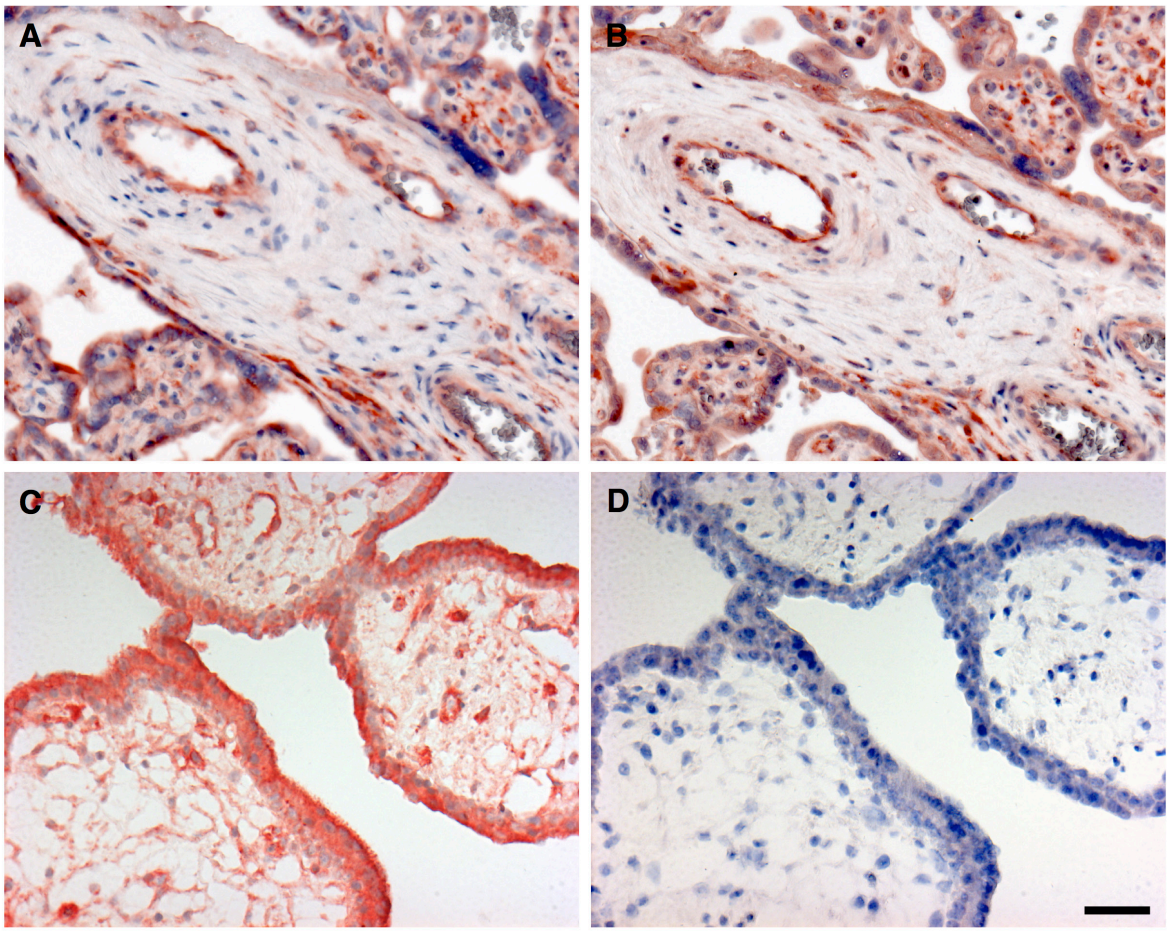

Figure 2: *Evaluation of anti-PLSCR1 antibodies.*

Immunohistochemical staining of sections of term placental tissues with (**A**) rabbit polyclonal anti-PLSCR1 antibody (1:500; Proteintech™) and (**B**) polyclonal anti-scramblase 1 antibody (1:100; Abcam®). (**C**) Incubation with anti-PLSCR1 antibody (Proteintech™) alone compared to (**D**) pre-adsorption of the antibody with blocking peptide. (**A-D**) Nuclear counterstaining: hemalaun. Scale bar represents 50 µm. This data has been published in Berghold V.M. et al., *Histochemistry and Cell Biology*, 2014.

4.3 Spatio-temporal expression of PLSCR1 in the human placenta

After anti-PLSCR1 antibody evaluation, spatio-temporal expression of PLSCR1 was analysed. PLSCR1 was abundantly expressed in syncytiotrophoblast, macrophages (Hofbauer cells) and endothelium with a distinct staining pattern found in first trimester and term placental sections (Fig. 3A, B). In contrast, PLSCR1 was hardly present in mononucleated cytotrophoblasts. In first trimester sections a continuous layer of cytotrophoblasts can be identified. This layer seems to thin out in term sections, although still intact, and only single cytotrophoblast nuclei are detectable (Fig. 3A, B).

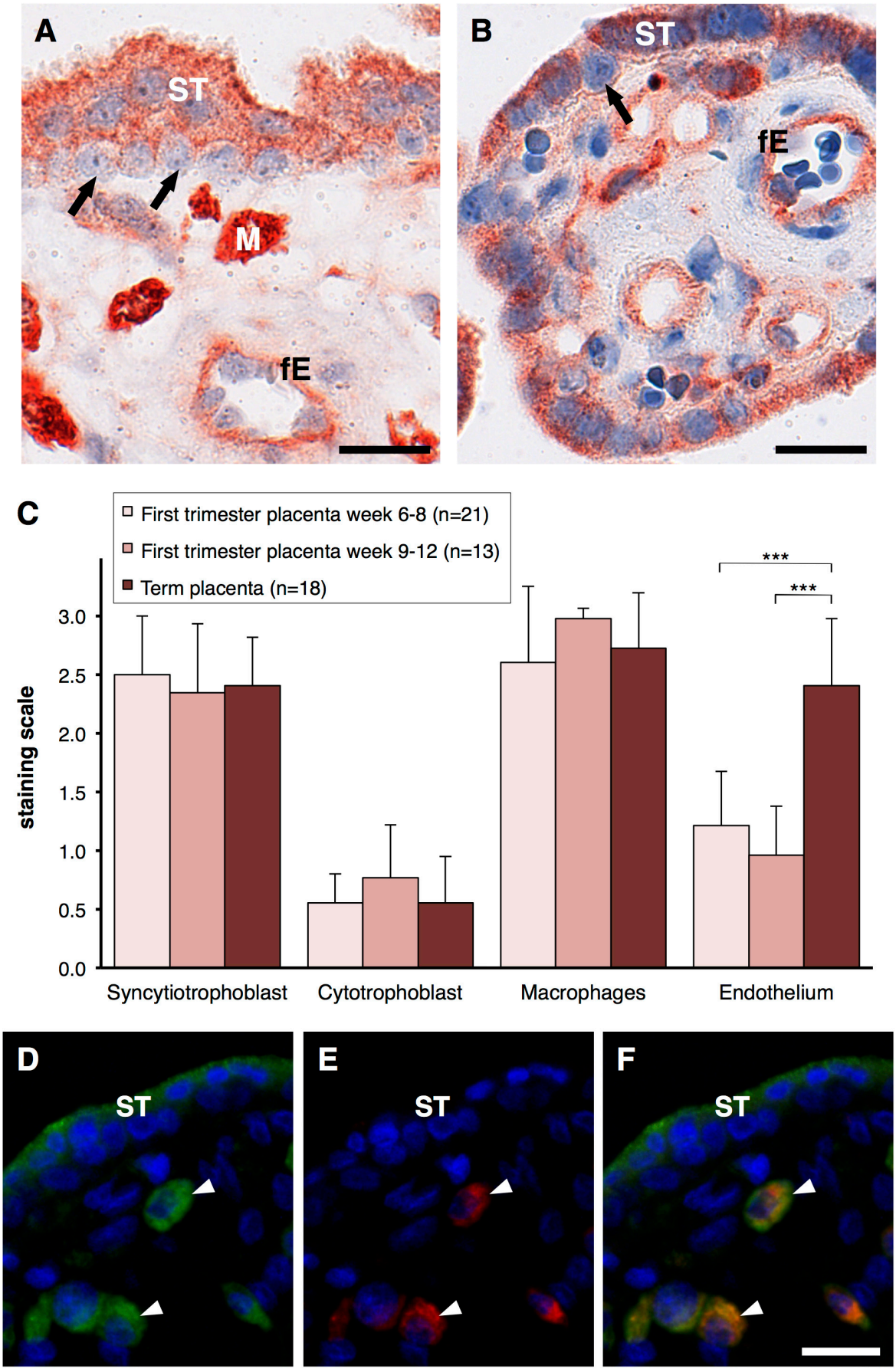

Figure 3: *PLSCR1 expression in first trimester and term placenta.*

(A, B) Representative PLSCR1 staining in sections from **(A)** first trimester (week 8+0) and **(B)** term placenta. Syncytiotrophoblast (ST), cytotrophoblasts (arrows), macrophages (M), fetal endothelium (fE). Nuclear counterstaining: hemalaun. Scale bar represents 20 µm. **(C)** Immunolocalization of PLSCR1 in three groups of placental tissues (mid first trimester week 6-8, n=21; late first trimester week 9-12, n=13; and term placentas >37 weeks, n=18). Classification by three independent observers. Staining scale: 3: strong, 2: moderate, 1: weak, 0: no staining. Results are presented as mean ± SD, ***p<0.001. **(D-F)** Immunofluorescence staining in first trimester placenta. **(D)** PLSCR1 (green), **(E)** CD68 (red), a specific marker for macrophages and **(F)** merge of D and E. Macrophages are pointed out with an arrowhead. Syncytiotrophoblast (ST). Nuclei were stained with DAPI. Scale bar represents 20 µm. This data has been published in Berghold V.M. et al., *Histochemistry and Cell Biology*, 2014.

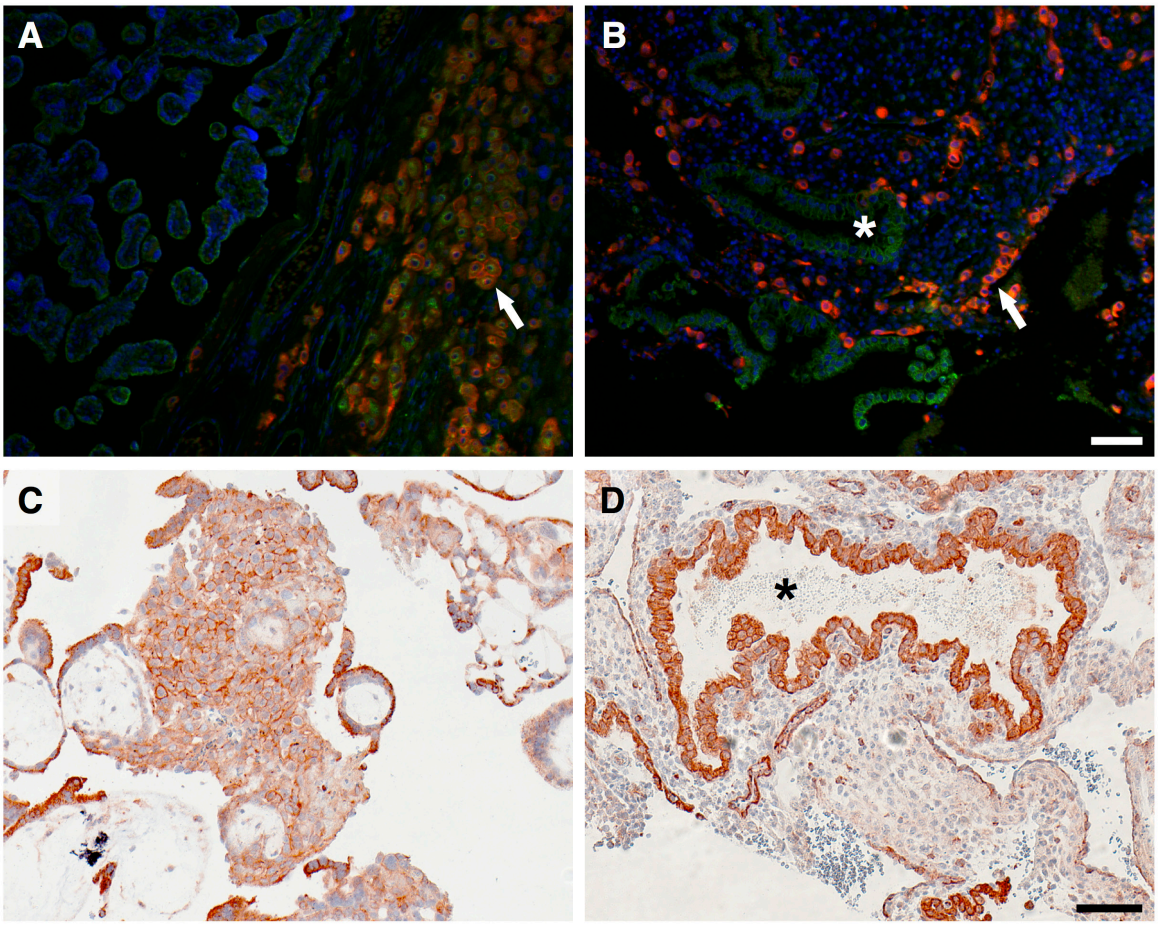

Figure 4: *PLSCR1 expression in first trimester extravillous trophoblasts and decidual glands.*

(A, B) Immunofluorescene staining for PLSCR1 (green) and HLA-G (red), a specific marker for extravillous trophoblasts. **(A)** Extravillous trophoblasts of term placental basal plate. **(B)** Decidual glands of first trimester placenta. Nuclei were stained with DAPI. **(C, D)** Immunohistochemical staining with anti-PLSCR1 antibody in first trimester placenta (week 9+0). PLSCR1 is expressed in **(C)** trophoblastic cell columns and **(D)** decidual glands. Nuclei are counterstained with hemalaun. Extravillous trophoblasts are pointed out with arrows, lumen of a decidual gland is indicated with an asterisk (*). Scale bar represents 100 µM.

In order to confirm that PLSCR1 positive cells within the placental stroma are true macrophages, sections were co-stained with antibodies directed against PLSCR1 (green) and CD68 (red), labelling macrophages (Fig. 3D-F). Further, sections of first trimester decidua basalis were stained for PLSCR1 (green) and HLA-G (red), a specific marker for extravillous trophoblasts (Fig. 4). Immunofluorescence and immunohistochemical staining confirmed the presence of PLSCR1 in extravillous trophoblasts (Fig. 4A), cell columns (Fig. 4C) and decidual glands (Fig. 4 B, D).

The PLSCR1 expression pattern was assessed with a staining scale from 0 to 3 (0 indicating no staining, 3 strong staining) by three independent observers, including three gestational age groups: mid first trimester (week 6 to 8, group 1, n=21), late first trimester (week 9 to 12, group 2, n=13) and term placentas (> 37 weeks, group 3, n=18). Additionally, groups of placentas with preeclampsia at term (n=4) and < 37 weeks of gestation (n=11), were compared to age matched control groups (control group term, n=18 and control group < 37 weeks of gestation, n=4) (Fig. 5). Here, the staining pattern as described above for control placentas was also found in placenta sections from specimens with preeclampsia (Fig. 5).

PLSCR1 protein was abundantly expressed in syncytiotrophoblast (group 1: 2.50 ± 0.50 (mean ± SD); group 2: 2.35 ± 0.59; group 3: 2.41 ± 0.41) and macrophages (group 1: 2.60 ± 0.65; group 2: 2.97 ± 0.09; group 3: 2.72 ± 0.47). In contrast, PLSCR1 was hardly present in mononucleated cytotrophoblasts (group 1: 0.56 ± 0.24; group 2: 0.77 ± 0.45; group 3: 0.56 ± 0.40). Endothelial PLSCR1 expression increased significantly between first trimester and term placenta, group 1: 1.21 ± 0.46; group 2: 0.96 ± 0.41; group 3: 2.4 ± 0.57; $p<0.001$; Fig. 3C).

In preeclampsia PLSCR1 protein was also expressed in syncytiotrophoblast (preeclampsia term 2.42 ± 0.29 vs. controls term 2.41 ± 0.50 and preeclampsia < 37 weeks of gestation 1.91 ± 0.60 vs. controls < 37 weeks 2.42 ± 0.59) and macrophages (preeclampsia term 2.63 ± 0.48 vs. controls term 2.72 ± 0.65 and preeclampsia < 37 weeks of gestation 2.52 ± 0.74 vs. controls < 37 weeks 2.75 ± 0.32). There was only weak expression of PLSCR1 in cytotrophoblasts (preeclampsia term 0.33 ± 0.27 vs. controls term 0.56 ± 0.24 and preeclampsia < 37 weeks of gestation 0.38 ± 0.28 vs. controls < 37 weeks 0.25 ± 0.10). In endothelial cells PLSCR1 expression was lower in preeclampsia compared to the respective control (preeclampsia term 1.83 ± 0.49 vs. controls term 2.41 ± 0.46 and preeclampsia < 37 weeks of gestation 1.62 ± 0.50 vs. controls < 37 weeks 1.83 ± 0.41; Fig. 5C).

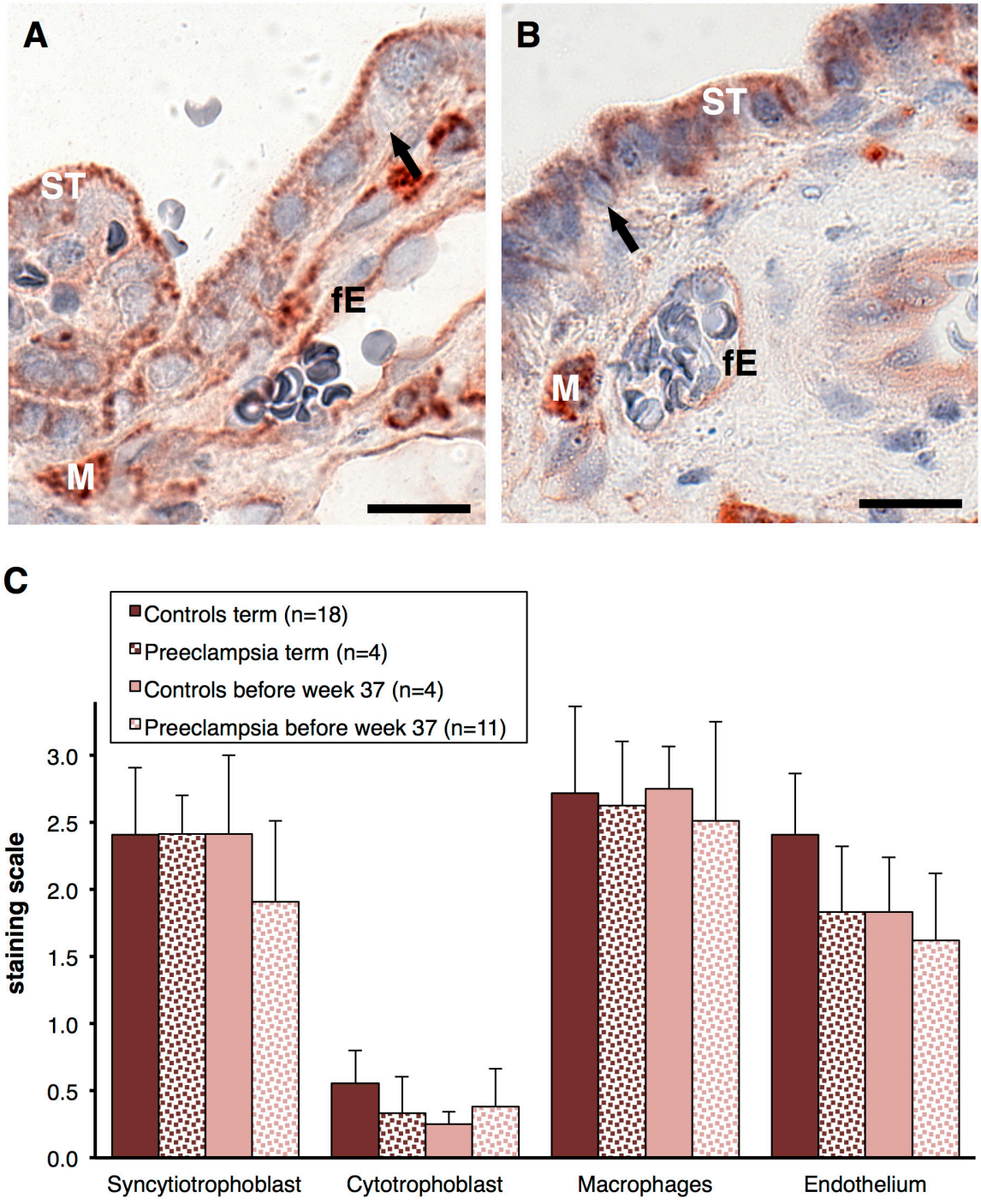

Figure 5: *PLSCR1 expression in placenta with preeclampsia.*

(A, B) Representative PLSCR1 staining in sections from **(A)** control and **(B)** preeclampsia, both week 31 of gestation. Syncytiotrophoblast (ST), cytotrophoblasts (arrows), macrophages (M), fetal endothelium (fE). Nuclear counterstaining: hemalaun. Scale bar represents 20 µm. **(C)** Immunolocalization of PLSCR1 in four groups of placental tissues (placenta controls at term, n=18; preeclampsia at term, n=4; controls < 37 week of gestation, n=4; preeclamspia < 37 week of gestation, n=11).Classification by three independent observers. Staining scale: 3: strong, 2: moderate, 1: weak, 0: no staining. Results are presented as mean ± SD.

4.4 BeWo cells as a useful model for villous trophoblast fusion

BeWo cells are a useful model to study villous trophoblast fusion. BeWo cells can be stimulated with forskolin (and other agents) to fuse and form multinucleated syncytia. Previously, the best fusion capacity with little to no effects on cell viability has been evaluated in our lab. Cells were treated with increasing concentrations of forskolin ranging from 0 to 100 µM (data not shown). 20 µM showed to be the best concentration to induce cellular fusion without any increased cell death. BeWo cells change their morphology after treatment with forskolin. Untreated BeWo show a more or less confluent monolayer of cobblestone-shaped cells. After treatment with forskolin the cells and nuclei increase in size, and their nuclei become clustered (Fig. 6).

Additionally, successful fusion and syncytialization in BeWo cells can be assessed using markers such as E-cadherin and desmosomal protein. These cell adhesion molecules disappear within a syncytium due to the loss of cell membranes, while mononucleated cells remain their cell boarders (Fig. 7A). Further, BeWo cells change their expression pattern and start producing beta-hCG predominantly in multinucleated syncytia (Fig. 7B, 8B, C). *Beta-hCG* mRNA expression analysis was performed in a time course experiment with forskolin treatment. Over the course of 6, 12, 24 and 48 h *beta-hCG* expression increased continuously normalized to the respective vehicle control (Fig. 8A).

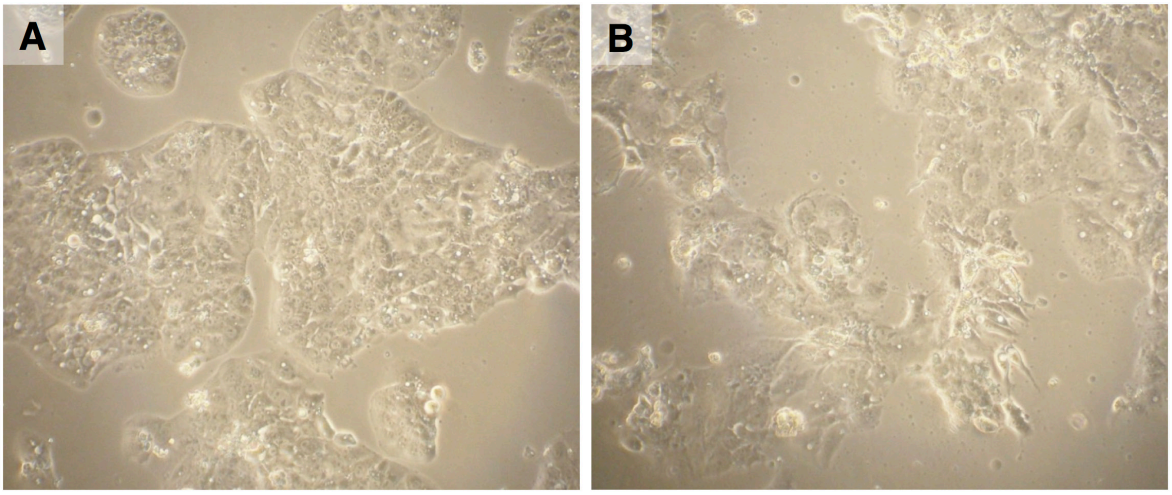

Figure 6: *BeWo cells stimmulated with forskolin/DMSO.*
BeWo cells were stimulated with **(A)** 0.2% DMSO control and **(B)** 20 µM forskolin for 48 h.

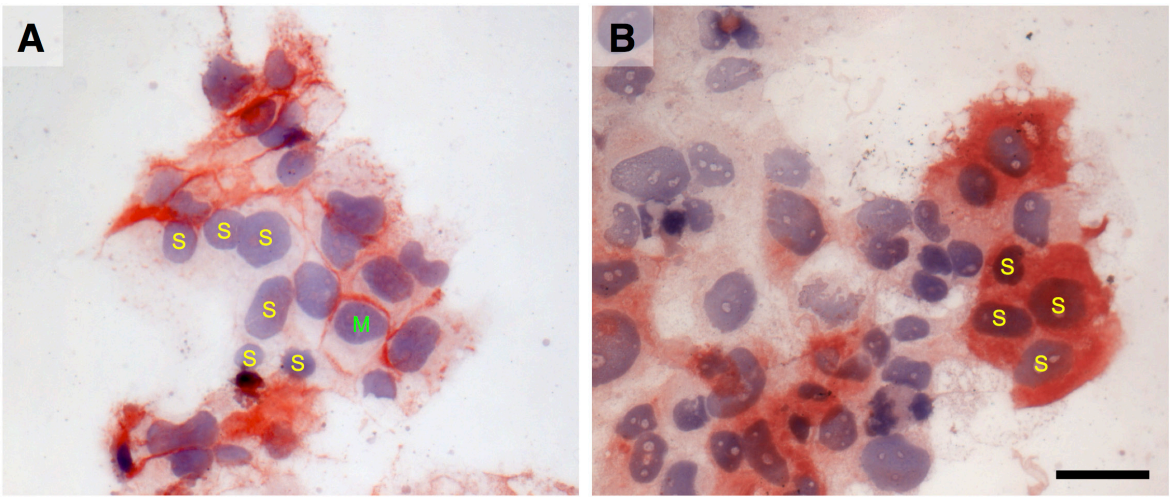

Figure 7: *BeWo cells are able to fuse and form multinucleated syncytia.*

(A) E-cadherin and **(B)** beta-hCG immunohistochemical staining of BeWo cells stimmulated with forskolin for 48 h. Mulitnucleated syncytia (S), mononucleated cells (M). Nuclear counterstaining: hemalaun. Scale bar represents 50 µM.

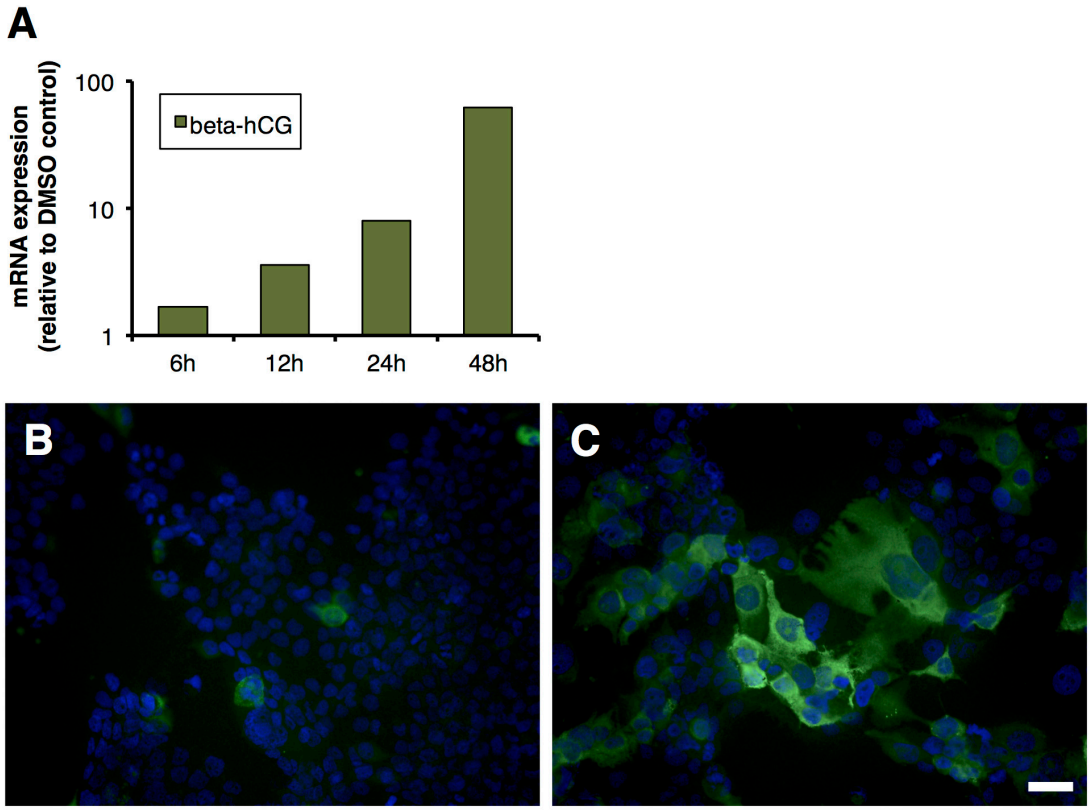

Figure 8: *Beta-hCG expression in BeWo cells after stimulation with forskolin.*

(A) qRT-PCR expression after time-course experiments in BeWo cells stimmulated with 20 µM forskolin after 6, 12, 24 and 48 h. Values represent fold changes relative to 0.2% DMSO control. Results are presented from one representative experiment. **(B,C)** Immuno-fluorescence staining of beta-hCG (green). **(B)** DMSO control and **(C)** forskolin treated cells after 48 h. Nuclei were stained with DAPI. Scale bar represents 50 µm.

4.5 PLSCR1 expression during BeWo cell differentiation

BeWo cells were treated with 20 µM forskolin and the respective 0.2% DMSO control for 48 h. *PLSCR1* mRNA expression remained constant (Fig. 9A). Semi-quantitative band densitometry of immunoblots revealed no change in PLSCR1 protein levels in treated versus untreated cells (93.1% ± 6.8% band intensity, Fig. 9B, C). PLSCR1 expression was also evaluated with immunohistochemical and further immunofluorescence double staining of PLSCR1 (red) and beta-hCG (green). A slight increase in PLSCR1 expression in forskolin treated cells could be detected (Fig. 10, 11). Nevertheless, this observation was not confirmed on mRNA and protein level. Additionally, immunofluorescence double staining indicated that PLSCR1 and beta-hCG do not completely co-localize in beta-hCG positive multinucleated syncytia (Fig. 11C, D).

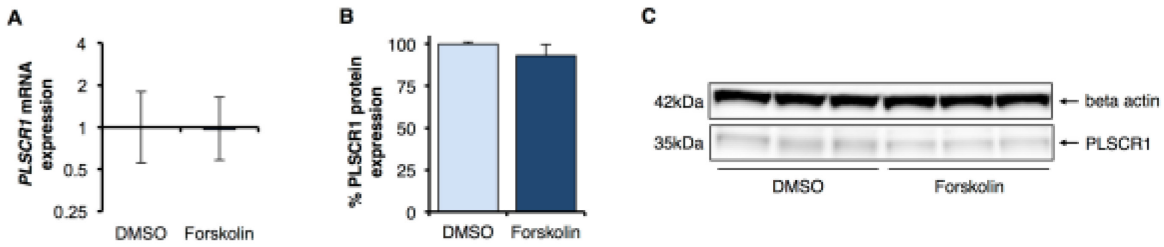

Figure 9: *PLSCR1 expression in BeWo cells.*

Analysis of PLSCR1 mRNA and protein expression in DMSO (0.2%) and forskolin (20 µM) treated BeWo cells after 48 h. **(A)** qRT-PCR results are presented as mean ± SEM from three different experiments performed in duplicates. **(B)** Semi-quantitative band densitometry of PLSCR1 protein expression related to beta-actin in DMSO or forskolin-treated BeWo cells. Band densities were normalized to DMSO control, which was set to 100%. Data are presented as mean ± SEM from five different experiments performed in triplicates. **(C)** Representative immunoblot of PLSCR1 protein expression (*Method I*). Parts of this data has been published in Berghold V.M. et al., *Histochemistry and Cell Biology*, 2014.

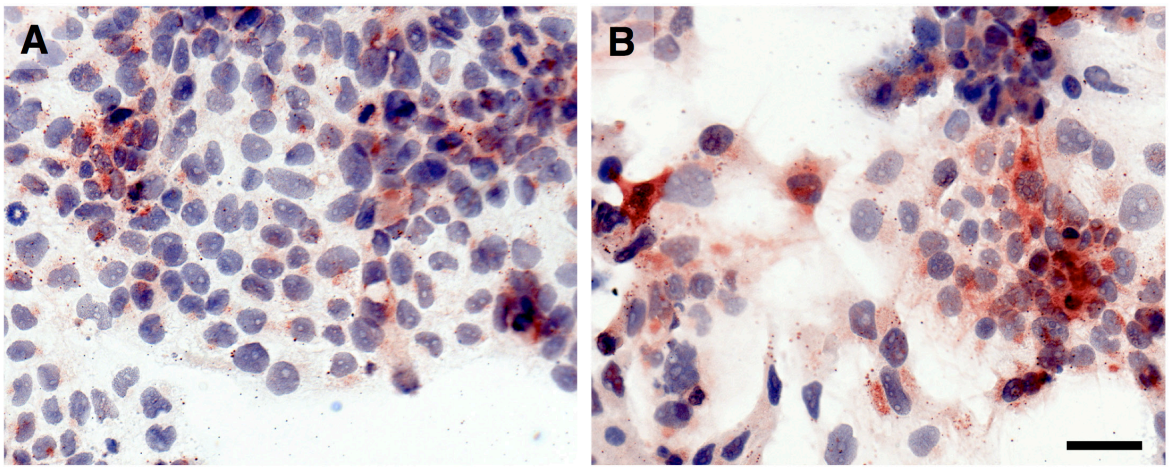

Figure 10: *Immunhistochemistry for PLSCR1 in BeWo cells.*

(A) DMSO control and **(B)** forskolin treatment for 48 h of BeWo cells cultivated on plastic chamber slides. Immunohistochemical staining with anti-PLSCR1 antibody. Nuclear counterstaining: hemalaun. Scale bar represents 50 µm.

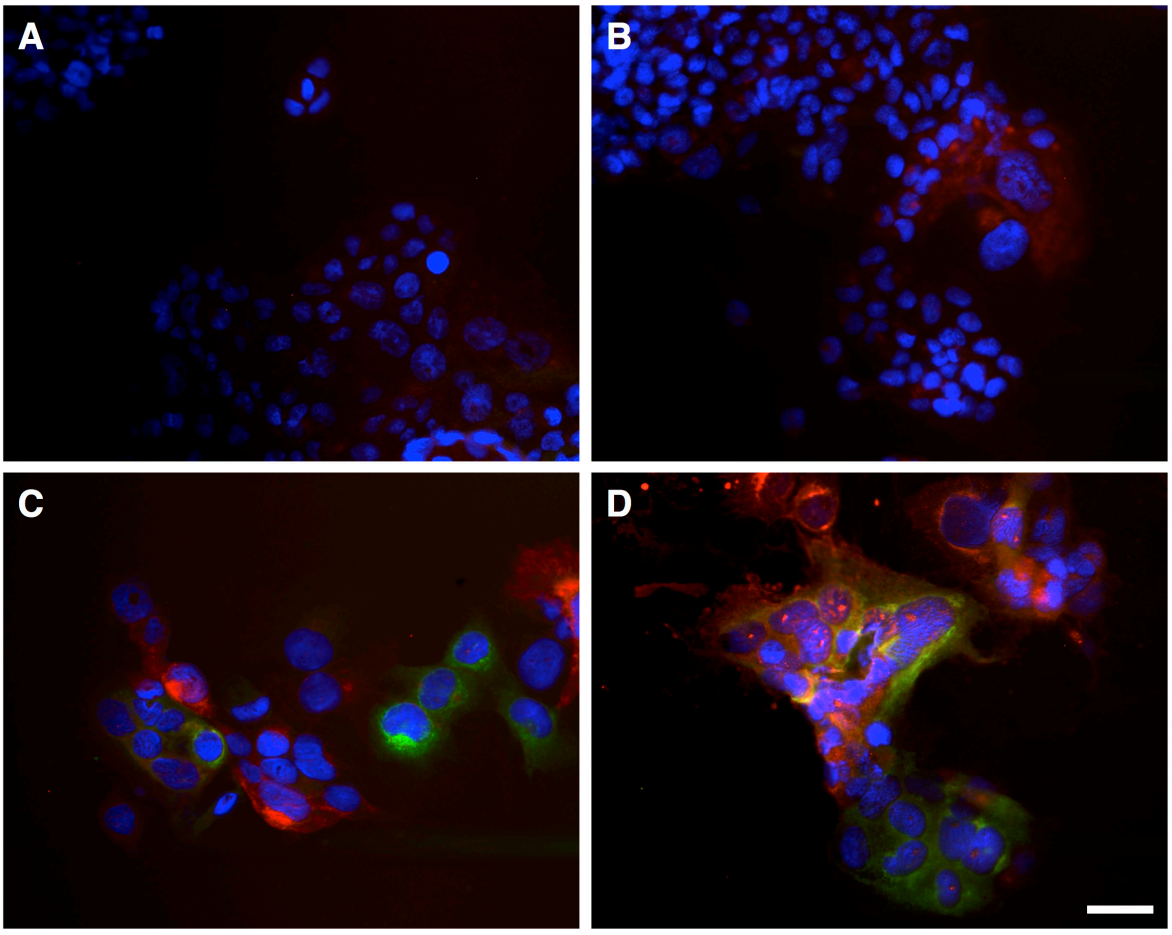

Figure 11: *PLSCR1 is not completely restricted to beta-hCG positive syncytia.*

Immunofluorescence double staining of PLSCR1 (red) and beta-hCG (green) in BeWo cells. **(A, B)** DMSO control **(C, D)** forskolin treatment. Nuclei were stained with DAPI. Scale bar represents 50 µm.

4.6 Phospholipid profile of BeWo cells after syncytialization

Mass spectrometry of PS, PC and PE was performed in DMSO vehicle controls and after successful fusion in BeWo cells treated with forskolin for 48 h (n=2). No significant changes in the phospholipid profile were detectable (Fig. 11).

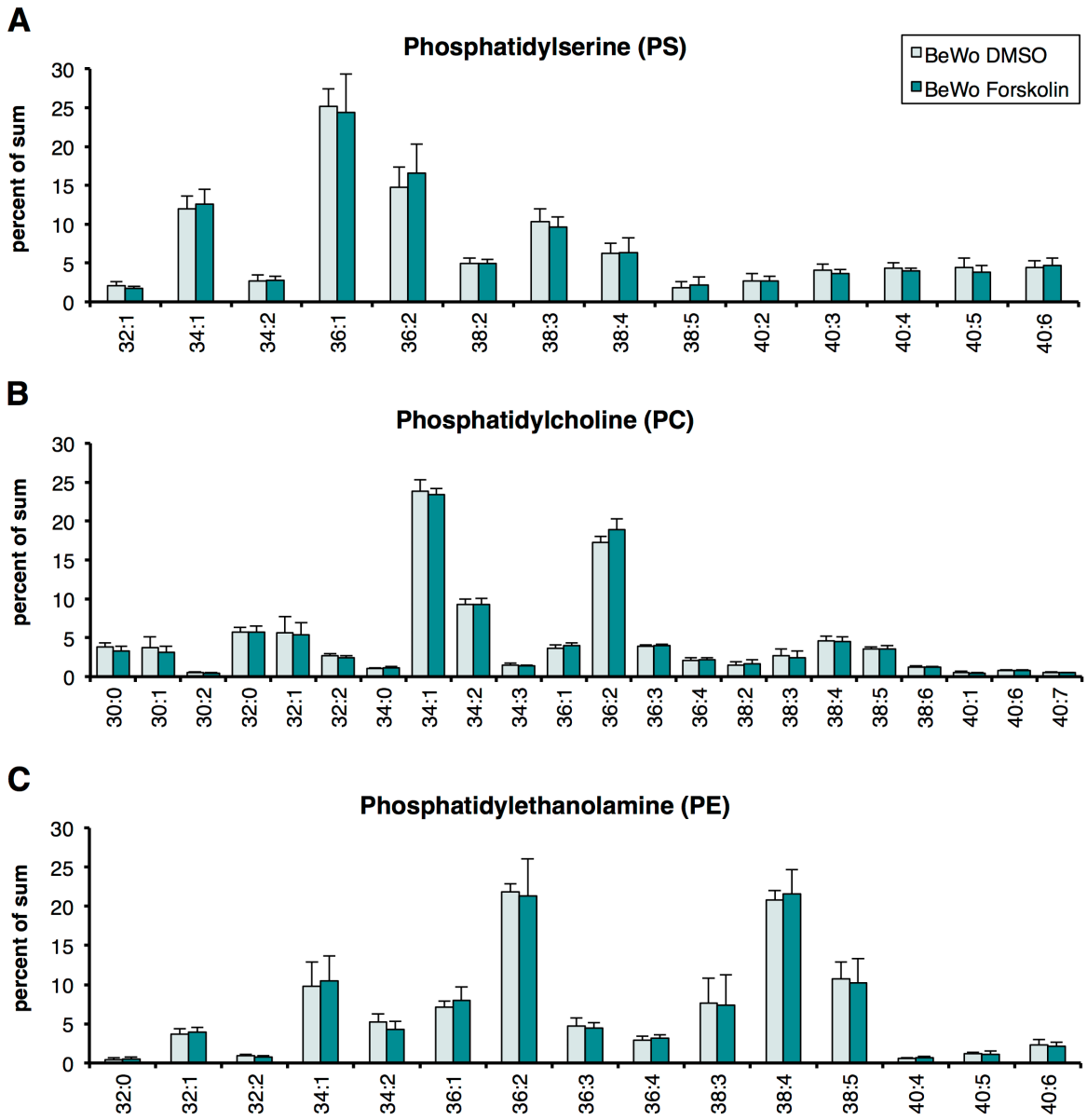

Figure 12: *Phospholipid profile of BeWo cells.*

Mass spectrometry of **(A)** phosphatidylserine (PS), **(B)** phosphatidylcholine (PC), and **(C)** phosphatidylethanolamine (PE) in BeWo cells with forskolin treatment for 48 h versus untreated controls. Results are presented as mean ± SD from two independent experiments performed in triplicates. X-axis indicates the different species of phospholipids (first digit: total length of fatty acids, second digit: number of double bounds).

4.7 PLSCR1 expression during primary trophoblast cell differentiation

In primary trophoblasts *PLSCR1* mRNA was significantly down-regulated by a mean factor of 0.31 after Br-cAMP treatment compared to DMSO control (Fig. 13A). Similarly, PLSCR1 protein levels decreased when fusion was induced with Br-cAMP compared to control cells (77.5% ± 6.5% band intensity; Fig. 13B, C).

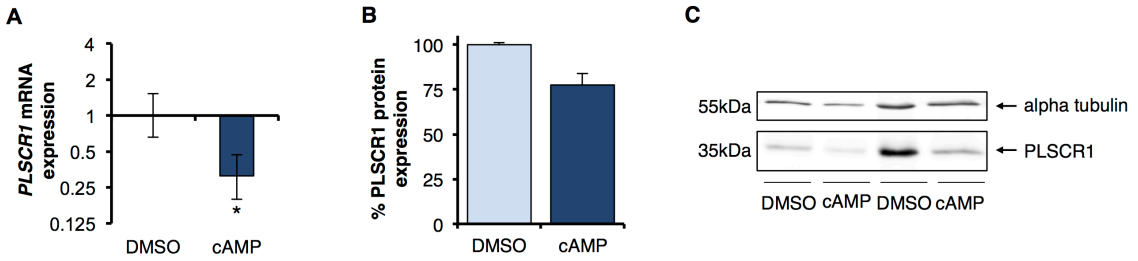

Figure 13: *PLSCR1 expression in primary trophoblasts.*

Analysis of *PLSCR1* mRNA and protein expression of DMSO (0.25%) and Br-cAMP (100 µM) treated primary trophoblasts after 72 h. **(A)** qRT-PCR results are presented as mean ± SEM from three differeent experiments performed in duplicates, *p<0.05. **(B)** Semi-quantitative band densitometry of PLSCR1 protein expression related to alpha-tubulin in DMSO or Br-cAMP-treated primary trophoblasts. Band densities were normalized to DMSO control, which was set to 100%. Data are presented as mean ± SEM from three different experiments, cells were pooled from two wells. **(C)** Representative immunoblot of PLSCR1 protein expression of two experiments (*Method II*). Parts of this data has been published in Berghold V.M. et al., *Histochemistry and Cell Biology*, 2014.

4.8 PLSCR1 expression in other cell lines (JAR, JEG-3, HEK-293 and Hep G2)

PLSCR1 mRNA and protein has been additionally tested in other cell lines. JAR and Jeg-3, two other choriocarcinoma cell lines, HEK-293, derived from embryonic kidney cells and Hep G2, derived from a hepatocellular carcinoma were used (Fig. 14). JAR cells revealed lower *PLSCR1* mRNA levels in comparison to BeWo cells. *PLSCR1* was down-regulated by a mean factor of 0.675. In contrast PLSCR1 protein expression was higher than in BeWo cells. In JEG-3 cells *PLSCR1* mRNA expression was up-regulated by a mean factor of 4.634, also protein level was higher compared to BeWo cells. In HEK-293 *PLSCR1* mRNA expression was not different to *PLSCR1* mRNA expression in BeWo cells. However, protein levels were higher. In Hep G2 *PLSCR1* mRNA was down-regulated by a mean factor of 0.677, PLSCR1 protein expression was nearly 5 times of the protein expression in BeWo cells

(Fig. 14A, B, D). Immunohistochemical staining showed high expression of PLSCR1 in Hep G2 cells (Fig. 14C).

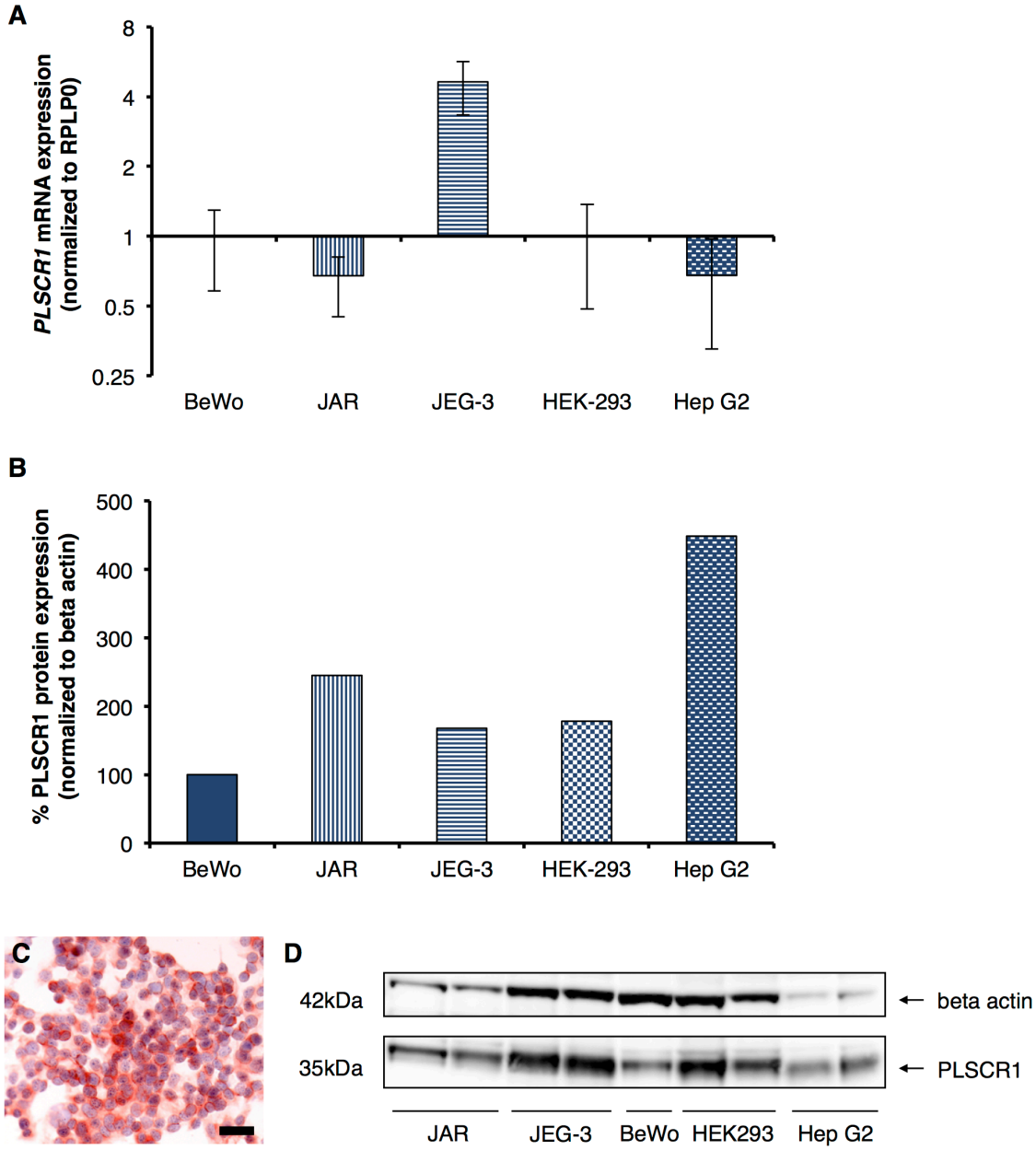

Figure 14: *PLSCR1 mRNA and protein expression in other cell lines.*

(A) qRT-PCR of mRNA expression level of PLSCR1 in different cell lines, BeWo JAR, JEG-3, HEK-293 and Hep G2. Results are presented as mean ± SEM from two separate experiments performed in triplicates. Values represent fold changes relative to BeWo cells. **(B)** Semi-quantitative band densitometry of PLSCR1 expression normalized to beta-actin. Band densities were normalized to PLSCR1 expression in BeWo cells, which was set to 100%. **(C)** Immunohistochemical staining of PLSCR1 in Hep G2 cells. Nuclear counterstaining: hemalaun. Scale bar represents 50 µm. **(D)** Representative immunoblot (*Method I*).

4.9 Silencing of PLSCR1 had no effect on BeWo cell fusion

Evaluation of PLSCR1 function on BeWo cell fusion was carried out with RNA interference. BeWo cells were transfected with small interfering RNA (siRNA) directed against *PLSCR1* or scrambled (non-silencing) control siRNA. After 24 h, 20 µM forskolin or 0.2% DMSO was added for an additional 48 h. None of these treatments affected cell viability, as determined by measurement of released LDH activity and normalization to total protein levels per well (data not shown).

Immunocytochemical staining for PLSCR1 in silenced and forskolin treated cells revealed a visible knockdown of PLSCR1. In control cells the protein was abundantly expressed, while in silenced cells only a weak staining could be detected (Fig. 15A, B). In Western blot analysis a maximal knockdown of the protein with 22% remaining PLSCR1 expression was achieved with a mean knockdown of 40% and 49% in BeWo cells treated with forskolin and DMSO, respectively, compared to untreated cells (Fig. 15C, D). On mRNA level *PLSCR1* was knocked down by a mean factor of 0.46 in forskolin and 0.5 in DMSO treated cells, compared to scrambled control (Fig. 16).

The other potential scramblases *PLSCR3*, *PLSCR4* and *TMEMF16* were marginally altered in the presence of *PLSCR1* siRNA. *TMEMF16* mRNA seemed to be down-regulated by forskolin (Fig. 16).

To evaluate the effect of *PLSCR1* knockdown on BeWo cell fusion, the differentiation marker *GCM-1* was analysed. *GCM-1* mRNA was up-regulated in BeWo cells stimulated with forskolin independent of siRNA stimulation. *PLSCR1* siRNA treatment led to a moderately but significantly decreased *GCM-1* expression without forskolin (Fig. 16).

As a second approach to confirm successful fusion, beta-hCG as a marker of trophoblast differentiation was evaluated with immunohistochemical staining. Cells treated with forskolin independent of siRNA treatment showed positive hCG staining, indicating successful syncytialization (Fig. 17A, B). Additionally, beta-hCG secretion was measured in conditioned media and normalized to total cell protein levels. Cells treated with DMSO and either *PLSCR1* or control siRNA showed a low release of beta-hCG (110 ± 25 mIU/mg protein (mean ± SEM) and 117 ± 32 mIU/mg protein, respectively). When *PLSCR1* or control siRNA transfected cells were stimulated with forskolin, a tremendous increase in hCG secretion occurred (1720 ± 323 mIU/mg protein and 1935 ± 465 mIU/mg protein, respectively; Fig. 17C).

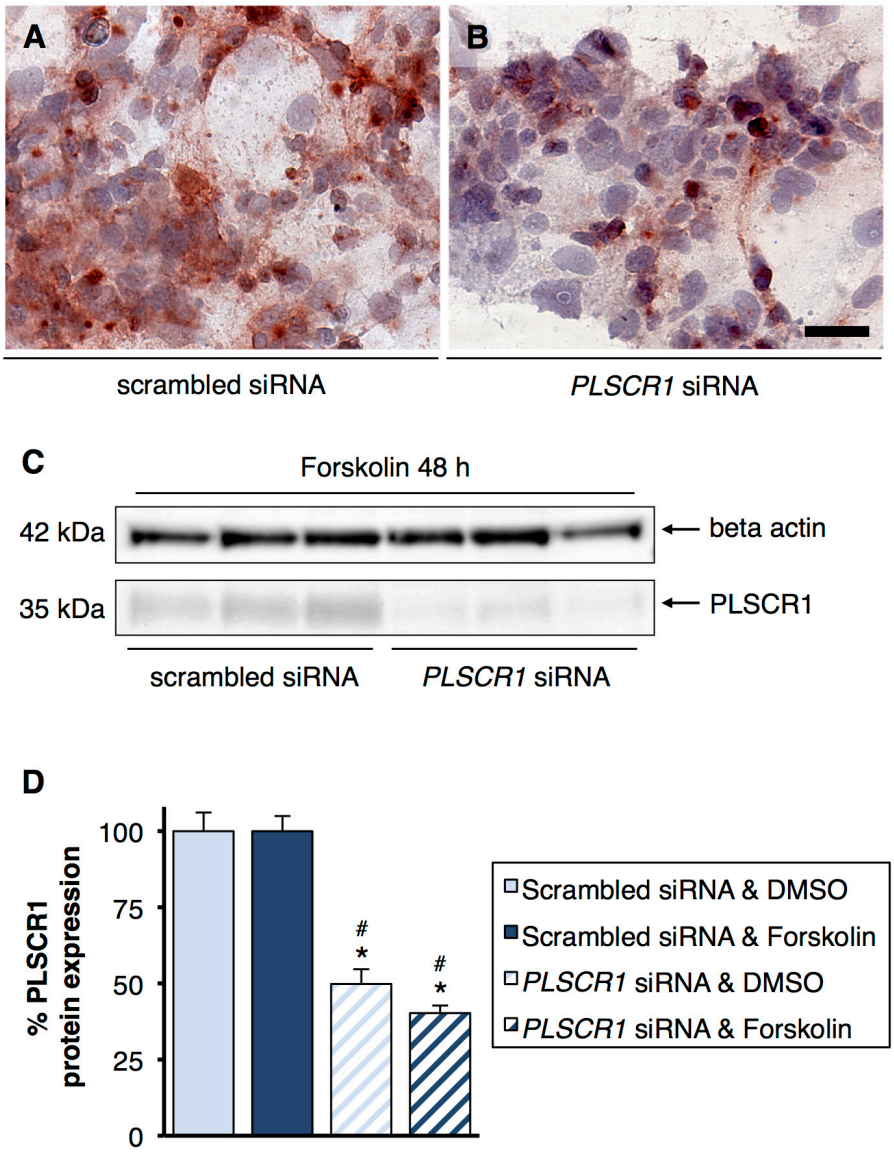

Figure 15: *Knockdown of PLSCR1 in BeWo cells.*

BeWo cells were transfected with either *PLSCR1* siRNA or a non-silencing scrambled control siRNA. 24 h after siRNA transfection cells were treated with forskolin (20 µM) or the vehicle control DMSO (0.2%) for 48 h. (**A, B**) Immunocytochemical staining of PLSCR1 after forskolin stimulation in (**A**) non-silencing control siRNA and (**B**) *PLSCR1* siRNA treated BeWo cells. Nuclear counterstaining: hemalaun. Scale bar represents 100 µm. (**C**) A representative immunoblot (*Method I*) and (**D**) semi-quantitative band densitometry of PLSCR1 expression normalized to beta-actin. Band densities were normalized to scrambled siRNA & DMSO control, which was set to 100%. Results are presented as mean ± SEM from five separate experiments performed in triplicates. Significant differences to the control are marked with an asterisk (*), significant differences to scrambled siRNA and forskolin treated cells are marked with a hash (#),); $p<0.05$. Parts of this data has been published in Berghold V.M. et al., *Histochemistry and Cell Biology*, 2014.

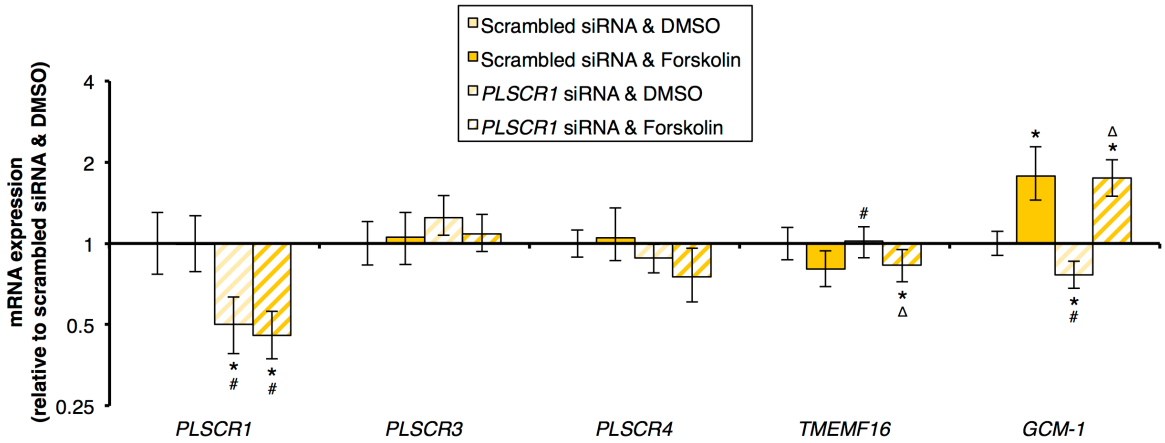

Figure 16: *mRNA expression after successful PLSCR1 knockdown in BeWo cells.*
qRT-PCR analysis of mRNA expression levels of *PLSCR1*, *PLSCR3*, *PLSCR4*, *TMEMF16* and *GCM-1* in BeWo cells after *PLSCR1* or scrambled siRNA treatment with further stimulation with 20 µM forskolin or 0.2% DMSO. Results are presented as mean ± SEM from three separate experiments performed in triplicates. Values represent fold changes relative to the scrambled siRNA and DMSO control. Significant differences to the control are marked with an asterisk (*), significant differences to scrambled siRNA and forskolin treated cells are marked with a hash (#) and significant differences to *PLSCR1* siRNA and DMSO treated cells are marked with a triangle (Δ); $p<0.05$. This data has been published in Berghold V.M. et al., *Histochemistry and Cell Biology*, 2014.

Furthermore, E-cadherin expression was evaluated. There have been reports that E-cadherin, a transmembrane glycoprotein which mediates cell to cell adhesion is present in cytotrophoblast cell contacts, however, missing after cellular differentiation and fusion (Coutifaris et al. 1991, Ng, Zhu & Leung 2011). Immunohistochemical staining of E-cadherin in forskolin treated cells indicated loss of membrane and formation of multinucleated syncytia independent of siRNA treatment (Fig. 18A, B). E-cadherin protein expression was analysed in silenced and non-silenced BeWo cell lysates with Western blot. No differences could be detected in E-cadherin protein expression (Fig. 18C, D).
Immunofluorescence staining for PLSCR1 in silenced and forskolin treated cells showed a clear knockdown of PLSCR1 in accordance with immunocytochemical and Western blot results (Fig. 19A-D).

Quantification of fusion in immunohistochemical stainings demonstrated spontaneous fusion in DMSO treated cells of about 7.4% with *PLSCR1* siRNA and 9.2% with scrambled siRNA. Forskolin treatment increased fusion events to 28.1% with *PLSCR1* siRNA and 26.8% with scrambled siRNA (Fig. 19E).

Taken together, no differences in fusion rates, beta-hCG release, E-cadherin protein and *GCM-1* mRNA expression were detected when BeWo cells were treated

with *PLSCR1* siRNA versus scrambled siRNA control, shedding doubts on the involvement of PLSCR1 in BeWo cell fusion.

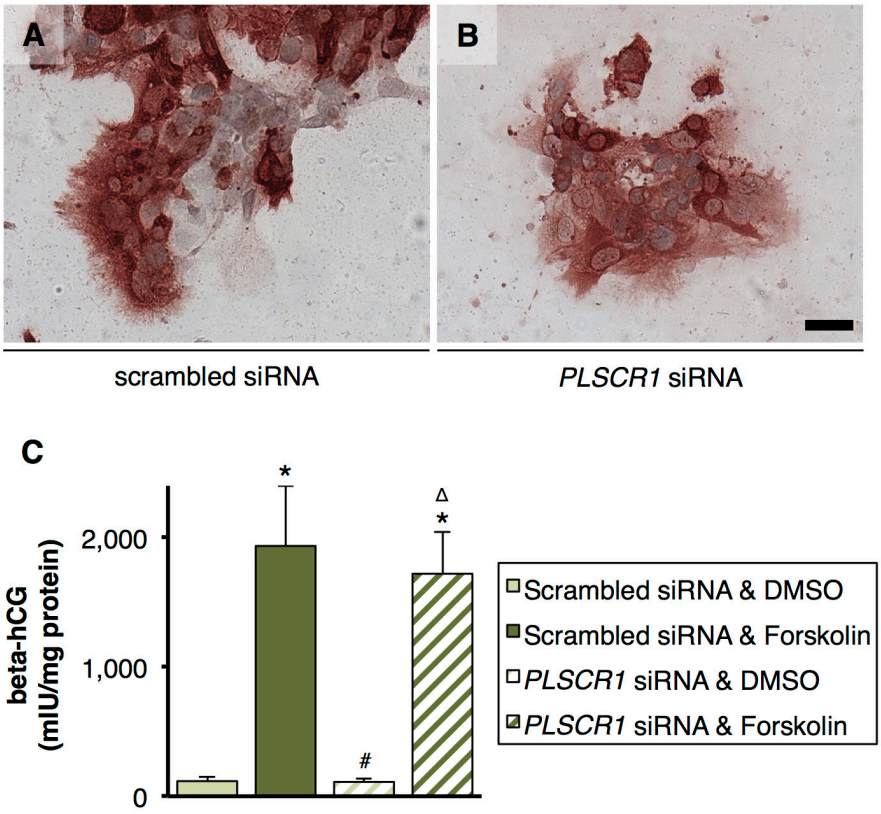

Figure 17: *Beta-hCG expression after PLSCR1 silencing in BeWo cells.*

BeWo cells were treated with siRNA, 24 h later forskolin (20 µM) or DMSO (0.2%) was added to the media for 48 h. **(A, B)** Immunocytochemical staining of beta-hCG after forskolin stimulation in **(A)** non-silencing control siRNA and **(B)** *PLSCR1* siRNA treated BeWo cells. Nuclear counterstaining: hemalaun. Scale bar represents 100 µm. **(C)** Measurements of beta-hCG in conditioned media after 72 h of siRNA treatment normalized to total cell protein (*Method I*). Results are presented as mean ± SEM from five separate experiments performed in triplicates. Significant differences to scrambled siRNA and DMSO treated cells are marked with an asterisk (*), significant differences to scrambled siRNA and forskolin treated cells are marked with a hash (#) and significant differences to *PLSCR1* siRNA and DMSO treated cells are marked with a triangle (Δ); $p<0.05$. Parts of this data has been published in Berghold V.M. et al., *Histochemistry and Cell Biology*, 2014.

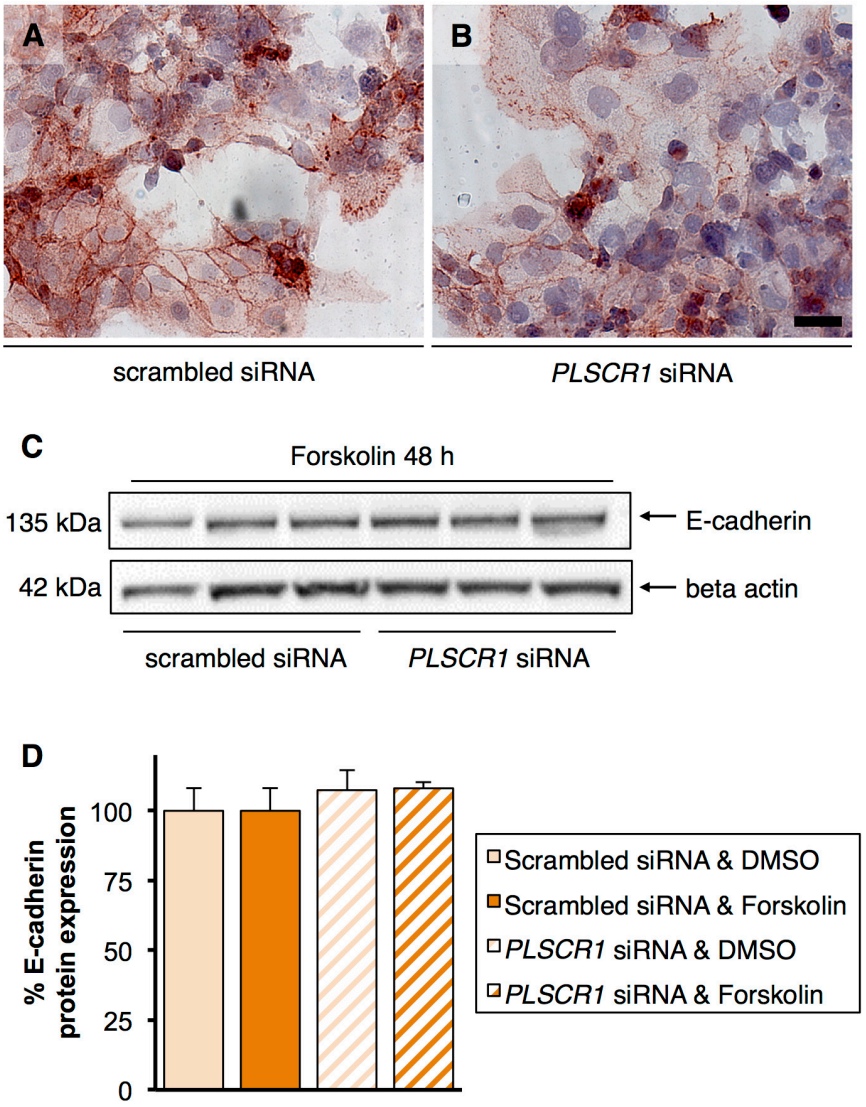

Figure 18: *E-cadherin in PLSCR1 siRNA treated BeWo cells.*

BeWo cells were transfected with either *PLSCR1* siRNA or a non-silencing scrambled control siRNA and 24 h after siRNA transfection cells were treated with forskolin (20 µM) or the vehicle control DMSO (0.2%) for 48 h. **(A, B)** Immunocytochemical staining of E-cadherin after forskolin stimulation in **(A)** non-silencing control siRNA and **(B)** *PLSCR1* siRNA treated BeWo cells. Nuclear counterstaining: hemalaun. Scale bar represents 100 µm. **(C)** A representative immunoblot (*Method I*) and **(D)** semi-quantitative band densitometry of E-cadherin expression normalized to beta-actin. Band densities were normalized to scrambled siRNA & DMSO control, which was set to 100%. Results are presented as mean ± SEM from two separate experiments performed in triplicates.

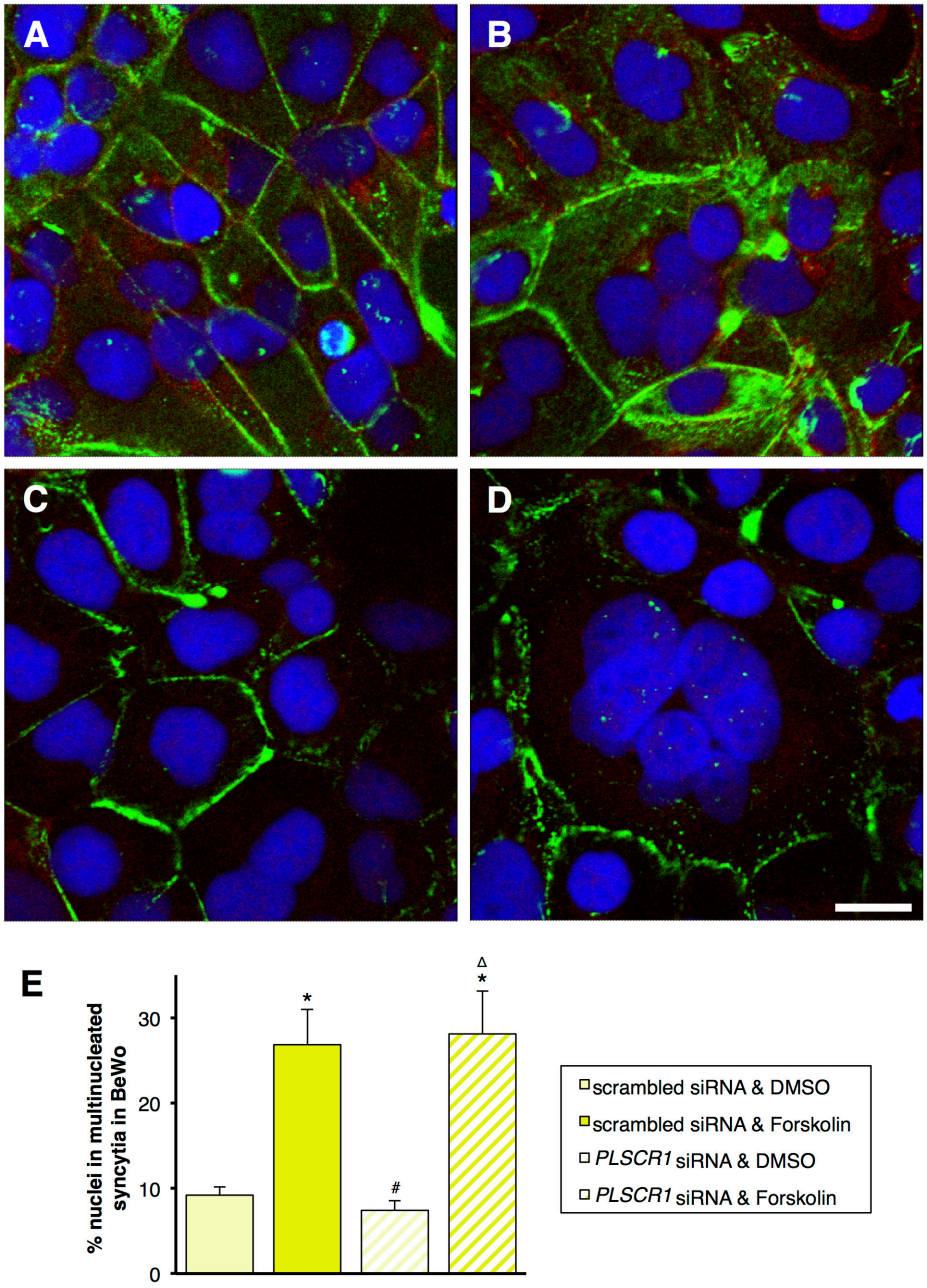

Figure 19: *Syncytialization after PLSCR1 knockdown in BeWo cells.*

Confocal imaging of a single z-axis of immunofluorescence staining of PLSCR1 (red), desmosomal protein (green) and DAPI stained nuclei (blue) in BeWo cells after siRNA treatment and stimulation with forskolin (20 µM) or DMSO (0.2%). (**A**) BeWo cells with scrambled control siRNA and vehicle control DMSO, (**B**) scrambled control siRNA and fusion induction with forskolin, (**C**) *PLSCR1* siRNA and DMSO, (**D**) *PLSCR1* siRNA and forskolin. Scale bar represents 20 µm. (**E**) Assessment of syncytialization by counting nuclei within syncytia versus total number of nuclei. Data are presented as mean ± SEM from three independent experiments. Significant differences to the control (scrambled siRNA and DMSO) are marked with an asterisk (*), significant differences to scrambled siRNA and forskolin treated cells are marked with a hash (#) and significant differences to *PLSCR1* siRNA and DMSO treated cells are marked with a triangle (Δ); $p<0.05$. Parts of this data has been published in Berghold V.M. et al., *Histochemistry and Cell Biology*, 2014.

4.10 Scramblase inhibitor R5421 and platelet aggregation

Besides RNA interference, a second strategy to inhibit PLSCR1 function was applied using a scramblase inhibitor (R5421), which prevents the exposure of phosphatidylserine on the cell surface (Smith et al. 2001, Gonzalez et al. 2009). The efficiency of R5421 was assessed using a platelet aggregation assay. Human platelets from healthy blood donors were incubated with 0.1 µM, 1 µM, 2.5 µM, 5 µM, 10 µM and 25 µM R5421 or the solvent control DMSO (0.4%) for 10 min. To induce submaximal platelet aggregation, ADP was added at concentrations individually adjusted for each blood donor. The efficiency testing of R5421 revealed a concentration dependent inhibitory effect of the inhibitor. ADP induced aggregation was almost completely reversed by R5421 at a concentration of 25 µM (99.7%). Inhibitor concentrations of 10 µM and 5 µM still resulted in 98.4% and 87.7% inhibition, respectively, when compared to the DMSO vehicle control (Fig. 20).

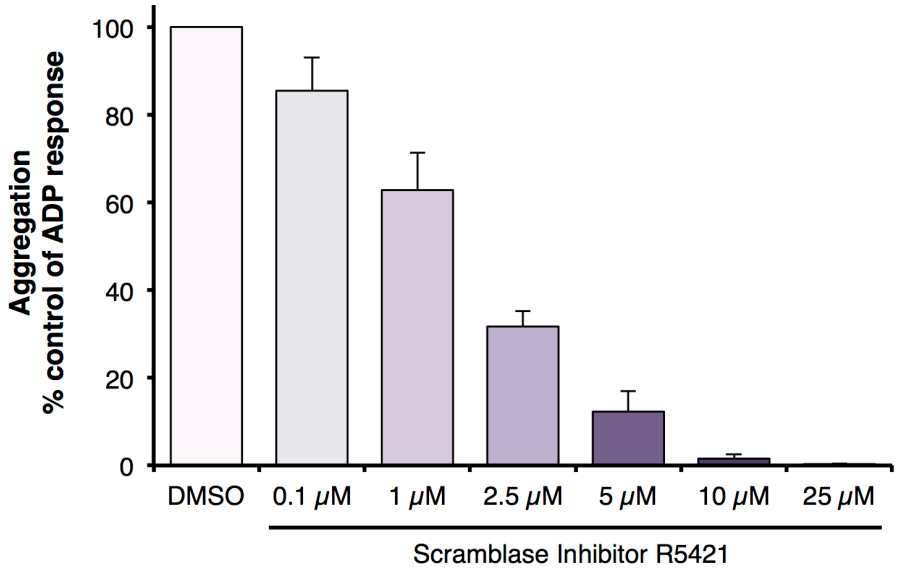

Figure 20: *Efficiency of scramblase inhibitor R5421 on platelet aggregation.*

Washed human platelets were pre-incubated with different concentrations of R5421 or the solvent control DMSO (0.4%) for 10 min. Platelet aggregation was induced with ADP at concentrations individually adjusted for each blood donor . Results are presented as mean percent ± SEM of the control response (DMSO) from three donors. This data has been published in Berghold V.M. et al., *Histochemistry and Cell Biology*, 2014.

4.11 Inhibition of PLSCR1 activity had no direct effect on BeWo cell fusion

After confirmation of inhibition of scramblase activity by R5421 with the platelet aggregation assay, the effect of R5421 on BeWo cell viability was tested. Therefore, cells were cultivated in media containing increasing concentrations of R5421 (5 µM, 10 µM, 15 µM, 20 µM, 25 µM, 30 µM, 50 µM) or DMSO (0.5%) alone as a control for 48 h. Cell death and survival was evaluated by microscopy (Fig. 21). Subsequently, LDH release was measured and normalized to total cell protein (data not shown). According to the results of the platelet aggregation assay, the concentration of R5421 for BeWo cells of 25 µM was chosen for further experiments based on minimal toxicity (Fig. 21E). Higher concentrations of R5421 were not tolerated by the BeWo cells and resulted in increased cell death (Fig. 21F).

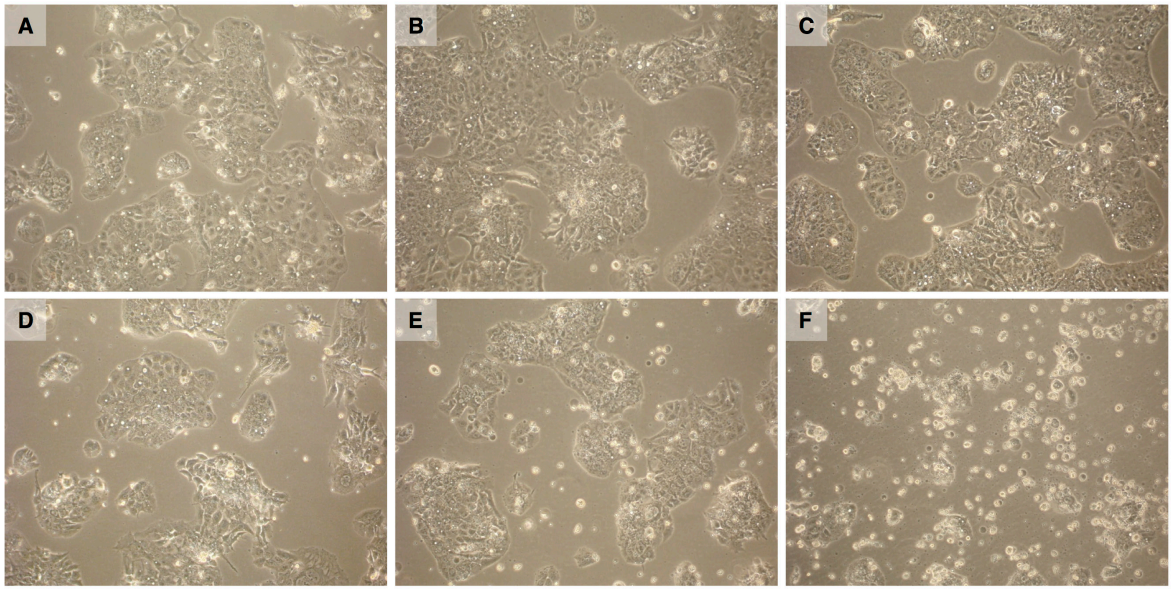

Figure 21: *BeWo cells after treatment with different concentrations of R5421.*
BeWo cells treated with DMSO **(A)** 0.1%, **(B)** 0.24%, **(C)** 0.5% and scramblase inhibitor R5421 **(D)** 10 µM, **(E)** 25 µM, **(F)** 50 µM for 48 h.

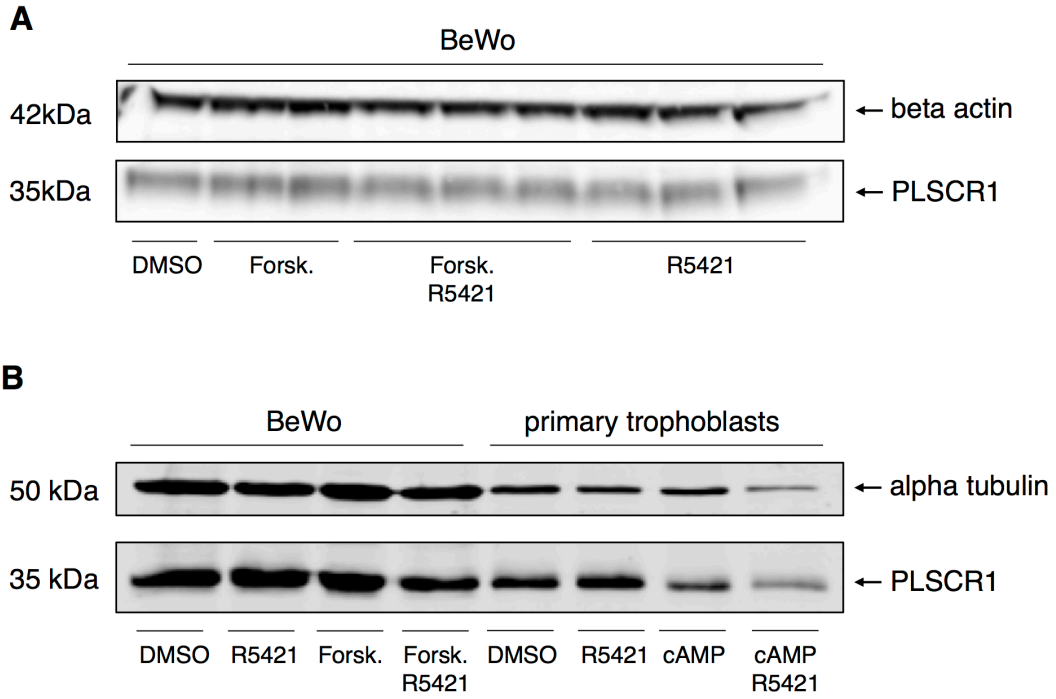

Figure 22: *Western blot of BeWo cells and primary trophoblasts after scramblase inhibitor R5421 treatement.*

BeWo cells and primary trophoblasts were treated with forskolin (20 µM) or Br-cAMP (100 µM) respectively or solvent control DMSO in the presence or absence of the scramblase inhibitor R5421 (25 µM) for 48 h. **(A)** Representative immunoblots for PLSCR1 and beta actin of BeWo cells (*Method I*). **(B)** Representative immunoblot for PLSCR1 and alpha tubulin of BeWo cells and primary trophoblasts (*Method II*).

For scramblase inhibitor experiments BeWo cells were treated with 0.45% DMSO control, 20 µM forskolin, 25 µM R5421 or 25 µM R5421 plus 20 µM forskolin for 48 h. R5421 treatment had no effect on PLSCR1 protein expression in BeWo cells as revealed by Western blot (Fig. 22A).

Expression levels of *PLSCR1*, *PLSCR3*, *PLSCR4*, *TMEMF16* and *GCM-1* in BeWo cells were assessed by qRT-PCR. *GCM-1* served as a marker for successful syncytialization and increased significantly after forskolin treatment with and without R5421. A smaller increase was also detected after R5421 stimulation alone. *PLSCR1* expression increased after combined stimulation with forskolin and R5421, but not after forskolin or R5421 treatment alone. *PLSCR3*, *PLSCR4* and *TMEMF16* expression decreased with forskolin and R5421 stimulation, but did not reach significance for *PLSCR4*. Additionally, *PLSCR4* and *TMEMF16* expression decreased after R5421 treatment alone (Fig. 23A).

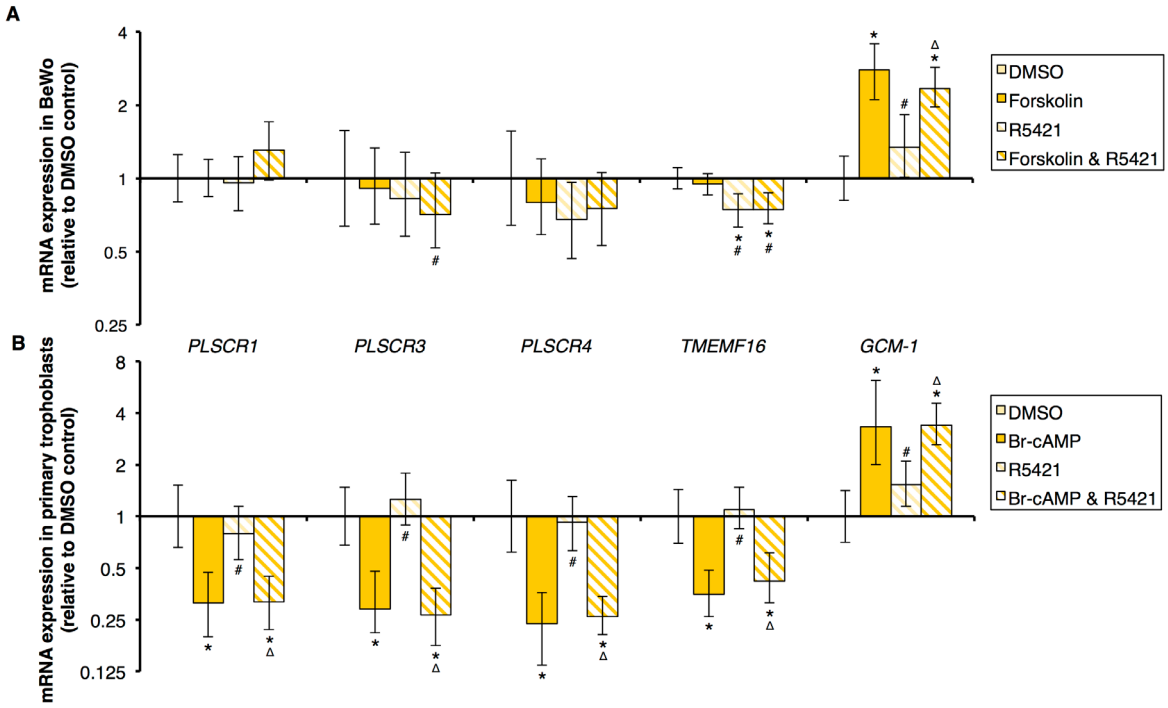

Figure 23: *mRNA expression after scramblase inhibitor R5421 treatment in BeWo cells and primary trophoblasts.*

qRT-PCR expression analysis of *PLSCR1*, *PLSCR3*, *PLSCR4*, *TMEMF16* and *GCM-1* in **(A)** BeWo cells and in **(B)** term primary trophoblasts. qRT-PCR results are presented as mean ± SEM from three separate experiments performed in triplicates (BeWo) or in duplicates (primary trophoblasts). Values represent fold changes relative to DMSO. Significant differences to DMSO treated cells are marked with an asterisk (*), significant differences to cells induced to fuse (forskolin and Br-cAMP treatment) are marked with a hash (#) and significant differences to R5421 treatment are marked with a triangle (Δ); p<0.05. This data has been published in Berghold V.M. et al., *Histochemistry and Cell Biology*, 2014.

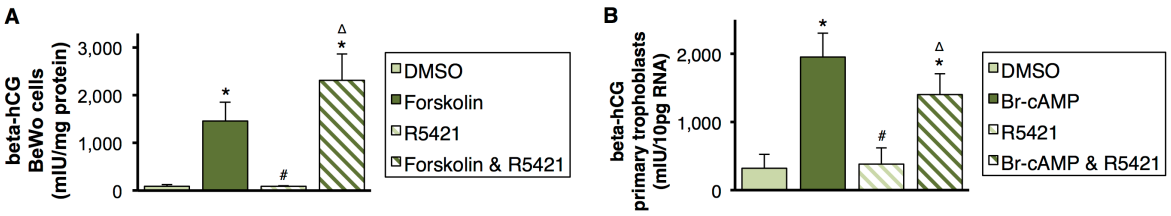

Figure 24: *Effect of scramblase inhibitor R5421 on BeWo cells and primary trophoblasts.*

Measurement of beta-hCG in **(A)** conditioned media of BeWo cells normalized to total cell protein (*Method I*) and **(B)** conditioned media of primary trophoblasts normalized to total cell RNA (*Method II*). Beta-hCG results are presented as mean ± SEM from three different experiments performed in triplicates (BeWo) or in duplicates (primary trophoblasts). Significant differences to DMSO treated cells are marked with an asterisk (*), significant differences to cells induced to fuse (forskolin and Br-cAMP treatment) are marked with a hash (#) and significant differences to R5421 treatment are marked with a triangle (Δ); p<0.05. This data has been published in Berghold V.M. et al., *Histochemistry and Cell Biology*, 2014.

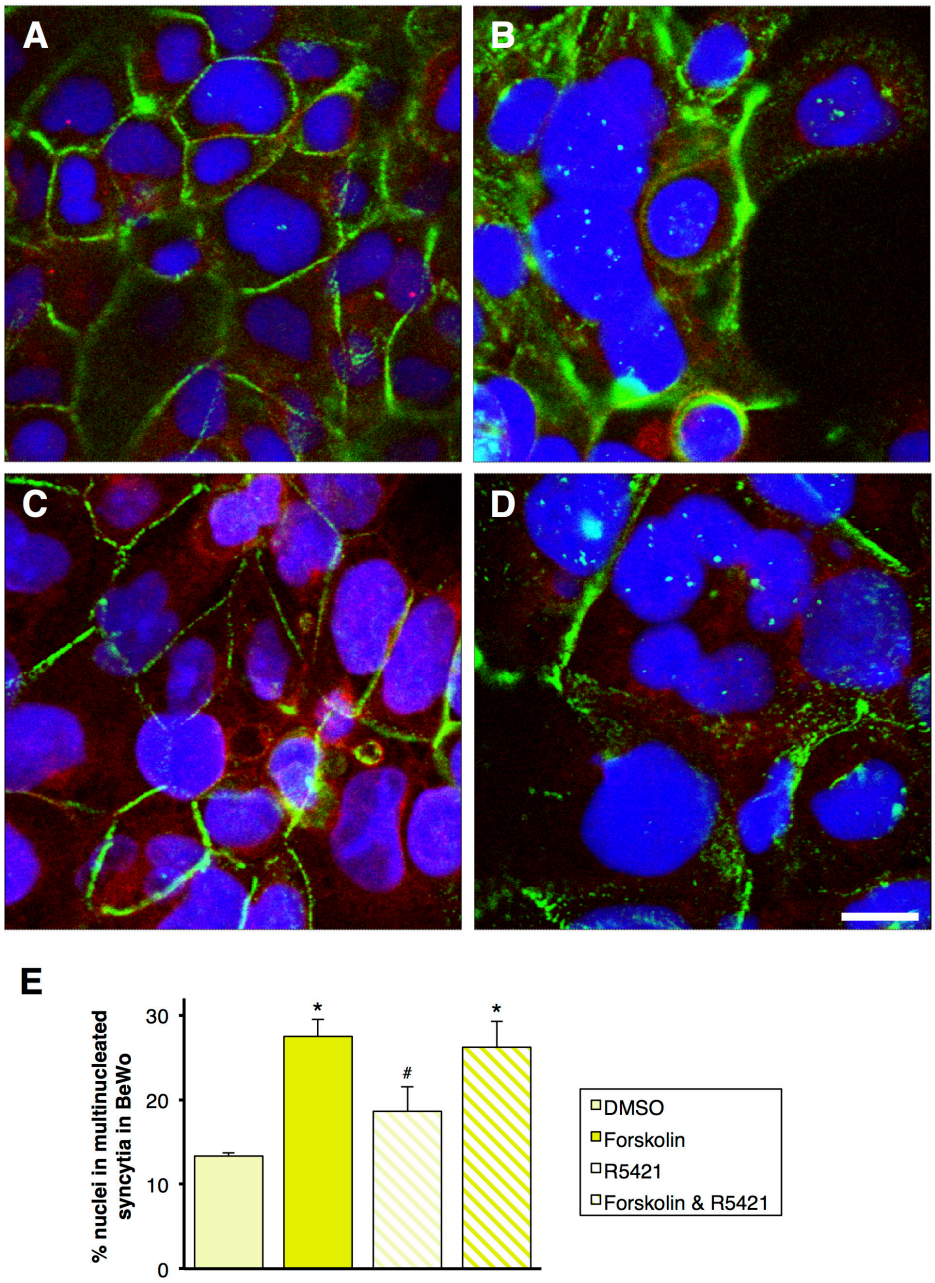

Figure 25: *Effect of scramblase inhibitor R5421 on BeWo cell syncytialization.*

Confocal imaging of a single z-axis of immunofluorescence staining of PLSCR1 (red), desmosomal protein (green) and DAPI stained nuclei (blue) in BeWo cells after treatment with forskolin (20 µM) or DMSO in the presence or absence of the scramblase inhibitor R5421 (25 µM) for 48 h. BeWo cells treated with (**A**) DMSO alone, (**B**) forskolin alone, (**C**) R5421 alone, (**D**) R5421 and forskolin together. Scale bar represents 20 µm. (**E**) Assessment of syncytialization by counting nuclei within syncytia versus total number of nuclei. Data are presented as mean ± SEM from three independent experiments. Significant differences to DMSO treated cells are marked with an asterisk (*) and significant differences to cells induced with forskolin are marked with a hash (#); $p<0.05$. Parts of this data has been published in Berghold V.M. et al., *Histochemistry and Cell Biology*, 2014.

Beta-hCG measured in the supernatant showed little secretion activity in DMSO-treated control BeWo cells regardless of R5421 treatment (without R5421: 90 ± 33 mIU/mg protein (mean ± SEM); with R5421: 90 ± 8 mIU/mg protein). Higher amounts of beta-hCG were released by BeWo cells stimulated with forskolin alone (1461 ± 401 mIU/mg protein). Beta-hCG secretion even increased after R5421 addition (2315 ± 551 mIU/mg protein; Fig. 24A).

Immunofluorescence double staining of PLSCR1 and desmosomal protein indicated increased PLSCR1 protein expression after R5421 treatment in presence or absence of forskolin (Fig. 25A-D). Consequent fusion assessment revealed a spontaneous fusion rate of 13.3% with DMSO treatment and 18.6% with R5421 treatment alone. BeWo cells treated with forskolin showed 27.5% fusion and with forskolin and R5421 25.6% fusion (Fig. 25E).

4.12 Inhibiton of scrambling activity in primary trophoblasts had no effect on fusion

To complement our findings scramblase inhibitor R5421 experiments were carried out in primary trophoblasts as well. The cells were stimulated with 0.25% DMSO, 100 µM Br-cAMP, 25 µM R5421 and 25 µM R5421 and 100 µM Br-cAMP together for 48 h and harvested after a total of 72 h.

R5421 treatment had no effect on PLSCR1 protein expression as determined by Western blot (Fig. 22B). On mRNA level *PLSCR1* mRNA was significantly down-regulated after Br-cAMP treatment alone and Br-cAMP and R5421 treatment together. *PLSCR1* mRNA expression decreased after Br-cAMP treatment to a relative mean value of 0.31 and together with R5421 to a relative mean value of 0.32 compared to DMSO control (Fig. 23B). A similar pattern was detected for the other scramblases *PLSCR3*, *PLSCR4* and *TMEMF16*. Treatment with Br-cAMP alone and Br-cAMP and R5421 together resulted in significant mRNA decrease, while R5421 treatment alone did not alter mRNA expression. *GCM-1* was up-regulated after Br-cAMP treatment with and without R5421, confirming successful syncytialization (Fig. 23B).

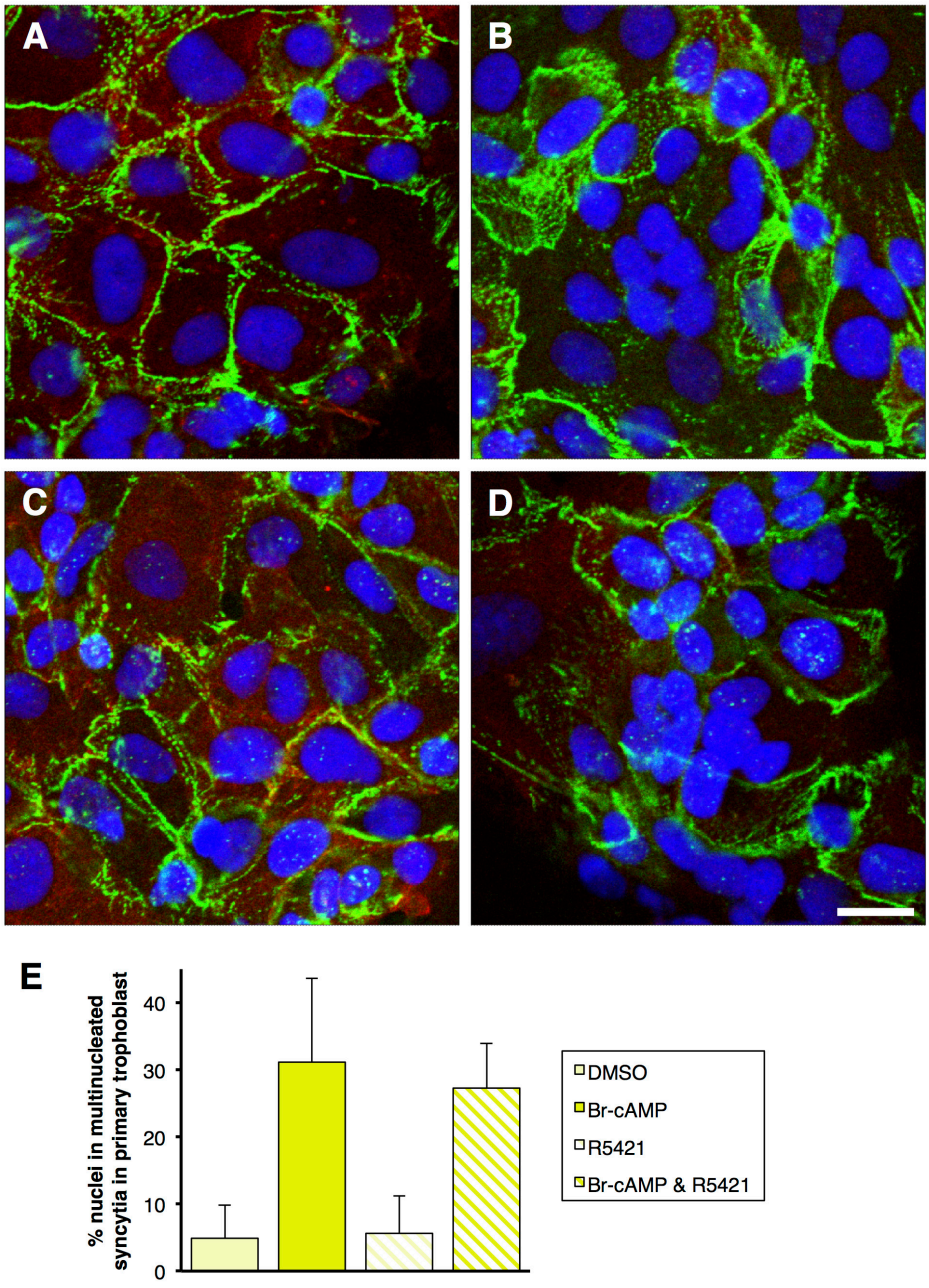

Figure 26: *Effect of scramblase inhibitor R5421 on primary trophoblast syncytialization.*

Confocal imaging of a single z-axis of immunofluorescence staining of PLSCR1 (red), desmosomal protein (green) and DAPI stained nuclei (blue) in primary trophoblasts after treatment with Br-cAMP (100 µM) or DMSO in the presence or absence of the scramblase inhibitor R5421 (25 µM) for 48 h. Primary trophoblasts were treated with (**A**) DMSO control, (**B**) Br-cAMP alone (**C**) R5421 alone, (**D**) R5421 and Br-cAMP together. Scale bar represents 20 µm. (**E**) Assessment of syncytialization by counting nuclei within syncytia versus total number of nuclei. Data are presented as mean ± SEM from two independent experiments. Parts of this data has been published in Berghold V.M. et al., *Histochemistry and Cell Biology*, 2014.

Beta-hCG measurement of the supernatant showed basal expression in DMSO treated control cells independent of R5421 treatment (without R5421: 321 ± 205 mIU/10ng RNA (mean ± SEM); with R5421: 382 ± 239 mIU/10ng RNA). After fusion induction with Br-cAMP beta-hCG increased in the supernatant (without R5421: 1953 ± 346 mIU/10ng RNA, with R5421: 1402 ± 308 mIU/10ng RNA; Fig. 24B).

Further, immunofluorescence double staining of primary trophoblasts with PLSCR1 and desmosomal protein confirmed the observations on protein and mRNA level. After fusion induction with Br-cAMP (with/without R5421 treatment) reduced expression of PLSCR1 was observed (Fig. 26A-D).

Successful fusion was evaluated by cell counting. Primary trophoblasts treated with DMSO control and R5421 showed spontaneous fusion of 4.9% and 5.6%, respectively. Br-cAMP treatment increased the fusion rate to 31.1% without R5421 and to 27.3% with R5421 (Fig. 26E).

4.13 Inhibition of PLSCR1 activity in first trimester villous explant cultures

To further confirm the observations in BeWo cells and isolated primary trophoblasts, first trimester explant cultures were treated with different concentrations of R5421 (1 to 50 µM) at 2.5% O_2 for 48 h. The scramblase inhibitor did not cause any changes on PLSCR1 protein expression in the explant cultures (Fig. 27A). Additionally, it did not provoke any change in beta-hCG release (Fig. 26B) or tissue survival, determined by LDH measured in the supernatants (Fig. 27C).

Tissue sections of first trimester explants were immunohistochemically stained for PLSCR1, Ki67, cytokeratin-7 and cleaved caspase-8. PLSCR1 showed a similar expression pattern as in first trimester placental sections; syncytiotrophoblast and macrophages were clearly stained whereas cytotrophoblasts were barely stained (Fig. 28A-D). Ki67, cytokeratin-7 and cleaved caspase-8 did not change with increasing concentrations of scramblase inhibitor R5421 (Fig. 28E-P).

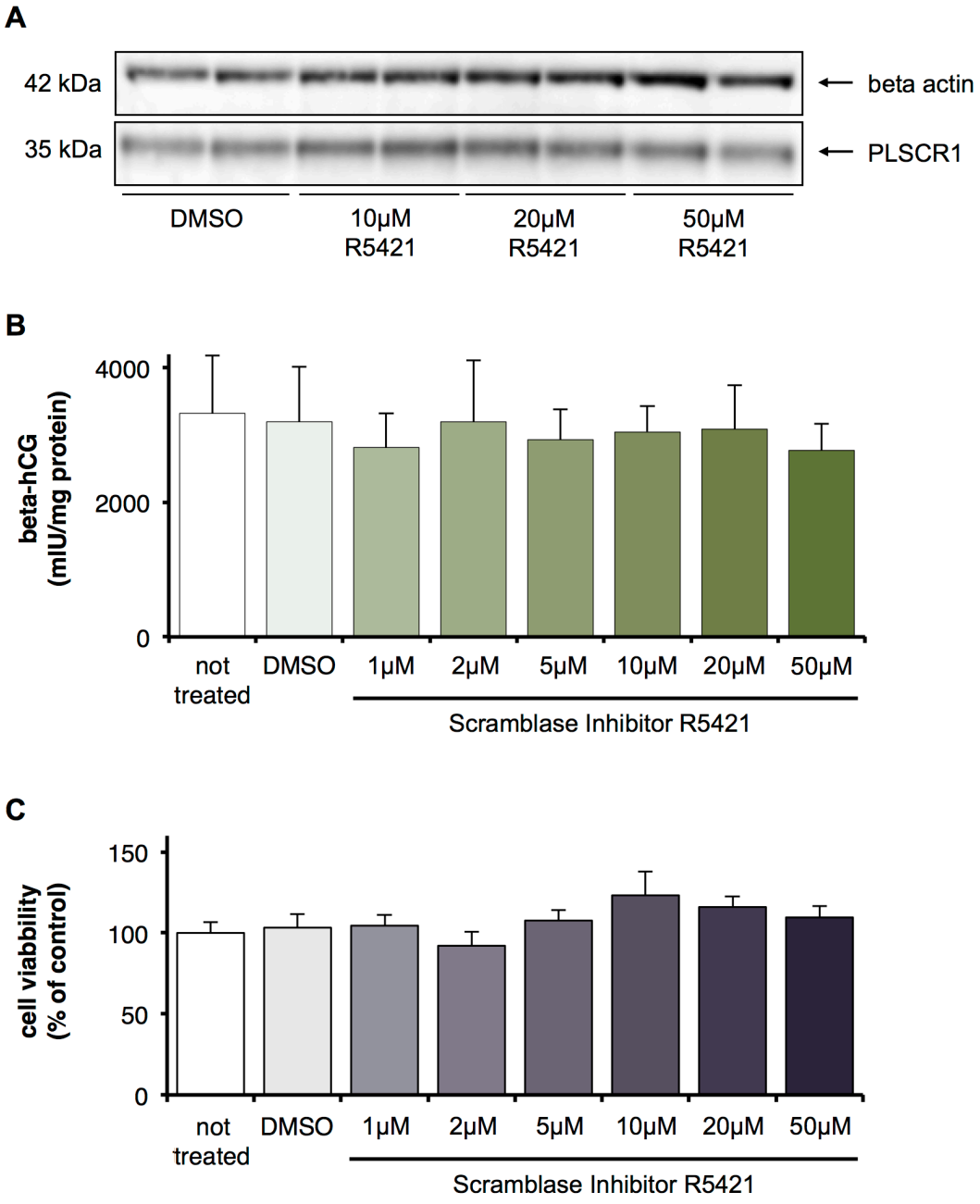

Figure 27: *Effects of scramblase inhibitor R5421 on first trimester explants.*

First trimester explants were cultivated for 48 h in medium containing different concentrations of scramblase inhibitor (1 µM, 2 µM, 5 µM, 10 µM, 20 µM and 50 µM) at 2.5% O_2 for 48 h. (**A**) Representative immunoblots for PLSCR1 and beta-actin as loding control (*Method I*). (**B**) Beta-hCG measurements were performed in collected culture supernatants and normalized to total tissue protein (*Method I*). **(C)** LDH release measured in the supernatant and consequently normalized to total tissue protein. Data are presented as mean ± SEM from six different first trimester placentas analyzed in triplicates.

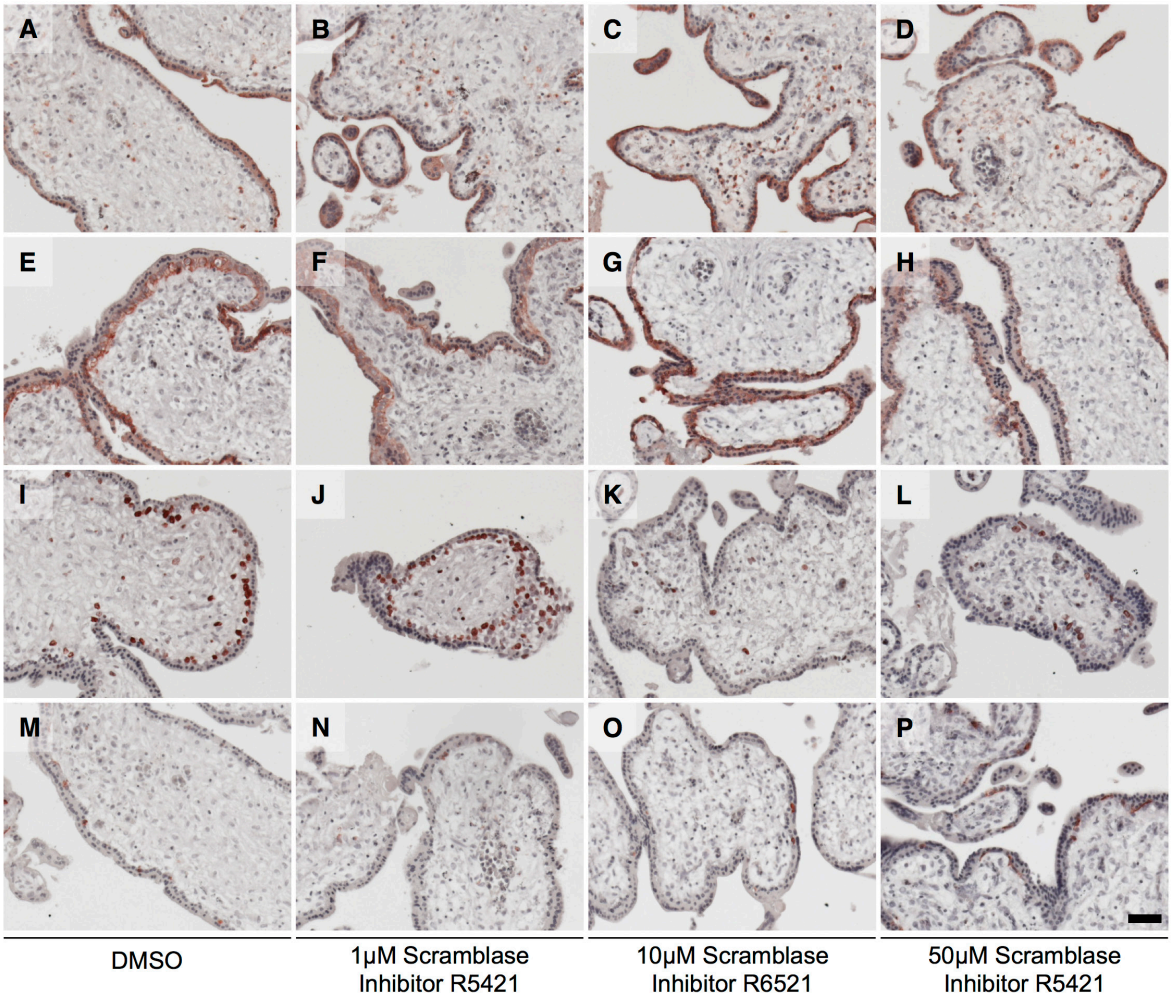

Figure 28: *Protein expression in first trimester explants after scramblase inhibitor treatment.*
Immunohistochemistry in human first trimester placenta (week 8 + 3). First trimester placental villous explants were cultured at 2.5% O_2 for 48 h in presence or absence of R5421. 0.5% DMSO served as vehicle control. Concentrations of R5421 were 1 µM, 10 µM, and 50 µM. There was no difference in staining pattern when sections were stained for (**A-D**) PLSCR1, (**E-H**) cytokeratin-7, (**I-L**) Ki67 and (**M-P**) cleaved caspase-8. Nuclear counterstaining: hemalaun. Scale bar represents 50 µm.

4.14 Microdissection, analysis of subgroups of cells

In order to evaluate the possible involvement of PLSCR1 in villous trophoblast fusion a single cell approach was investigated. The P.A.L.M. laser capture microdissection device enables to identify and cut out the desired cells, i.e. beta-hCG positive multinucleated syncytia (Fig. 29). Many syncytia may be cut and combined for consequent analysis. Different approaches to preserve RNA integrity throughout the process including RNAlater and ProtectRNA™ RNase Inhibitor were investigated.

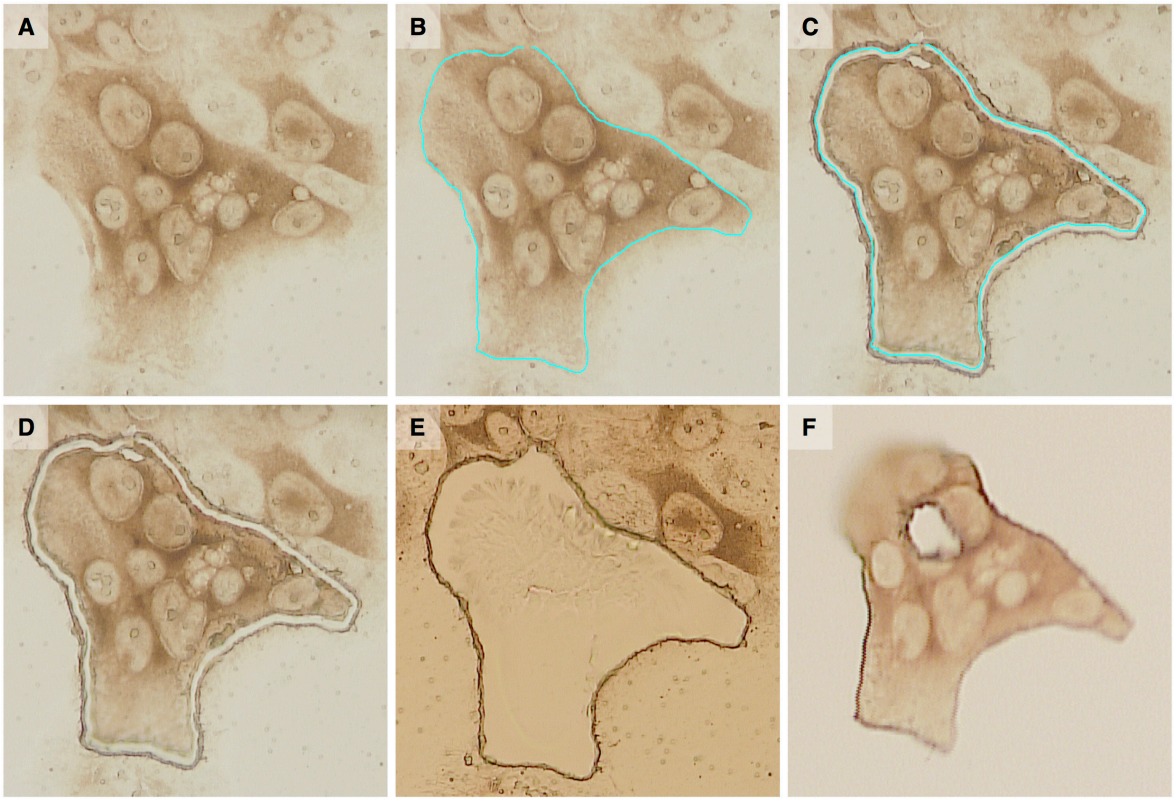

Figure: 29: *Microdissction of a beta-hCG positive syncytium.*

Slides were stained against beta-hCG and screened for positive synytia. **(A)** Identification of syncytium **(B)** picked and marked syncytium, **(C)** cutting along the marked lined with P.A.L.M. laser capture microdissection device **(D)** fully cut piece, **(E)** empty place on membrane, **(F)** catapulted piece into cap of a tube.

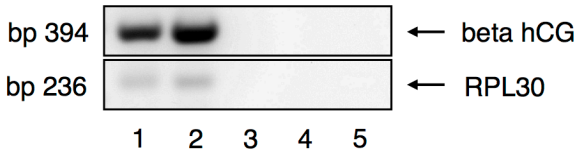

Figure 30: *RT-PCR after RNA isolation of microdissected cells.*

BeWo cells were stimulated with forskolin for 48 h. Slides were treated with RNAlater® for 1 h. After microdissection and RNA isolation RT-PCR with beta-hCG and RPLP0 primer pairs was performed. Products were separated on 1.5% denaturing agarose gels containing GelRed™.
1: approximately 100 BeWo cells, without beta-hCG staining
2: approximately 300 BeWo cells, without beta-hCG staining
3: approximately 100 BeWo cells, with beta-hCG staining
4: approximately 300 BeWo cells, with beta-hCG staining
5: H_2O negative control

However, after one-step RT-PCR and evaluation of products on 1.5% denaturing agarose gels no amplification products were observed after immunocytochemical staining for beta-hCG (Fig. 30). When the staining procedure was omitted one-step RT-PCR products were detected (Fig. 30).

Analysis of RIN factor with the Bio Analyzer confirmed these results by showing only maximally degraded RNA of RNA samples after beta-hCG staining and microdissection (data not shown).

4.15 Cytomegalovirus transfection of isolated primary trophoblasts

Since PLSCR1 was described to play a role in viral response, preliminary experiments were conducted to elucidate a potential antiviral role of PLSCR1 in the human placenta. Isolated primary trophoblasts were treated with HCMV virus for 6 h. Infection was confirmed with immunofluorescence staining with anti-cytomegalovirus antibody (Fig. 31A, B). PLSCR1 also seemed to be present in infected cells (Fig. 31A, B). Semi-quantitative band densitometry of immunoblot of one preliminary experiment revealed no changes in PLSCR1 protein expression after HCMV infection compared to uninfected control cells (Fig. 31C).

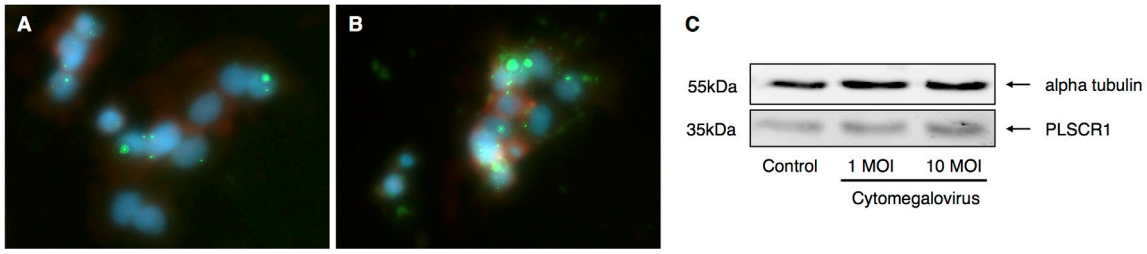

Figure 31: *Isolated primary trophoblasts infected with HCMV.*

(A, B) Immunofluoresence staining for cytomegalovirus (green) and PLSCR1 (red) of infected cells with **(A)** 1 MOI and **(B)** 10 MOI. **(C)** Immunoblot of primary trophoblast cells infected with HCMV.

5 Discussion

Please note that parts of this chapter have been published in Berghold V.M. et al., *Histochemistry and Cell Biology*, 2014.

Until now, there is hardly any available data on PLSCR1 in the human placenta. Merely, there have been reports that PLSCR1 might be involved in placental pathologies such as preeclampsia (Heikkila et al. 2005) and antiphospholipid syndrome with pregnancy morbidity (Amengual et al. 2013). General investigations on the scramblase family members revealed that *PLSCR1* mRNA is present in the placenta (Wiedmer et al. 2000). However, details on micro-anatomical localization and cellular function of PLSCR1 in the human placenta are quite unclear. In the present study we tested the hypothesis whether or not PLSCR1 plays a role in human trophoblast differentiation and fusion. For this purpose, we first determined the spatio-temporal expression pattern of PLSCR1 in human placental tissues.

5.1 PLSCR1 in the villous trophoblast compartment

PLSCR1 expression was tested with immunohistochemistry staining on a large number of placental sections. Specificity of the antibodies directed against PLSCR1 from two different companies were critically evaluated. This included a pre-adsorption approach with a respective blocking peptide. Based on these aspects the obtained immunohistochemistry results can be accepted as reliable. Accordingly, PLSCR1 is present in the syncytiotrophoblast as well as placental macrophages and endothelial cells of first trimester and term placenta. Within the cell, PLSCR1 is an integral membrane protein and is normally detected in the plasma membrane and various internal membrane pools (Zhao et al. 1998, Sun et al. 2002). In syncytiotrophoblast the distribution of this specific pattern seems to be correlating. Especially in first trimester placentas on the apical membrane of the syncytiotrophoblast a predominant location within the brush border facing maternal blood was observed. Surprisingly, PLSCR1 was virtually absent in the cytotrophoblast layer. Expression in other cell types but the villous cytotrophoblast does not per se exclude PLSCR1 to be involved in the differentiation and fusion process. Many of the yet described factors are rather part of a multifactorial mechanism than acting solely. Given PLSCR1 was really involved in the fusion process, its marginal expression in the cytotrophoblast rather

suggests the process of merging of neighboring membranes to be initiated from the syncytiotrophoblast (Potgens et al. 2004, Gauster, Huppertz 2010).

5.2 PLSCR1 expression outside the villous trophoblast compartment

Besides the villous trophoblast compartment, PLSCR1 expression was also observed in placental macrophages and endothelial cells within the villous stroma, as well as in extravillous trophoblasts, cell columns, and decidual glands.

In immunohistochemical staining of placenta sections PLSCR1 was highest expressed in placental macrophages (Hofbauer cells). These cells remove dead cells, cellular debris and microorganisms by phagocytosis/endocytosis. Apoptotic cells expose PS on the surface, which macrophages recognize as a signal to consequently remove these cells (Henson, Bratton & Fadok 2001). A possible explanation for the high expression in placental macrophages might be a regulatory role of PLSCR1 in this process. So far, PLSCR1 has been described to play a role in phospholipid reorganization of calcium-dependent neuroendocrine compensatory endocytosis (Ory et al. 2013). Additionally, PLSCR1 was found to interact with proteinase 3 on neutrophils interfering with macrophage phagocytosis (Kantari et al. 2007). This observed involvement in endocytosis might be necessary for PLSCR1 function in endothelial and trophoblast cells as well.

The only difference of PLSCR1 expression levels between first trimester and term placenta was found in fetal endothelial cells. The observed expression levels increased significantly from first trimester to term; however, the reason for this increase is currently unknown. To date, PLSCR1 has only been investigated in human umbilical vein endothelial cells (HUVEC). In HUVEC the scramblase was induced by interferon and contributes to cytokine-regulated cell proliferation and differentiation (Warke et al. 2003).

5.3 PLSCR1 in preeclampsia

In an array study on severe early onset preeclampsia PLSCR1 was demonstrated to be up-regulated in these placentas compared to healthy controls (Heikkila et al. 2005). In the present study, PLSCR1 expression was evaluated with immunohistochemical staining of sections of placentas with preeclampsia before and

after week 37 of gestation and compared to age-matched controls. In contrast to the array study the results of the present study indicate that PLSCR1 might be less expressed in the syncytiotrophoblast in early onset preeclampsia as well as in endothelial cells in both preeclampsia before and after week 37 of gestation. However, this observed trend has to be interpreted carefully due to the limited number of samples. Unfortunately, it was not possible to further evaluate PLSCR1 in placentas with preeclampsia. The obtained samples of frozen placenta tissue were unusable for qRT-PCR analysis. The attempted RNA isolations with the TRIzol® or RNeasy® Mini Kit method resulted in only degraded RNA.

5.4 Models for studying villous trophoblast fusion

In order to evaluate PLSCR1 during villous trophoblast fusion, we used three valuable model systems, the choriocarcinoma cell line BeWo, isolated primary trophoblasts from term placentas and first trimester villous explant cultures.

So far, one of the most valuable *in vitro* models for studying trophoblast fusion is the trophoblast-derived cell line BeWo with similar characteristics to freshly isolated human villous cytotrophoblasts. BeWo cells possess the tendency to fuse and form multinucleated syncytia after stimulation with forskolin or cAMP and analogues (Wice et al. 1990). Furthermore, after fusion the multinucleated cells adopt the morphology of the placental syncytiotrophoblast presenting clustered nuclei, massive areas of nuclei-free cytoplasm and a syncytiotrophoblast-like brush border on the apical surface (Wice et al. 1990). Further PS is found on the surface of BeWo cells during forskolin-induced fusion (Das et al. 2004). Therefore, BeWo cells are frequently used and generally accepted as a suitable *in vitro* model for studying villous trophoblast differentiation and consequent fusion (Mi et al. 2000, Benaitreau et al. 2010, Dunk et al. 2012).

As a second model we used primary trophoblast preparations isolated from term placentas. We performed the majority of our experiments with these cells, to support and complement our findings from the BeWo cell line model. Primary trophoblasts are also able to differentiate in culture, aggregate and form multinucleated syncytia (Kliman et al. 1986, Yui et al. 1994). In contrast to BeWo cells, primary trophoblasts were stimulated to fuse with Br-cAMP. Primary trophoblasts are probably a better model than carcinoma cells such as BeWo cells. However, there are some disadvantages including limited access to tissues, elaborate and time-consuming

isolation procedures resulting in relative small numbers of cells, which limits number of experiments and a short cultivation timeframe.

To mimic the in vivo situation even closer we used as a third in vitro model human first trimester villous explant cultures. These explants consist of intact placental tissue, where villous trophoblast fusion can be studied. Villous cytotrophoblasts continue to proliferate; moreover, the double-layered villous trophoblast structure remains intact for several days (Black et al. 2004, Miller et al. 2005). Explant cultures need to be cultivated at appropriate physiological oxygen tension of about 2.5% to resemble the situation as in utero (Jauniaux et al. 2000). However, only short-term cultures are possible and assessment of single cells and fusion events is very difficult.

Despite suitable and useful models, evaluation of factors involved in villous trophoblast fusion is generally difficult. The fusion process takes place in a limited amount of time, after which potentially involved proteins might be down-regulated or altered again, before these changes can be observed or measured. Additionally, not all cells undergo fusion; in this study we were able to reach fusion rates of about 30% in BeWo cells as well as in primary trophoblasts. This makes it very difficult to evaluate the possible involvement of PLSCR1 in villous trophoblast fusion. Therefore, a single cell analysis approach was performed with the intention to precisely investigate only syncytialized structures versus mononucleated cells. With the P.A.L.M laser microdissection device it was possible to cut and catapult beta-hCG positive syncytia into a tube and consequently perform RNA isolation and analysis. However, the problem was the immunohistochemical staining for beta-hCG that allows the identification of multinucleated syncytia. After the fast staining protocol it was not possible to obtain decent RNA quality; even when DEPC-water, ProtectRNA™ RNase Inhibitor and RNAlater® were used. Without staining against beta-hCG, it was possible to isolate RNA after the microdissection procedure. After several unsuccessful attempts this approach had to be discontinued.

5.5 Assessment of successful fusion into multinucleated cells

Successful syncytial fusion and functional response was evaluated with three different methods: (1) beta-hCG release into supernatants, (2) *GCM-1* mRNA expression and (3) counting of total number of nuclei versus number of nuclei in syncytia by visualization of cell borders.

In the human placenta the pregnancy related beta-subunit of hCG is only produced by the syncytiotrophoblast; correspondingly, in BeWo cells it is mainly produced, however, not solely in multinucleated syncytia (Orendi et al. 2010). BeWo cells were stimulated to fuse by forskolin, an adenylyl cyclase activator, which induces an increase of intracellular cyclic adenosine monophosphate (cAMP) (Seamon, Padgett & Daly 1981) and consequently BeWo cell differentiation (Wice et al. 1990). For differentiation and fusion induction in primary trophoblasts Br-cAMP, a brominated derivate of cAMP was used. Increased intracellular cAMP elevates the pregnancy related hormone beta-hCG (Albanese et al. 1991) among other fusion-related processes. Hence, beta-hCG may be seen as a marker for differentiation in these cells. In BeWo cells and primary trophoblasts significant increase of beta-hCG after fusion induction was observed.

The fusion stimulating compound forskolin is dissolved in DMSO. DMSO alone at the same volume (up to 0.45%) was added to the media and served as vehicle control. DMSO itself may affect the differentiation process. However, the amounts used in this study are considerably smaller than those where alterations have been reported (Da Violante et al. 2002, Rebourcet et al. 2004).

As a second approach the mRNA expression of the transcription factor *GCM-1* was analysed with qRT-PCR. GCM-1 plays a crucial role in regulation of villous trophoblast differentiation (Baczyk et al. 2009) and is an upstream regulator of syncytin 1, which is a captive retroviral protein necessary for trophoblast fusion (Mi et al. 2000). Therefore, on mRNA level elevated *GCM-1* expression confirmed the successful formation of multinucleated syncytia in trophoblasts. In all our experiments with forskolin or Br-cAMP treatment increased *GCM-1* expression was detected.

Thirdly, intercellular boundaries were visualized by staining for desmosomal protein (Douglas, King 1990) or E-cadherin (Coutifaris et al. 1991, Ng, Zhu & Leung 2011). Desmosomes are complex structures of cell adhesion proteins, which connect neighbouring cells found in the placenta between cytotrophoblasts and between cytotrophoblasts and syncytiotrophoblast (Douglas, King 1990). E-cadherins, transmembrane glycoproteins, mediate calcium-dependent cell-cell adhesion in neighbouring cells and are present in cytotrophoblast cell contacts; however, it is missing after cell fusion (Coutifaris et al. 1991, Ng, Zhu & Leung 2011).

Successful cell fusion has been assessed after cultivation on coverslips and staining with a respective membrane associated protein. Reported fusion rates of forskolin stimulated BeWo cells show large variations ranging from 10% (Kudo et al.

2003, Borges et al. 2003) up to 80% (Das et al. 2004, Lin, Xu & Rote 1999). This large discrepancy is probably due to the quantification approach as well as to the evaluator. Counting of cell nuclei and evaluation of cell borders is done by eye and estimation of mononucleated cells and multinucleated syncytia depends on the individual person. Different concentrations of forskolin (10 µM versus 100 µM) did not seem to result in diverging fusion rates, performed by the same group (Das et al. 2004, Lin, Xu & Rote 1999). Further, different BeWo cell clones might have different fusion tendencies (Gauster, Huppertz 2010), which also makes comparisons difficult. Taken together, assessment of villous trophoblast fusion is essential to study potential factors involved in this process; however, fusion rates have to be critically reviewed and should be supported by another method to assess fusion such as measurement of hCG secretion into the supernatant or expression analysis of known contributing factors.

5.6 PLSCR1 during the fusion process

Phospholipid scramblases are responsible for unspecific scrambling of phospholipids across the lipid bilayer of the plasma membrane (Basse et al. 1996, Zhou et al. 1997). They are activated when intracellular calcium is increased due to cell injury or apoptosis (Basse et al. 1996, Zhou et al. 1997). This results in PS exposure on the cell's surface and in the transient collapse of regular phospholipid membrane asymmetry, which is also a crucial event in villous trophoblast fusion (Huppertz et al. 1998).

In this study we hypothesized that PLSCR1 plays a role in villous trophoblast fusion, either by inducing transient abolishment of membrane asymmetry or by signaling between the syncytiotrophoblast and cytotrophoblast layer.

BeWo cells stimulated with forskolin to fuse into multinucleated syncytia did not result in PLSCR1 expression changes neither on mRNA nor on protein level when compared to DMSO treated cells. The phospholipid profile of BeWo cells was evaluated. Again no significant changes in phospholipid profile were detectable between treated and untreated cells. However, it has to be considered that this method does not allow the distinction between outer and inner membrane leaflet. Here, only the distinct profiles of the different phospholipid species in BeWo cells can be presented.

5.7 Inhibition of PLSCR1 with siRNA and scramblase inhibitor R5421

In order to evaluate a functional role of PLSCR1 in trophoblast fusion two experimental strategies including siRNA mediated silencing of *PLSCR1* expression on the one hand and inhibition of PLSCR1 activity by a scramblase inhibitor on the other hand were used. Silencing mediated by *PLSCR1* siRNA led to a considerable decrease of PLSCR1 protein in the trophoblast cell line BeWo, as evaluated by Western blot, qRT-PCR and immunocytochemistry. Attempts in primary trophoblasts to knockdown *PLSCR1* via siRNA were unsuccessful due to insufficient transfection efficiency. This is a well-known difficulty in primary cells (Holder et al. 2012, Meade, Ma & Guller 2007).

Although PLSCR1 was silenced by more than 50%, which can be considered sufficient to study PLSCR1 function, no effect on forskolin induced hCG secretion was observed between silenced and control cells. Similarly, no change in E-cadherin expression was detected.

Since initiation of fusion, i.e. merger of cytoplasmic membranes and formation of the fusion pore, is locally restricted to a very small area, one may argue that a knockdown of more than 50% is not high enough to rule out sufficient activity of the remaining PLSCR1 portion. Therefore, the second strategy to test PLSCR1 involvement in trophoblast fusion was based on the scramblase inhibitor R5421, which has been demonstrated in human erythrocytes and platelets (Dekkers et al. 1998) and hence, inhibits the exposure of PS on the cell surface (Smith et al. 2001, Gonzalez et al. 2009). At the same time, it does not affect aminophospholipid flippases (Dekkers et al. 1998). In platelets, exposure of PS serves to form a procoagulant surface initiating the blood coagulation cascade (Williamson et al. 1995). Consequently, a platelet aggregation assay was used to determine effective concentrations of R5421 inhibiting platelet aggregation, i.e. inhibition of lipid scrambling.

According to the literature inhibition was obtained to a great extend by adding R5421 at a final concentration of 50 µM. Unfortunately, BeWo cells and first trimester villous explants did not tolerate this high concentration for the duration of the experiments in this study; therefore, lower concentrations had to be used. 25 µM of R5421 led to a nearly complete inhibition of platelet aggregation and was well tolerated by the cells. Therefore, to ensure effective inhibition of lipid scrambling in our cell culture experiments, 25 µM of R5421 was chosen. The inhibitor did not cause any

alterations on PLSCR1 protein expression. Although comparison between platelets and BeWo cells is almost impossible one may assume that the applied R5421 concentration is sufficient to inhibit most of the scramblase activity in BeWo cells as well.

Despite the presence of R5421 the cells were able to fuse and even resulted in a slight increase in *GCM-1* mRNA expression without any fusion stimulation. A similar effect was observed when counting of nuclei assessed fusion rates. In BeWo cells the fusion rate increased whereas in primary trophoblasts R5421 showed no effect on fusion rates. Surprisingly, there was an increase in beta-hCG secretion when BeWo cells were treated with forskolin and scramblase activity was inhibited by R5421. Whether the size of the syncytia remains the same between treated and untreated cells is not clear. R5421 might lead to the formation of rather small syncytia containing only two to three nuclei.

Our results indicate that inhibition of scramblase activity by scramblase inhibitor R5421 leads to increased differentiation (*GCM-1* up-regulation) and cell fusion (beta-hCG secretion and fusion rate) in BeWo cells. In primary trophoblasts this effects seems to be less prominent.

5.8 Other members of the scramblase family in the human placenta and during fusion

According to the data presented here PLSCR1 is not directly involved in differentiation and fusion of BeWo and primary trophoblast cells. Although microarray analysis revealed PLSCR1 to be the most expressed scramblase protein in placental cells, other members of the scramblase family could potentially compensate for the loss of PLSCR1 to maintain successful phospholipid scrambling and fusion. Thus, PLSCR3 and PLSCR4, other members of the phospholipid scramblase family, were included in this study (Wiedmer et al. 2000). PLSCR2, the last to date known member of the phospholipid scramblase family, had to be excluded as it is only expressed in testis and has not been found in any other tissue including the placenta (Wiedmer et al. 2000). Another candidate that mediates PS externalization is TMEM16F. TMEM16F has been linked to Scott Syndrome, a rare bleeding disorder where phospholipid scrambling is impaired (Suzuki et al. 2010b, Yang et al. 2012a). Originally, PLSCR1 was suspected to be responsible for this disease (Stout et al. 1997).

Analysis of *PLSCR3*, *PLSCR4* and *TMEMF16* mRNA expression in BeWo cells and primary trophoblasts showed no increase after forskolin or Br-cAMP treatment, indicating that these scramblases have no effect on fusion. In contrast, in BeWo cells there was a marginal down-regulation of *TMEMF16* after *PLSCR1* siRNA and R5421 treatment.

Surprisingly, Br-cAMP induced syncytialization in primary trophoblasts resulted in a decrease in *PLSCR1* mRNA expression as well as the other tested scramblases *PLSCR3*, *PLSCR4* and *TMEMF16*. This effect was not enhanced by simultaneous R5421 treatment. On the contrary, forskolin did not induce such an effect in BeWo cells. The underlying mechanisms of these effects are unclear. cAMP binds to the transcriptional regulator cAMP responsive element modulator alpha (Rauen et al. 2013) and other transcription factors such as the cAMP receptor protein or the virulence factor regulator (Gancedo 2013). In turn these factors have regulatory functions on gene expression (Rauen et al. 2013, Gancedo 2013). One of these properties might be involved in down-regulating PLSCR1 and the other scramblases in primary trophoblasts after incubation with Br-cAMP.

5.9 PLSCR1 plays a role in negatively regulating trophoblast fusion

According to the data presented in this study, we can exclude a direct propagating role of phospholipid scramblase activity of PLSCR1 in mechanisms of the trophoblast fusion process. On the contrary, our data suggest a potential role of PLSCR1 in negatively regulating fusion rather than facilitating trophoblast fusion. PLSCR1 is present in the syncytiotrophoblast; however, virtually absent in the cytotrophoblast layer underneath. Signaling from the syncytiotrophoblast to the cytotrophoblast indicating the necessity for fusion may be a potential function of PLSCR1 in trophoblast fusion.

PLSCR1 has been described to be involved in signaling pathways including interactions with immunoglobulin E type 1 receptor, c-Abl tyrosine kinase and epidermal growth factor receptor (Sahu et al. 2007).

Due to the high expression in syncytiotrophoblast, another role of PLSCR1 besides fusion in villous trophoblast should be considered, e.g., in the formation of syncytial knots and/or antiviral defense.

6 Conclusion

Overall, our results rather exclude PLSCR1 to be directly involved in trophoblast cell differentiation and fusion. Nevertheless, the data presented points out a potential role of PLSCR1 negatively regulating this process. When PLSCR1 activity was blocked, increased fusion could be observed. The specific underlying signaling pathways are not known and require more research in this field.

Since PS exposure to the cell surface has been discussed to be crucial for the fusion process (Das et al. 2004), a compensatory activity of other phospholipid transporters should also be kept in mind. None of the tested transporters in this study seem to possess this activity in trophoblast. However, due to the presence of PLSCR1 at the apical side of the syncytiotrophoblast, involvement of PLSCR1 in other aspects of trophoblast biology, such as lipid metabolism or antiviral response, are conceivable. Further in–depth studies will help to improve understanding the effects on syncytiotrophoblast growth and maintenance. Beyond that the role in pregnancy pathologies such as preeclampsia, where impaired fusion is considered to be part of the causative process needs further evaluation.

7 Bibliography

Albanese, C., Kay, T.W., Troccoli, N.M. & Jameson, J.L. 1991, "Novel cyclic adenosine 3',5'-monophosphate response element in the human chorionic gonadotropin beta-subunit gene", *Molecular endocrinology (Baltimore, Md.),* vol. 5, no. 5, pp. 693-702.

Amengual, O., Atsumi, T., Oku, K., Suzuki, E., Horita, T., Yasuda, S. & Koike, T. 2013, "Phospholipid scramblase 1 expression is enhanced in patients with antiphospholipid syndrome", *Modern rheumatology / the Japan Rheumatism Association,* vol. 23, no. 1, pp. 81-88.

Askelund, K.J. & Chamley, L.W. 2011, "Trophoblast deportation part I: review of the evidence demonstrating trophoblast shedding and deportation during human pregnancy", *Placenta,* vol. 32, no. 10, pp. 716-723.

Baczyk, D., Drewlo, S., Proctor, L., Dunk, C., Lye, S. & Kingdom, J. 2009, "Glial cell missing-1 transcription factor is required for the differentiation of the human trophoblast", *Cell death and differentiation,* vol. 16, no. 5, pp. 719-727.

Basse, F., Stout, J.G., Sims, P.J. & Wiedmer, T. 1996, "Isolation of an erythrocyte membrane protein that mediates Ca2+-dependent transbilayer movement of phospholipid", *The Journal of biological chemistry,* vol. 271, no. 29, pp. 17205-17210.

Benaitreau, D., Dos Santos, E., Leneveu, M.C., De Mazancourt, P., Pecquery, R. & Dieudonne, M.N. 2010, "Adiponectin promotes syncytialisation of BeWo cell line and primary trophoblast cells", *Reproductive biology and endocrinology : RB&E,* vol. 8, pp. 128-7827-8-128.

Benirschke, K., Burton, G.J. & Baergen, R.N. 2012a, "Basic Structure of the Villous Trees" in *Pathology of the Human Placenta*, eds. K. Benirschke, G.J. Burton & R.N. Baergen, 6th edn, Springer Science & Business Media, New York, pp. 55-100.

Benirschke, K., Burton, G.J. & Baergen, R.N. 2012b, "Early Development of the Human Placenta" in *Pathology of the Human Placenta*, eds. K. Benirschke, G.J. Burton & R.N. Baergen, 6th edn, Springer Science & Business Media, New York, pp. 41-53.

Benirschke, K., Burton, G.J. & Baergen, R.N. 2012c, "Nonvillous Parts and Trophoblast Invasion" in *Pathology of the Human Placenta*, eds. K. Benirschke, G.J. Burton & R.N. Baergen, 6th edn, Springer Science & Business Media, New York, pp. 157-240.

Bevers, E.M., Smeets, E.F., Comfurius, P. & Zwaal, R.F. 1994, "Physiology of membrane lipid asymmetry", *Lupus,* vol. 3, no. 4, pp. 235-240.

Bitbol, M. & Devaux, P.F. 1988, "Measurement of outward translocation of phospholipids across human erythrocyte membrane", *Proceedings of the National*

Academy of Sciences of the United States of America, vol. 85, no. 18, pp. 6783-6787.

Black, S., Kadyrov, M., Kaufmann, P., Ugele, B., Emans, N. & Huppertz, B. 2004, "Syncytial fusion of human trophoblast depends on caspase 8", *Cell death and differentiation,* vol. 11, no. 1, pp. 90-98.

Borges, M., Bose, P., Frank, H.G., Kaufmann, P. & Potgens, A.J. 2003, "A two-colour fluorescence assay for the measurement of syncytial fusion between trophoblast-derived cell lines", *Placenta,* vol. 24, no. 10, pp. 959-964.

Bretscher, M.S. 1972, "Asymmetrical lipid bilayer structure for biological membranes", *Nature: New biology,* vol. 236, no. 61, pp. 11-12.

Coleman, J.A., Quazi, F. & Molday, R.S. 2013, "Mammalian P4-ATPases and ABC transporters and their role in phospholipid transport", *Biochimica et biophysica acta,* vol. 1831, no. 3, pp. 555-574.

Coutifaris, C., Kao, L.C., Sehdev, H.M., Chin, U., Babalola, G.O., Blaschuk, O.W. & Strauss, J.F.,3rd 1991, "E-cadherin expression during the differentiation of human trophoblasts", *Development (Cambridge, England),* vol. 113, no. 3, pp. 767-777.

Cui, W., Li, S.Y., Du, J.F., Zhu, Z.M. & An, P. 2012, "Silencing phospholipid scramblase 1 expression by RNA interference in colorectal cancer and metastatic liver cancer", *Hepatobiliary & pancreatic diseases international : HBPD INT,* vol. 11, no. 4, pp. 393-400.

Da Violante, G., Zerrouk, N., Richard, I., Provot, G., Chaumeil, J.C. & Arnaud, P. 2002, "Evaluation of the cytotoxicity effect of dimethyl sulfoxide (DMSO) on Caco2/TC7 colon tumor cell cultures", *Biological & pharmaceutical bulletin,* vol. 25, no. 12, pp. 1600-1603.

Daleke, D.L. 2003, "Regulation of transbilayer plasma membrane phospholipid asymmetry", *Journal of lipid research,* vol. 44, no. 2, pp. 233-242.

Das, M., Xu, B., Lin, L., Chakrabarti, S., Shivaswamy, V. & Rote, N.S. 2004, "Phosphatidylserine efflux and intercellular fusion in a BeWo model of human villous cytotrophoblast", *Placenta,* vol. 25, no. 5, pp. 396-407.

Dekkers, D.W., Comfurius, P., Vuist, W.M., Billheimer, J.T., Dicker, I., Weiss, H.J., Zwaal, R.F. & Bevers, E.M. 1998, "Impaired Ca2+-induced tyrosine phosphorylation and defective lipid scrambling in erythrocytes from a patient with Scott syndrome: a study using an inhibitor for scramblase that mimics the defect in Scott syndrome", *Blood,* vol. 91, no. 6, pp. 2133-2138.

Der, S.D., Zhou, A., Williams, B.R. & Silverman, R.H. 1998, "Identification of genes differentially regulated by interferon alpha, beta, or gamma using oligonucleotide arrays", *Proceedings of the National Academy of Sciences of the United States of America,* vol. 95, no. 26, pp. 15623-15628.

Dong, B., Zhou, Q., Zhao, J., Zhou, A., Harty, R.N., Bose, S., Banerjee, A., Slee, R., Guenther, J., Williams, B.R., Wiedmer, T., Sims, P.J. & Silverman, R.H. 2004,

"Phospholipid scramblase 1 potentiates the antiviral activity of interferon", *Journal of virology,* vol. 78, no. 17, pp. 8983-8993.

Douglas, G.C. & King, B.F. 1990, "Differentiation of human trophoblast cells in vitro as revealed by immunocytochemical staining of desmoplakin and nuclei", *Journal of cell science,* vol. 96 (Pt 1), no. Pt 1, pp. 131-141.

Drewlo, S., Levytska, K. & Kingdom, J. 2012, "Revisiting the housekeeping genes of human placental development and insufficiency syndromes", *Placenta,* vol. 33, no. 11, pp. 952-954.

Dunk, C.E., Gellhaus, A., Drewlo, S., Baczyk, D., Potgens, A.J., Winterhager, E., Kingdom, J.C. & Lye, S.J. 2012, "The molecular role of connexin 43 in human trophoblast cell fusion", *Biology of reproduction,* vol. 86, no. 4, pp. 115.

Fischer, U., Janicke, R.U. & Schulze-Osthoff, K. 2003, "Many cuts to ruin: a comprehensive update of caspase substrates", *Cell death and differentiation,* vol. 10, no. 1, pp. 76-100.

Fisher, S., Genbacev, O., Maidji, E. & Pereira, L. 2000, "Human cytomegalovirus infection of placental cytotrophoblasts in vitro and in utero: implications for transmission and pathogenesis", *Journal of virology,* vol. 74, no. 15, pp. 6808-6820.

Frasch, S.C., Henson, P.M., Nagaosa, K., Fessler, M.B., Borregaard, N. & Bratton, D.L. 2004, "Phospholipid flip-flop and phospholipid scramblase 1 (PLSCR1) co-localize to uropod rafts in formylated Met-Leu-Phe-stimulated neutrophils", *The Journal of biological chemistry,* vol. 279, no. 17, pp. 17625-17633.

Gancedo, J.M. 2013, "Biological roles of cAMP: variations on a theme in the different kingdoms of life", *Biological reviews of the Cambridge Philosophical Society,* vol. 88, no. 3, pp. 645-668.

Gauster, M. & Huppertz, B. 2010, "The paradox of caspase 8 in human villous trophoblast fusion", *Placenta,* vol. 31, no. 2, pp. 82-88.

Gauster, M., Moser, G., Orendi, K. & Huppertz, B. 2009, "Factors involved in regulating trophoblast fusion: potential role in the development of preeclampsia", *Placenta,* vol. 30 Suppl A, pp. S49-54.

Gauster, M., Siwetz, M., Orendi, K., Moser, G., Desoye, G. & Huppertz, B. 2010, "Caspases rather than calpains mediate remodelling of the fodrin skeleton during human placental trophoblast fusion", *Cell death and differentiation,* vol. 17, no. 2, pp. 336-345.

Gonzalez, L.J., Gibbons, E., Bailey, R.W., Fairbourn, J., Nguyen, T., Smith, S.K., Best, K.B., Nelson, J., Judd, A.M. & Bell, J.D. 2009, "The influence of membrane physical properties on microvesicle release in human erythrocytes", *PMC biophysics,* vol. 2, no. 1, pp. 7-5036-2-7.

Guilbert, L.J., Winkler-Lowen, B., Sherburne, R., Rote, N.S., Li, H. & Morrish, D.W. 2002, "Preparation and functional characterization of villous cytotrophoblasts free of syncytial fragments", *Placenta,* vol. 23, no. 2-3, pp. 175-183.

Harrison, R.A. & Gadella, B.M. 2005, "Bicarbonate-induced membrane processing in sperm capacitation", *Theriogenology,* vol. 63, no. 2, pp. 342-351.

Heikkila, A., Tuomisto, T., Hakkinen, S.K., Keski-Nisula, L., Heinonen, S. & Yla-Herttuala, S. 2005, "Tumor suppressor and growth regulatory genes are overexpressed in severe early-onset preeclampsia--an array study on case-specific human preeclamptic placental tissue", *Acta Obstetricia et Gynecologica Scandinavica,* vol. 84, no. 7, pp. 679-689.

Henson, P.M., Bratton, D.L. & Fadok, V.A. 2001, "Apoptotic cell removal", *Current biology : CB,* vol. 11, no. 19, pp. R795-805.

Hiden, U., Maier, A., Bilban, M., Ghaffari-Tabrizi, N., Wadsack, C., Lang, I., Dohr, G. & Desoye, G. 2006, "Insulin control of placental gene expression shifts from mother to foetus over the course of pregnancy", *Diabetologia,* vol. 49, no. 1, pp. 123-131.

Holder, B.S., Tower, C.L., Forbes, K., Mulla, M.J., Aplin, J.D. & Abrahams, V.M. 2012, "Immune cell activation by trophoblast-derived microvesicles is mediated by syncytin 1", *Immunology,* vol. 136, no. 2, pp. 184-191.

Huang, Y., Zhao, Q., Zhou, C.X., Gu, Z.M., Li, D., Xu, H.Z., Wiedmer, T., Sims, P.J., Zhao, K.W. & Chen, G.Q. 2006, "Antileukemic roles of human phospholipid scramblase 1 gene, evidence from inducible PLSCR1-expressing leukemic cells", *Oncogene,* vol. 25, no. 50, pp. 6618-6627.

Huppertz, B., Frank, H.G., Kingdom, J.C., Reister, F. & Kaufmann, P. 1998, "Villous cytotrophoblast regulation of the syncytial apoptotic cascade in the human placenta", *Histochemistry and cell biology,* vol. 110, no. 5, pp. 495-508.

Huppertz, B., Frank, H.G., Reister, F., Kingdom, J., Korr, H. & Kaufmann, P. 1999, "Apoptosis cascade progresses during turnover of human trophoblast: analysis of villous cytotrophoblast and syncytial fragments in vitro", *Laboratory investigation; a journal of technical methods and pathology,* vol. 79, no. 12, pp. 1687-1702.

Huppertz, B., Tews, D.S. & Kaufmann, P. 2001, "Apoptosis and syncytial fusion in human placental trophoblast and skeletal muscle", *International review of cytology,* vol. 205, pp. 215-253.

Jauniaux, E., Watson, A.L., Hempstock, J., Bao, Y.P., Skepper, J.N. & Burton, G.J. 2000, "Onset of maternal arterial blood flow and placental oxidative stress. A possible factor in human early pregnancy failure", *The American journal of pathology,* vol. 157, no. 6, pp. 2111-2122.

Kantari, C., Pederzoli-Ribeil, M., Amir-Moazami, O., Gausson-Dorey, V., Moura, I.C., Lecomte, M.C., Benhamou, M. & Witko-Sarsat, V. 2007, "Proteinase 3, the Wegener autoantigen, is externalized during neutrophil apoptosis: evidence for a functional association with phospholipid scramblase 1 and interference with macrophage phagocytosis", *Blood,* vol. 110, no. 12, pp. 4086-4095.

Kenneson, A. & Cannon, M.J. 2007, "Review and meta-analysis of the epidemiology of congenital cytomegalovirus (CMV) infection", *Reviews in medical virology,* vol. 17, no. 4, pp. 253-276.

Kilani, R.T., Chang, L.J., Garcia-Lloret, M.I., Hemmings, D., Winkler-Lowen, B. & Guilbert, L.J. 1997, "Placental trophoblasts resist infection by multiple human immunodeficiency virus (HIV) type 1 variants even with cytomegalovirus coinfection but support HIV replication after provirus transfection", *Journal of virology,* vol. 71, no. 9, pp. 6359-6372.

Kliman, H.J., Nestler, J.E., Sermasi, E., Sanger, J.M. & Strauss, J.F.,3rd 1986, "Purification, characterization, and in vitro differentiation of cytotrophoblasts from human term placentae", *Endocrinology,* vol. 118, no. 4, pp. 1567-1582.

Kudo, Y., Boyd, C.A., Kimura, H., Cook, P.R., Redman, C.W. & Sargent, I.L. 2003, "Quantifying the syncytialisation of human placental trophoblast BeWo cells grown in vitro", *Biochimica et biophysica acta,* vol. 1640, no. 1, pp. 25-31.

Kuo, Y.B., Chan, C.C., Chang, C.A., Fan, C.W., Hung, R.P., Hung, Y.S., Chen, K.T., Yu, J.S., Chang, Y.S. & Chan, E.C. 2011, "Identification of phospholipid scramblase 1 as a biomarker and determination of its prognostic value for colorectal cancer", *Molecular medicine (Cambridge, Mass.),* vol. 17, no. 1-2, pp. 41-47.

Langbein, M., Strick, R., Strissel, P.L., Vogt, N., Parsch, H., Beckmann, M.W. & Schild, R.L. 2008, "Impaired cytotrophoblast cell-cell fusion is associated with reduced Syncytin and increased apoptosis in patients with placental dysfunction", *Molecular reproduction and development,* vol. 75, no. 1, pp. 175-183.

Lee, X., Keith, J.C.,Jr, Stumm, N., Moutsatsos, I., McCoy, J.M., Crum, C.P., Genest, D., Chin, D., Ehrenfels, C., Pijnenborg, R., van Assche, F.A. & Mi, S. 2001, "Downregulation of placental syncytin expression and abnormal protein localization in pre-eclampsia", *Placenta,* vol. 22, no. 10, pp. 808-812.

Lin, L., Xu, B. & Rote, N.S. 1999, "Expression of endogenous retrovirus ERV-3 induces differentiation in BeWo, a choriocarcinoma model of human placental trophoblast", *Placenta,* vol. 20, no. 1, pp. 109-118.

Lindau, M. & Almers, W. 1995, "Structure and function of fusion pores in exocytosis and ectoplasmic membrane fusion", *Current opinion in cell biology,* vol. 7, no. 4, pp. 509-517.

Lu, B., Sims, P.J., Wiedmer, T., Moser, A.H., Shigenaga, J.K., Grunfeld, C. & Feingold, K.R. 2007, "Expression of the phospholipid scramblase (PLSCR) gene family during the acute phase response", *Biochimica et biophysica acta,* vol. 1771, no. 9, pp. 1177-1185.

McMaster, M.T., Librach, C.L., Zhou, Y., Lim, K.H., Janatpour, M.J., DeMars, R., Kovats, S., Damsky, C. & Fisher, S.J. 1995, "Human placental HLA-G expression is restricted to differentiated cytotrophoblasts", *Journal of immunology (Baltimore, Md.: 1950),* vol. 154, no. 8, pp. 3771-3778.

Meade, E.S., Ma, Y.Y. & Guller, S. 2007, "Role of hypoxia-inducible transcription factors 1alpha and 2alpha in the regulation of plasminogen activator inhibitor-1 expression in a human trophoblast cell line", *Placenta,* vol. 28, no. 10, pp. 1012-1019.

Metz, P., Dazert, E., Ruggieri, A., Mazur, J., Kaderali, L., Kaul, A., Zeuge, U., Windisch, M.P., Trippler, M., Lohmann, V., Binder, M., Frese, M. & Bartenschlager, R. 2012, "Identification of type I and type II interferon-induced effectors controlling hepatitis C virus replication", *Hepatology (Baltimore, Md.),* vol. 56, no. 6, pp. 2082-2093.

Mi, S., Lee, X., Li, X., Veldman, G.M., Finnerty, H., Racie, L., LaVallie, E., Tang, X.Y., Edouard, P., Howes, S., Keith, J.C.,Jr & McCoy, J.M. 2000, "Syncytin is a captive retroviral envelope protein involved in human placental morphogenesis", *Nature,* vol. 403, no. 6771, pp. 785-789.

Miller, R.K., Genbacev, O., Turner, M.A., Aplin, J.D., Caniggia, I. & Huppertz, B. 2005, "Human placental explants in culture: approaches and assessments", *Placenta,* vol. 26, no. 6, pp. 439-448.

Monck, J.R. & Fernandez, J.M. 1996, "The fusion pore and mechanisms of biological membrane fusion", *Current opinion in cell biology,* vol. 8, no. 4, pp. 524-533.

Ng, Y.H., Zhu, H. & Leung, P.C. 2011, "Twist regulates cadherin-mediated differentiation and fusion of human trophoblastic cells", *The Journal of clinical endocrinology and metabolism,* vol. 96, no. 12, pp. 3881-3890.

Orendi, K., Gauster, M., Moser, G., Meiri, H. & Huppertz, B. 2010, "The choriocarcinoma cell line BeWo: syncytial fusion and expression of syncytium-specific proteins", *Reproduction (Cambridge, England),* vol. 140, no. 5, pp. 759-766.

Ory, S., Ceridono, M., Momboisse, F., Houy, S., Chasserot-Golaz, S., Heintz, D., Calco, V., Haeberle, A.M., Espinoza, F.A., Sims, P.J., Bailly, Y., Bader, M.F. & Gasman, S. 2013, "Phospholipid scramblase-1-induced lipid reorganization regulates compensatory endocytosis in neuroendocrine cells", *The Journal of neuroscience : the official journal of the Society for Neuroscience,* vol. 33, no. 8, pp. 3545-3556.

Pfaffl, M.W., Horgan, G.W. & Dempfle, L. 2002, "Relative expression software tool (REST) for group-wise comparison and statistical analysis of relative expression results in real-time PCR", *Nucleic acids research,* vol. 30, no. 9, pp. e36.

Potgens, A.J., Drewlo, S., Kokozidou, M. & Kaufmann, P. 2004, "Syncytin: the major regulator of trophoblast fusion? Recent developments and hypotheses on its action", *Human reproduction update,* vol. 10, no. 6, pp. 487-496.

Potgens, A.J., Schmitz, U., Bose, P., Versmold, A., Kaufmann, P. & Frank, H.G. 2002, "Mechanisms of syncytial fusion: a review", *Placenta,* vol. 23 Suppl A, pp. S107-13.

Rauen, T., Hedrich, C.M., Tenbrock, K. & Tsokos, G.C. 2013, "cAMP responsive element modulator: a critical regulator of cytokine production", *Trends in molecular medicine,* vol. 19, no. 4, pp. 262-269.

Rebourcet, R., Mignot, T.M., Robert, B. & Ferre, F. 2004, "Endothelin-2 down-regulation occurs in parallel with the anti-proliferative effect of dimethylsulfoxide in BeWO human choriocarcinoma cell line", *Cellular and molecular biology (Noisy-le-Grand, France),* vol. 50 Online Pub, pp. OL701-12.

Richart, R. 1961, "Studies of placental morphogenesis. I. Radioautographic studies of human placenta utilizing tritiated thymidine", *Proceedings of the Society for Experimental Biology and Medicine.Society for Experimental Biology and Medicine (New York, N.Y.),* vol. 106, pp. 829-831.

Sahu, S.K., Gummadi, S.N., Manoj, N. & Aradhyam, G.K. 2007, "Phospholipid scramblases: an overview", *Archives of Biochemistry and Biophysics,* vol. 462, no. 1, pp. 103-114.

Seamon, K.B., Padgett, W. & Daly, J.W. 1981, "Forskolin: unique diterpene activator of adenylate cyclase in membranes and in intact cells", *Proceedings of the National Academy of Sciences of the United States of America,* vol. 78, no. 6, pp. 3363-3367.

Seigneuret, M. & Devaux, P.F. 1984, "ATP-dependent asymmetric distribution of spin-labeled phospholipids in the erythrocyte membrane: relation to shape changes", *Proceedings of the National Academy of Sciences of the United States of America,* vol. 81, no. 12, pp. 3751-3755.

Silverman, R.H., Halloum, A., Zhou, A., Dong, B., Al-Zoghaibi, F., Kushner, D., Zhou, Q., Zhao, J., Wiedmer, T. & Sims, P.J. 2002, "Suppression of ovarian carcinoma cell growth in vivo by the interferon-inducible plasma membrane protein, phospholipid scramblase 1", *Cancer research,* vol. 62, no. 2, pp. 397-402.

Sims, P.J. & Wiedmer, T. 2001, "Unraveling the mysteries of phospholipid scrambling", *Thrombosis and haemostasis,* vol. 86, no. 1, pp. 266-275.

Smith, S.K., Farnbach, A.R., Harris, F.M., Hawes, A.C., Jackson, L.R., Judd, A.M., Vest, R.S., Sanchez, S. & Bell, J.D. 2001, "Mechanisms by which intracellular calcium induces susceptibility to secretory phospholipase A2 in human erythrocytes", *The Journal of biological chemistry,* vol. 276, no. 25, pp. 22732-22741.

Song, G., Fleming, J.A., Kim, J., Spencer, T.E. & Bazer, F.W. 2011, "Pregnancy and interferon tau regulate DDX58 and PLSCR1 in the ovine uterus during the peri-implantation period", *Reproduction (Cambridge, England),* vol. 141, no. 1, pp. 127-138.

Stout, J.G., Basse, F., Luhm, R.A., Weiss, H.J., Wiedmer, T. & Sims, P.J. 1997, "Scott syndrome erythrocytes contain a membrane protein capable of mediating Ca2+-dependent transbilayer migration of membrane phospholipids", *The Journal of clinical investigation,* vol. 99, no. 9, pp. 2232-2238.

Sun, J., Nanjundan, M., Pike, L.J., Wiedmer, T. & Sims, P.J. 2002, "Plasma membrane phospholipid scramblase 1 is enriched in lipid rafts and interacts with the epidermal growth factor receptor", *Biochemistry,* vol. 41, no. 20, pp. 6338-6345.

Suzuki, E., Amengual, O., Atsumi, T., Oku, K., Hashimoto, T., Kataoka, H., Horita, T., Yasuda, S., Ieko, M., Fukushima, K. & Koike, T. 2010a, "Increased expression of phospholipid scramblase 1 in monocytes from patients with systemic lupus erythematosus", *The Journal of rheumatology,* vol. 37, no. 8, pp. 1639-1645.

Suzuki, J., Umeda, M., Sims, P.J. & Nagata, S. 2010b, "Calcium-dependent phospholipid scrambling by TMEM16F", *Nature,* vol. 468, no. 7325, pp. 834-838.

Tanaka, K., Fujimura-Kamada, K. & Yamamoto, T. 2011, "Functions of phospholipid flippases", *Journal of Biochemistry,* vol. 149, no. 2, pp. 131-143.

van den Eijnde, S.M., van den Hoff, M.J., Reutelingsperger, C.P., van Heerde, W.L., Henfling, M.E., Vermeij-Keers, C., Schutte, B., Borgers, M. & Ramaekers, F.C. 2001, "Transient expression of phosphatidylserine at cell-cell contact areas is required for myotube formation", *Journal of cell science,* vol. 114, no. Pt 20, pp. 3631-3642.

Vignery, A. 2000, "Osteoclasts and giant cells: macrophage-macrophage fusion mechanism", *International journal of experimental pathology,* vol. 81, no. 5, pp. 291-304.

Warke, R.V., Xhaja, K., Martin, K.J., Fournier, M.F., Shaw, S.K., Brizuela, N., de Bosch, N., Lapointe, D., Ennis, F.A., Rothman, A.L. & Bosch, I. 2003, "Dengue virus induces novel changes in gene expression of human umbilical vein endothelial cells", *Journal of virology,* vol. 77, no. 21, pp. 11822-11832.

Wice, B., Menton, D., Geuze, H. & Schwartz, A.L. 1990, "Modulators of cyclic AMP metabolism induce syncytiotrophoblast formation in vitro", *Experimental cell research,* vol. 186, no. 2, pp. 306-316.

Wiedmer, T., Zhao, J., Nanjundan, M. & Sims, P.J. 2003, "Palmitoylation of phospholipid scramblase 1 controls its distribution between nucleus and plasma membrane", *Biochemistry,* vol. 42, no. 5, pp. 1227-1233.

Wiedmer, T., Zhou, Q., Kwoh, D.Y. & Sims, P.J. 2000, "Identification of three new members of the phospholipid scramblase gene family", *Biochimica et biophysica acta,* vol. 1467, no. 1, pp. 244-253.

Williamson, P., Bevers, E.M., Smeets, E.F., Comfurius, P., Schlegel, R.A. & Zwaal, R.F. 1995, "Continuous analysis of the mechanism of activated transbilayer lipid movement in platelets", *Biochemistry,* vol. 34, no. 33, pp. 10448-10455.

Yang, H., Kim, A., David, T., Palmer, D., Jin, T., Tien, J., Huang, F., Cheng, T., Coughlin, S.R., Jan, Y.N. & Jan, L.Y. 2012a, "TMEM16F forms a Ca2+-activated cation channel required for lipid scrambling in platelets during blood coagulation", *Cell,* vol. 151, no. 1, pp. 111-122.

Yang, J., Zhu, X., Liu, J., Ding, X., Han, M., Hu, W., Wang, X., Zhou, Z. & Wang, S. 2012b, "Inhibition of Hepatitis B virus replication by phospholipid scramblase 1 in vitro and in vivo", *Antiviral Research,* vol. 94, no. 1, pp. 9-17.

Yu, A., McMaster, C.R., Byers, D.M., Ridgway, N.D. & Cook, H.W. 2003, "Stimulation of phosphatidylserine biosynthesis and facilitation of UV-induced apoptosis in Chinese hamster ovary cells overexpressing phospholipid scramblase 1", *The Journal of biological chemistry,* vol. 278, no. 11, pp. 9706-9714.

Yu, C., Shen, K., Lin, M., Chen, P., Lin, C., Chang, G.D. & Chen, H. 2002, "GCMa regulates the syncytin-mediated trophoblastic fusion", *The Journal of biological chemistry,* vol. 277, no. 51, pp. 50062-50068.

Yui, J., Garcia-Lloret, M., Brown, A.J., Berdan, R.C., Morrish, D.W., Wegmann, T.G. & Guilbert, L.J. 1994, "Functional, long-term cultures of human term trophoblasts purified by column-elimination of CD9 expressing cells", *Placenta,* vol. 15, no. 3, pp. 231-246.

Zhao, J., Zhou, Q., Wiedmer, T. & Sims, P.J. 1998, "Level of expression of phospholipid scramblase regulates induced movement of phosphatidylserine to the cell surface", *The Journal of biological chemistry,* vol. 273, no. 12, pp. 6603-6606.

Zhao, K.W., Li, D., Zhao, Q., Huang, Y., Silverman, R.H., Sims, P.J. & Chen, G.Q. 2005, "Interferon-alpha-induced expression of phospholipid scramblase 1 through STAT1 requires the sequential activation of protein kinase Cdelta and JNK", *The Journal of biological chemistry,* vol. 280, no. 52, pp. 42707-42714.

Zhao, K.W., Li, X., Zhao, Q., Huang, Y., Li, D., Peng, Z.G., Shen, W.Z., Zhao, J., Zhou, Q., Chen, Z., Sims, P.J., Wiedmer, T. & Chen, G.Q. 2004, "Protein kinase Cdelta mediates retinoic acid and phorbol myristate acetate-induced phospholipid scramblase 1 gene expression: its role in leukemic cell differentiation", *Blood,* vol. 104, no. 12, pp. 3731-3738.

Zhou, Q., Zhao, J., Stout, J.G., Luhm, R.A., Wiedmer, T. & Sims, P.J. 1997, "Molecular cloning of human plasma membrane phospholipid scramblase. A protein mediating transbilayer movement of plasma membrane phospholipids", *The Journal of biological chemistry,* vol. 272, no. 29, pp. 18240-18244.

Zhou, Q., Zhao, J., Wiedmer, T. & Sims, P.J. 2002, "Normal hemostasis but defective hematopoietic response to growth factors in mice deficient in phospholipid scramblase 1", *Blood,* vol. 99, no. 11, pp. 4030-4038.